Measurement of Adsorption Isotherms by Means of Gas Chromatography

by

Martin Schaefer

A thesis submitted in partial fulfillment of the

requirements for the degree of

Master of Science

(Chemical Engineering)

at the

University of Wisconsin-Madison

1991

Abstract

This study investigates the feasibility of a chromatographic flow method to determine low concentration adsorption isotherms of acetone on activated carbon. The temperatures and concentrations studied range from 27°C to 130°C and from 2 ppm to 50.4 ppm, respectively. Different acetone concentrations are obtained by diluting an acetone-nitrogen mixture of known composition with a stream of pure nitrogen. All experiments are done on Calgon OL 20/50 activated carbon. At 40°C, the amount of adsorbed acetone ranges from 2.57 milligram per gram carbon at an acetone concentration of 2.41 ppm to 15.9 milligram at a concentration of 50.4 ppm.

The measured adsorption equilibrium data are useful for the modeling of static and regenerative adsorptive air filters to remove volatile organic compounds from indoor air. Several adsorption models, including the Langmuir model and the Dubinin-Polanyi theory are fitted to the data. It is shown that a single equation, derived from the Dubinin-Radushkevich expression correlates the data over the whole temperature and concentration range under investigation.

Adsorption measurements on crushed Calgon OL 20/50 activated carbon yield adsorption capacities which are 46% higher than those obtained from the uncrushed carbon. The isosteric heat of adsorption is found to be a function of the amount adsorbed. For 2 milligrams acetone adsorbed per gram of carbon, the value is 57 kJ per mole acetone.

Acknowledgements

This project was made possible by funds from the University of Wisconsin graduate school, the office of research services, and Johnson Controls Corporation. The German Academic Exchange Service provided me with the opportunity of attending graduate school in the United States of America. Frank-Detlef Drake initialized this program and introduced me to the Solar Energy Laboratory.

My stay in Madison has been a very challenging and remunerative experience. I am very grateful that I had the chance to meet and to work with people who were so interesting and helpful. I would like to thank my two advisors, Professor Sanford A. Klein and Professor John W. Mitchell. Their steady questions and ideas kept this project going. Professor William A. Beckman, the director of the Solar Energy Laboratory, and Krista Knight, also contributed substantially to the progress of my studies. Professor S.H. Langer provided a thorough background in gas chromatography and Richard Boor provided very welcome help in the experimental part of this work. Shirley Quamme from the Solar Lab staff never left one question unanswered. My friends in the Lab were great to work with and created a pleasant and inspiring atmosphere. Thanks to Tom, my roommate, for teaching me so much of the American culture and for all those deep discussions. A special thanks to Larissa for making my life outside of the Lab so wonderful. Finally, I want to thank my parents and my sister Barbara for their loving support over the distance. Their phone calls, letters, and packages were always greatly appreciated.

Table of Contents

Appendices

List of Figures

List of Tables

Nomenclature

English Letter Symbols

Symbol	Definition
A	composite area in frontal analysis chromatogram or adsorption potential
C	circumference
c	concentration
D	diameter
F	flowrate
h	convective heat transfer coefficient
j	pressure correction factor
K	adsorption equilibrium constant
k	(any) constant or heat conductivity coefficient
L	length
M	molecular weight
m	mass
N	number of data points
n	moles
p	partial pressure
Q	heat of adsorption
q	amount adsorbed
R	gas constant
r	rate
T	temperature
t	time or temperature
v	velocity
W	micropore volume

w	uncertainty
x	axial coordinate
y	mole fraction

Greek Symbols

Symbol	Definition
ε	error estimation or void fraction
θ	fractional surface coverage
μ	viscosity
ξ	mass fraction
ρ	density

Subscripts

Symbol	Definition
a	adsorption
atm	atmospheric
d	desorption
diff	differential
f	fluid
i	inlet condition or component
o	outlet condition
p	particle
res	resulting
s	solute or surface
sm	solute-nitrogen mixture
st	isosteric
vel	velocity
vp	vapor pressure

CHAPTER
ONE

Introduction

1.1 The Adsorption Process

Adsorption operations utilize the ability of certain solids to concentrate specific substances from solution onto their surface. This process is exploited in many technical applications [1], where the components of gaseous or liquid solutions are separated from each other in order to purify the solution or to recover a valuable product. On a molecular level, adsorption can be described as the adhesion of molecules to a surface. The reverse process is called desorption. The terms adsorbate and adsorbent refer to the molecules of the gas or liquid phase and to the solid respectively. Adsorption is a very general phenomenon. Even common solids will adsorb gases and vapors to a small extend but only some solids exhibit sufficient specificity and adsorptive capacity to make them useful as adsorbents. This capability was recognized in the eighteenth century by Scheele [2] and Fontana [3] who did experiments on adsorption phenomena. In terms of adsorption engineering, the knowledge of both the equilibrium distribution of the molecules between the two phases and of the rates approaching the equilibrium is the basis for calculations and modeling. The equilibrium distribution is a strong function of the temperature and pressure of the system. Upon adsorption, the adsorbate molecules

lose some of their kinetic energy. This makes adsorption an exothermic process, and lowering the temperature will result in an increased number of adsorbed molecules.

The adsorptive power of a solid mainly depends on the total area of exposed surface. In this respect, the outer surface area and the porosity play complementary parts in adsorption phenomena. The significant surface is usually not the gross surface of the granular particles, but the very much larger surface of the internal pores of the particles. The pores can be very small, sometimes of the order of a few molecular diameters in width, but their large number provides an enormous surface for adsorption.

Adsorption processes are widely used in commercial, municipal, and private applications. The scale of operations ranges from the use of a few grams of adsorbent in the laboratory to industrial plants with an adsorbent inventory exceeding 100 tons.

Typical applications in the field of gaseous separations are the dehumidification of air and other gases, the removal of odors and impurities from industrial gases like carbon dioxide, and the recovery of valuable solvent vapors from dilute mixtures with air and other gases. Adsorption processes are also used to fractionate mixtures of hydrocarbon gases containing such substances as methane, ethylene, ethane, propylene, and propane. Furthermore, gaseous adsorption processes control many hazardous substances including pesticides and the many halogenated organics coming under increased scrutiny for their health related effects. In household applications, adsorption processes are used in exhaust fans to reduce odors associated with cooking processes. A relatively new field is the use in commercial buildings (e.g., offices, hotels, restaurants) to remove a variety of pollutants from indoor air.

Liquid separations include the removal of moisture dissolved in gasoline, the decolorization of petroleum products and aqueous sugar solutions, and the fractionation

of mixtures of aromatic and paraffinic hydrocarbons. The increase in the amount of hazardous and toxic chemicals in public water supplies also leads directly to the use of adsorptive purification processes.

Adsorption processes can also be used for a totally different purpose: the precise measurement of the adsorption of vapors by a porous solid can be used to estimate the specific surface area and the pore size distribution of the solid [16, 17, 18, 19]. The specific surface area and the particle size are related in an inverse fashion. In this respect, the method yields also valuable information about the particle size of the porous solid under investigation. This is of special importance since microscopic methods fail for particle sizes below about 1μ.

1.1.1 Physical and Chemical Adsorption

Two different types of adsorption phenomena are distinguished, physical and chemical. Although this distinction is conceptually useful, there are many intermediate cases and it is not always possible to categorize a particular system unequivocally.

Physical adsorption is a readily reversible phenomenon. It is the result of intermolecular forces of attraction between molecules of the solid and the adsorbed substance. When the intermolecular attractive forces between a solid and a gas are greater than those existing between molecules of the gas itself, the gas will condense upon the surface of the solid. Condensation occurs even when the pressure in the gas phase is lower than the vapor pressure for the corresponding temperature. Such a condensation will be accompanied by an evolution of heat. The amount of generated heat is usually somewhat larger than the latent heat of vaporization and of the order of the heat of sublimation of the gas. Measurements for adsorption of acetone on charcoal at 30°C

yielded a value of approximately 60 kJ per mole of acetone [1]. By lowering the pressure of the gas phase or by raising the temperature, the adsorbed gas is readily removed from the solid. Industrial adsorption operations depend upon this reversibility for either recovery of the adsorbent for reuse, or for the recovery of the adsorbed substance. The forces involved in physical adsorption are of two main kinds, electrostatic interactions due to permanent dipoles in the adsorbed molecules and van der Waals forces. Electrostatic contributions are present only in the case of adsorbents which have an ionic structure. Van der Waals forces are common to all materials and will be present regardless of the nature of the solid or the fluid phase. They consist of attractive dispersion forces [4,5] and short range repulsive forces [6]. Gregg and Sing [7] give a thorough derivation of all involved aspects.

Chemisorption is the result of chemical interaction between the adsorbent and the adsorbed substance. A chemical interaction occurs when a transfer of electrons between the adsorbent and the adsorbed molecules occurs. Because of this electrical interaction, the term "valency forces" is used in the process of chemisorption [7]. The strength of the chemical bond may vary considerably, and identifiable chemical compounds in the usual sense do not actually form because the new species is confined to a single layer of atoms or molecules on the surface of the solid. Generally, the adhesive force is much greater than that found in physical adsorption. The heat liberated during chemisorption is usually large, of the order of the heat of chemical reaction. Because of the chemical nature, the process is often irreversible, and on desorption the original substance undergoes a chemical change. The same substance which, under conditions of low temperature, will undergo substantially only physical adsorption upon a solid will sometimes exhibit chemisorption at higher temperatures. As mentioned earlier, both phenomena can occur

at the same time. Chemisorption is of particular importance in the field of heterogeneous catalysis where the controlled chemical change of a substance is the main objective.

1.1.2 Charcoal as an Adsorbent

Many different solids are in general use as adsorbents. Adsorbents must possess certain engineering properties depending upon the application to which they are put. If they are used in a fixed bed through which a liquid or gas flows, they must not offer too great a pressure drop for flow nor must they easily be carried away by the flowing stream. Also, they must have adequate strength and hardness so as not to be reduced in size during handling or crushed in supporting their own weight in beds of the required thickness. As mentioned before, a large surface per unit weight is essential to all useful adsorbents. The most common adsorbents are charcoal, Fuller's earths, activated clays, bauxite, alumina, bone char, synthetic polymeric adsorbents, silica gel, and molecular sieves [1].

Charcoal, or activated carbon, is used in many industrial applications. A vast number of reports in the literature deal with adsorption experiments on charcoal [e.g., 8, 9, 10, 11, 12]. Charcoal is prepared from carbon containing source materials such as coconut shells, fruit pits, coal, lignite, and wood. These materials are first pyrolyzed and carbonized at several hundred degrees centigrade. During this process, the volatile fraction and low molecular products of pyrolysis are removed and the residual carbonaceous material undergoes the so-called "activation process". In this activation process, oxidizing gases, such as steam or carbon dioxide are passed over the product. The tarry carbonization products which were formed during the pyrolisis are removed and the pores are opened.

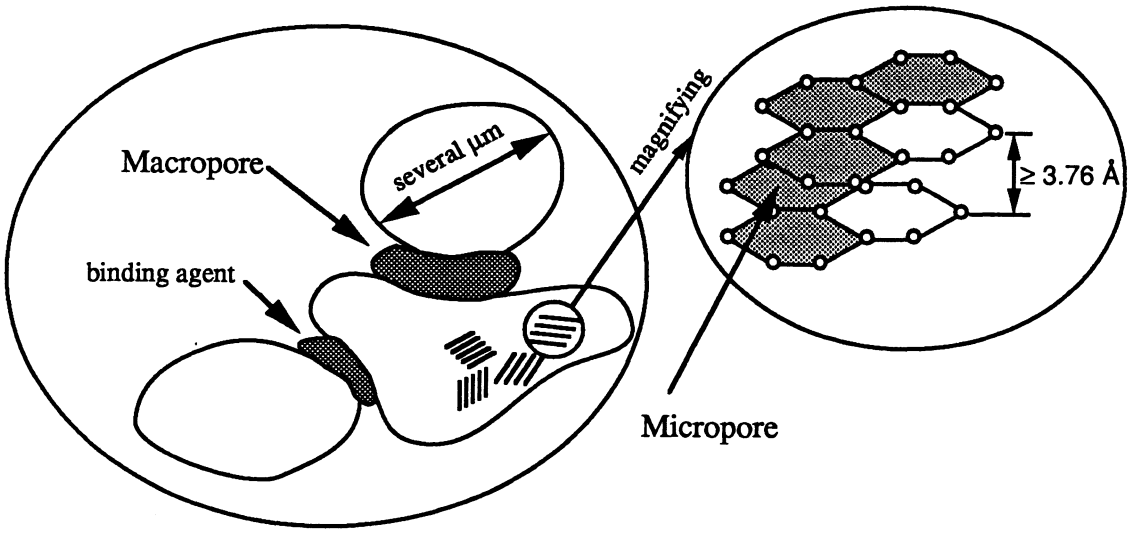

Figure 1.1 Structure of activated carbon

Dubinin [13, 14] proposed a classification of pores according to their average width. Pores of widths below 20 Å (2 nm) are described as micropores, those with widths above 200 Å (20 nm) as macropores. The term of "transitional pores" applies for openings with widths between those two values. For activated carbon, micropores are the space between two neighboring crystallite planes (Figure 1.1). For a perfect lattice, the distance between two planes can be calculated as 3.76 Å (0.376 nm). Since activated carbons usually have a rather disordered crystallite structure, the average figure must be somewhat larger. Macropores are the space between two crystals (Figure 1.1).

The surface of activated carbon is essentially nonpolar although a slight polarity may arise from surface oxidation. As a result, carbon adsorbents tend to be hydrophobic and organophilic. This means that they have little tendency to adsorb polar water molecules but have a high affinity for organic species. Furthermore, charcoal has a wide pore size

distribution and therefore does not exhibit the strong preferential adsorption apparent with other adsorbents. However, there is some degree of preferential adsorption, following a general trend of preference for molecules with higher molecular weight and higher boiling point [15].

The history of microporous carbonaceous adsorbents can be traced back for more than 3000 years. The ancient Egyptians used activated carbon for medicinal purposes. They also lined their water storage vessels with charcoal to remove unpleasant tastes and odors from water supplies. The same application was known to ancient mariners who crossed the seas in large sailing ships. Today activated carbon is used in many different applications like the recovery of solvent vapors from gas mixtures, collection of gasoline hydrocarbons from natural gas, and the fractionation of hydrocarbon gases [1]. Because charcoal so effectively removes toxic organics from air, it is also used in many types of breathing apparatuses, such as industrial respirators and gas masks for fire-fighting, mine safety and gas warfare. In various types of filters charcoal purifies air for plant employees, passengers in airplanes, and submarine personnel to name just a few.

1.2 Adsorption Data

Mass transfer effects involved in actual fluid-solid contacting processes are the cause for non instantaneous equilibria. When an adsorbent is in contact with the surrounding fluid of a certain composition, adsorption takes place and after a sufficiently long time, the adsorbent and the surrounding fluid reach equilibrium. In practical operations, this time can be relatively long and it might not be economically feasible to wait for complete

equilibrium. Three processes control the overall rate of mass transfer for adsorption in a packed bed:

1) film diffusion through the boundary layer surrounding the adsorbent particle

2) pore diffusion, a combination of molecular diffusion, Knudsen diffusion, Poiseuille flow, and surface diffusion

3) the kinetics of the actual adsorption process [20, 21]

The slowest and therefore rate-controlling step in most cases is the pore diffusion process [22]. Several methods of accounting for the mass transfer resistances are used, e.g. [23, 24]. Usually, the resistances are lumped and an overall mass transfer coefficient is derived [25, 26]. However, information and data on adsorption equilibria, without considering the rate of the process, are important in many engineering applications. This is the reason why the great bulk of experimental data pertaining to adsorption represent equilibrium measurements [e.g., 8, 9, 10, 11, 12]. This study is concerned with adsorption equilibrium measurements. Mass transfer rates are not measured.

1.2.1 Isotherms and Isosteres

The equilibrium relation between amount adsorbed, q, and concentration of adsorbate in the fluid phase, c, at a given temperature T is called the adsorption isotherm. Usually, q is plotted as a function of the adsorbate concentration. Since q is also a function of the adsorbate-adsorbent system, the general expression reads

$$q = f(c, T, \text{adsorbate}, \text{adsorbent}) \tag{1.1}$$

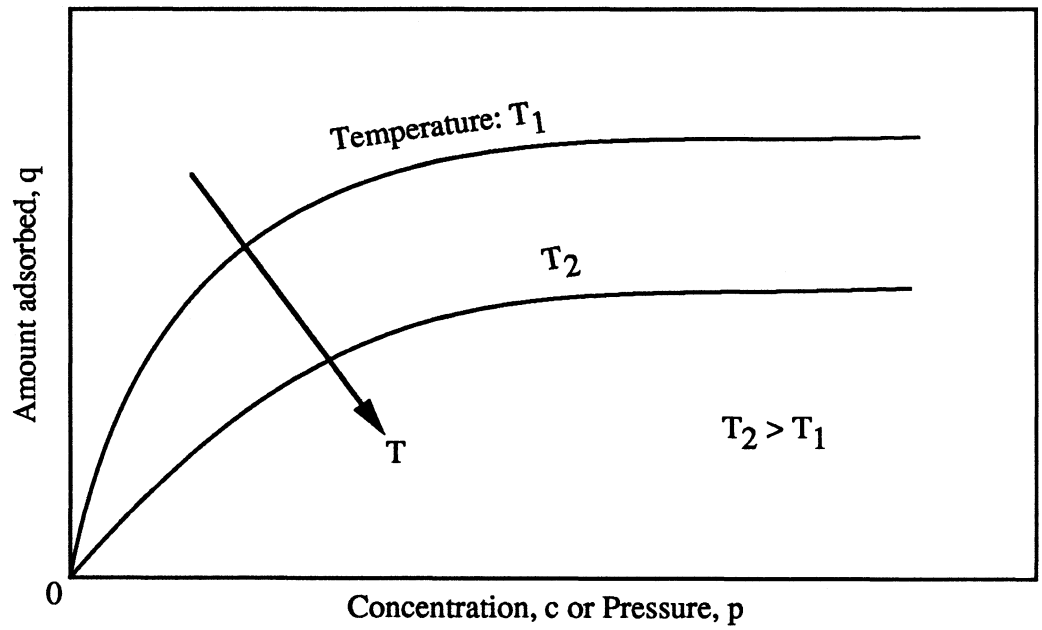

Figure 1.2 Adsorption Isotherms

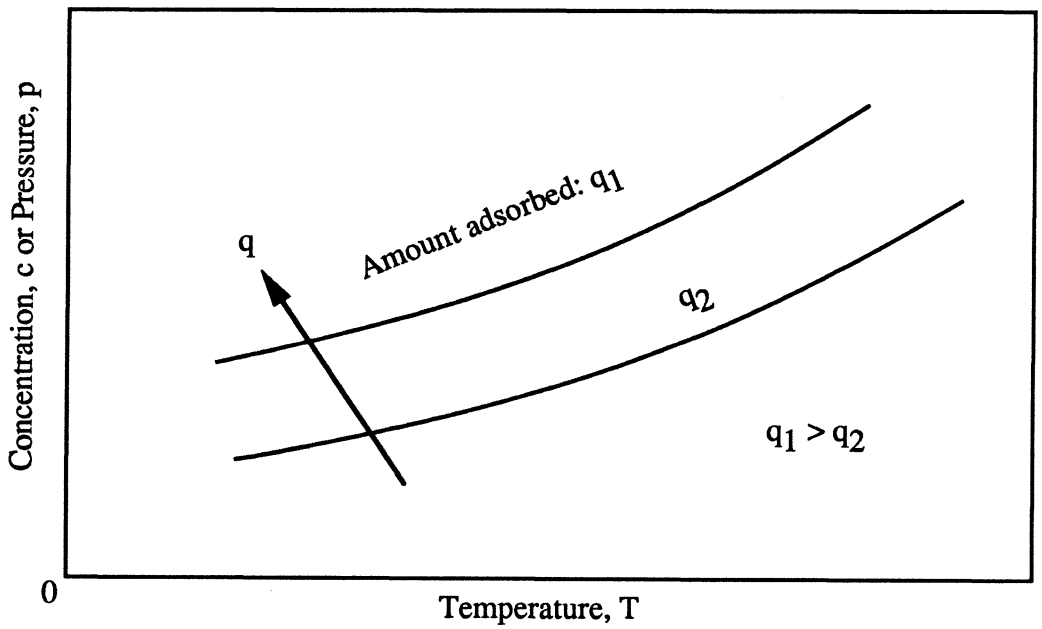

Figure 1.3 Adsorption Isosteres

The adsorbate concentration in the fluid phase can be expressed in any convenient unit such as partial pressure or fractions of mole, mass or volume. Accordingly, q can be expressed in many different ways such as mass or moles of adsorbate per mass of adsorbent. A plot of the concentration versus the temperature, for a given amount adsorbed, is called an adsorption isostere. Typical adsorption isotherms and isosteres are shown in Figure 1.2 and 1.3 respectively.

A main task of adsorption theory is to express the shape of the isotherms in terms of important parameters such as the specific surface area and the volume of the pores and to incorporate this in mathematical models. This has been done successfully in simple cases. In more complex cases, no completely satisfactory approach is known. The main difficulty is given by the fact that over-simplified models have to be used in order to get mathematically tractable equations. On the other hand, many purely empirical models have been developed. They intend to correlate the experimental data in simple equations with two or at most three empirical parameters. Of all these different approaches, a rather simple model, the so-called "Langmuir isotherm", has gained wide acceptance. It was derived with a theory in mind but it is not universally applicable, nor can it be predicted in which case it will apply.

1.2.2 The Langmuir Isotherm

The simplest theoretical model for adsorption was given by Langmuir [27]. It was developed from a kinetic viewpoint and assumes that adsorption takes place on an energetically uniform surface without any interactions between adsorbed molecules. Furthermore, it idealizes the adsorbed molecules to be of spherical shape and to form a monolayer on the adsorbent surface. In reality, several layers of molecules can be

adsorbed on the surface, creating the term "multilayer" adsorption (Figure 1.4). In Langmuir's model, the fractional coverage θ, also called the surface coverage, is expressed as

$$\theta = \frac{q}{q_0} \tag{1.2}$$

where q is the actual number and q_0 the theoretical possible value of adsorbed molecules per unit area of adsorbent. Assuming first order kinetics, that is when the rates are directly proportional to the concentration driving force, the adsorption rate r_a and the desorption rate r_d are given by

$$r_a = k_a\, p\, (1 - \theta) \tag{1.3}$$

and

$$r_d = k_d\, \theta \tag{1.4}$$

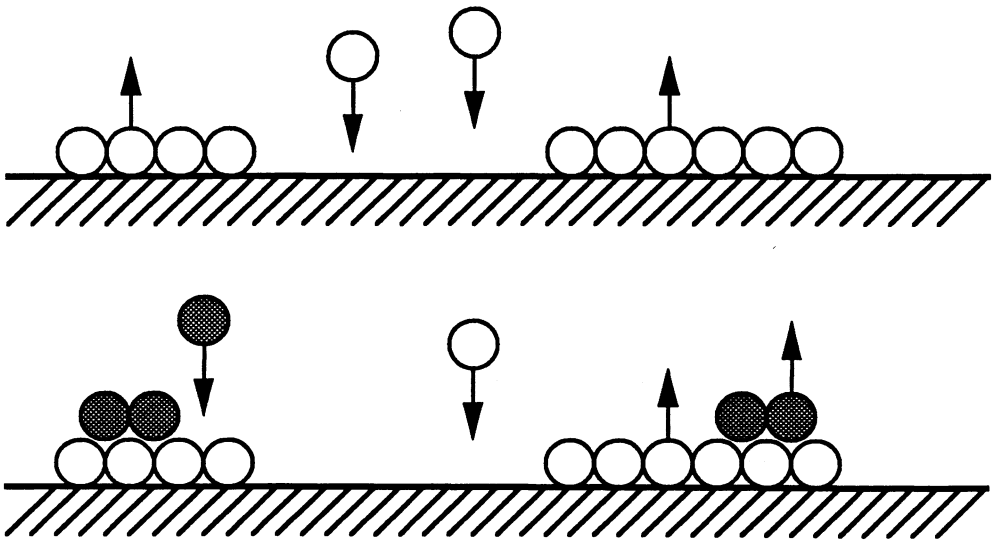

Figure 1.4 Monolayer and multilayer adsorption

The constants k_a and k_d are the adsorption and desorption rate constants and p is the partial pressure of the adsorbate in the gas phase. Equilibration of the adsorption rate and desorption rate gives the equilibrium relation as

$$k_a\, p\, (1-\theta) = k_d\, \theta \tag{1.5}$$

or

$$p = \frac{1}{K}\,\frac{\theta}{(1-\theta)} \tag{1.6}$$

where $K = k_a/k_d$ is the temperature dependent adsorption equilibrium constant. Equation (1.6) is called the Langmuir isotherm. When the amount adsorbed, q, is small compared with the adsorption capacity of the adsorbent, q_0, the term $\theta/(1-\theta)$ in equation (1.6) reduces approximately to θ and equation (1.6) can be written as

$$\theta = K\, p \tag{1.7}$$

For a constant K, the isotherm becomes a straight line through the origin. A more thorough mathematical analysis of the problem considers the initial slope of the function represented by equation (1.6) and yields

$$\frac{dp}{d\theta} = \frac{1}{K}\,\frac{1}{(1-\theta)^2} \tag{1.8}$$

and for the limit of θ approaching zero

$$\lim_{\theta \to 0} \left(\frac{1}{K}\,\frac{1}{(1-\theta)^2} \right) = \frac{1}{K} = \text{constant} \tag{1.9}$$

Equations (1.7) and (1.9) are of special importance to this study since they show that for adsorption on a uniform surface at sufficiently low concentrations ($\theta \longrightarrow 0$) the equilibrium relationship between adsorption and partial pressure of adsorbate will be

linear. Hence, the isotherm reduces to a straight line through the origin, as shown in Figure 1.5.

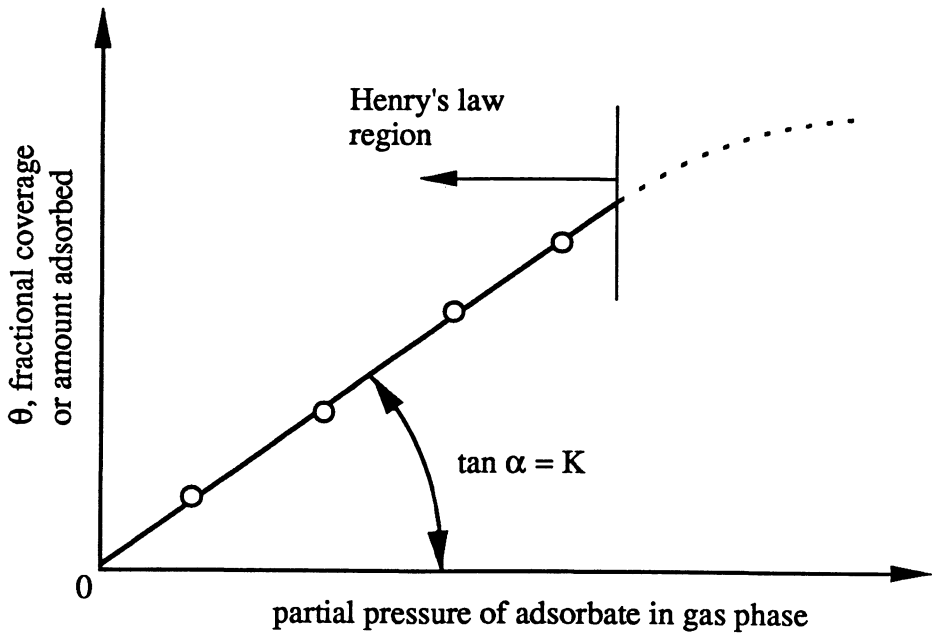

Figure 1.5 Henry's law region

The region of linearity is called the "Henry's law" region, in analogy to the ideal solubility of gases in liquids. Accordingly, K, the constant of proportionality is called the Henry constant. As mentioned before, Langmuir's derivation is based on two basic assumptions, a uniform surface and an absence of any interactions between adsorbed molecules. At low adsorbate concentrations (which is the concentration range of interest to this study), the second idealization seems to be justified whereas the assumption of a uniform surface appears to be too over-simplified, especially when looking at porous adsorbents like charcoal. Nevertheless, Langmuir's equation agrees with experimental

data in many cases and has hence become a very widely used tool in adsorption calculations.

The accuracy of equation (1.6) can be improved in several ways, especially by taking interactions between adsorbing molecules into account. Many refinements of Langmuir's original approach have been described in the literature [28, 29] but none of them has gained as widespread acceptance as the original approach.

1.2.3 The BET classification

A vast amount of adsorption isotherms were measured on a variety of solids and reported in the literature. In order to classify these, Brunauer et al. [30, 31] have divided the isotherms for physical adsorption into five types (Figure 1.6). This classification is commonly referred to as the Brunauer, Emmett and Teller (BET) classification. Although the grouping was originally done for convenience, it soon became clear that each class represents a specific physical system. Type I isotherms are obtained when true microporous adsorbents are used. These adsorbents have pore sizes which are not very much greater than the molecular diameter of the adsorbate molecule. In this case, a complete filling of the micropores refers to the definite saturation limit. If the adsorbent has a wide range of pore sizes, the isotherms follow the type II and III. When two distinct surface layers are formed, either on a plane surface or on the wall of a pore which has a much wider diameter than the molecular size, isotherms of type IV are obtained. Type V isotherms hint that intermolecular attraction effects are large. Not all isotherms clearly belong to one group and many borderline cases occur. Furthermore, some isotherms do not fit into this classification at all.

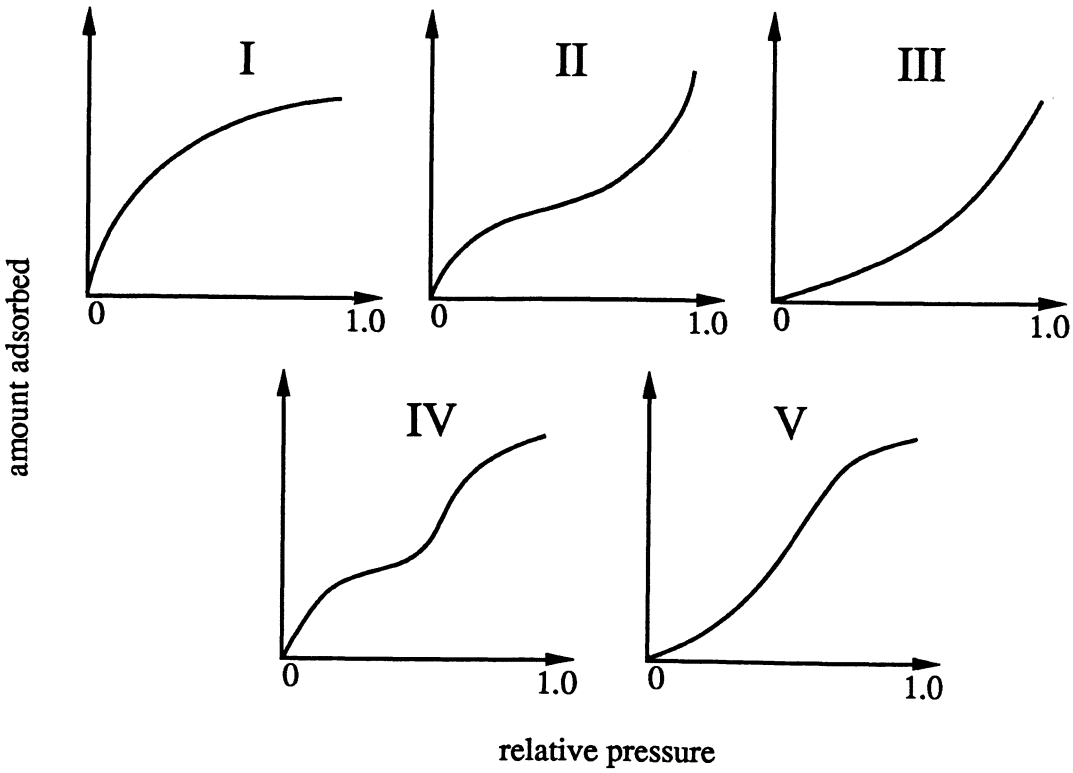

Figure 1.6 BET-classification of isotherms

1.2.4 Adsorption Hysteresis

The isotherms in Figure 1.2 and 1.6 represent true equilibrium values. In those cases, adsorption and desorption are completely reversible and one point on the curve can be obtained either by adsorption on a fresh adsorbent or by desorption from a sample with initially higher adsorbate concentration. In some cases, however, different equilibrium results are obtained, depending upon whether the sample was desorbed or adsorbed. This is called the hysteresis phenomenon and is shown in Figure 1.7. The hysteresis loop usually does not occur within the Henry's law region. When hysteresis is observed, the adsorption equilibrium pressure is always higher than that obtained by desorption.

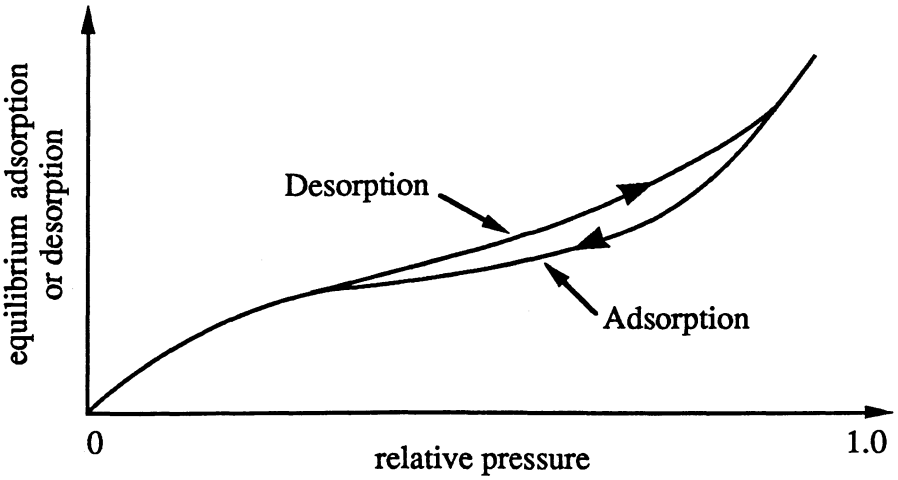

Figure 1.7 Hysteresis phenomenon

1.3 Measurement of Adsorption Isotherms

Adsorption isotherms can be determined by static or dynamic methods (section 1.3.2 and 1.3.3). In both cases, the adsorbent surface must be cleaned from previously adsorbed gases and brought to the same condition prior to each experiment in order to get accurate results.

1.3.1 Preparation of Sample

Accurate measurements of adsorption isotherms depend on the careful preparation of the adsorbent surface. All solids which have been exposed to a gas or vapor are covered with a physically adsorbed film which has to be removed in order to get reproducible results. The term "outgassing" usually applies to a procedure where the adsorbent is cleaned from initial loadings such as water vapor. "Desorption" is the term used when an adsorbent is recycled after use and previously adsorbed molecules leave the surface.

With many solids the preparation of gas free surfaces is complicated by the presence of an underlying layer of chemically adsorbed gas (section 1.1.1). In those cases not only the adsorbate molecules but also the solid surface can change its chemical structure upon forced removal of the adsorbed substance. If the chemisorbed layer cannot be entirely removed, the outgassing or desorption (from now on just referred to as "desorption") treatment must be designed so that the surface is brought to the same condition prior to each experiment. In this way, results from different runs can be compared. It is crucial that the desorption procedure is reported with each set of results. If not, the data lose much of their value because comparisons and verifications cannot be conducted.

All adsorption isotherms must start at the origin. It is therefore possible to desorb a sample completely by purging it with an inert gas like nitrogen (nitrogen can easily be adsorbed on adsorbents like charcoal at temperatures slightly above its boiling point, i.e. -196°C, it is not adsorbed at higher temperatures). By doing so, all physically adsorbed molecules will eventually leave the adsorbent surface. Since the equilibrium distribution of adsorbate molecules between fluid and solid phase is a strong function of the temperature and pressure of the system (see section 1.1), the desorption can be conveniently accelerated by raising the temperature or lowering the pressure. Both can be done at the same time. In the case of physical adsorption, a vacuum of the order of 1E-5 mmHg (1.3E-3 Pa) is generally considered to be sufficient [7]. The desorption treatment in most adsorption experiments described in the literature [e.g., 32, 33, 34] is done by means of elevated temperatures only. Because of the large number of adsorption systems, no practical manual to reproducible desorption procedures can be given. Each system has to be investigated separately.

1.3.2 Static Methods

Static methods can be divided into volumetric and gravimetric methods. In the first method, the adsorbent is placed into a dead space of accurately known volume. Successive charges of adsorbate are then admitted to the dead space from some form of volumetric measuring device such as a gas burette or pipette. Equilibrium is reached when the pressure of the gas in the dead space comes to a constant value. The amount of adsorbate remaining unadsorbed in the dead space is then calculated with the gas laws. The quantity which has been adsorbed can be computed by subtraction of the amount remaining unadsorbed from the total amount which has been admitted. A variety of procedures which allow static measurements have been described in the literature [35, 36, 37].

Gravimetric methods to determine adsorption isotherms are based on the principal of weighing the adsorbent during the adsorption process. The increase in mass can be directly related to the amount of adsorbed adsorbate molecules. The simplest method is that of intermittent weighing where the adsorbent is removed at intervals and weighed [38]. For convenience, the adsorbent is contained in a bulb which can easily be detached to the apparatus. Adsorption balances included in the experimental setup allow a continuously determination of the mass of adsorbent. Due to the small amounts of mass adsorbed, very sensitive balances have to be used. The increase in the mass of the adsorbent sample is usually in the mg range. Several suitable balances are described in the literature [39, 40, 41]. Equilibrium is reached when no further increase in the mass is detected.

Volumetric and gravimetric methods principally suffer from a decreasing accuracy with decreasing concentration of adsorbate.

1.3.3 Dynamic Methods

The term "dynamic" refers to a procedure where the adsorbate is passed in a continuous flow method through a test tube containing an adsorber bed. In its first applications [42], this method was combined with the gravimetric approach (section 1.3.2) and the attainment of adsorption equilibrium was checked by removal and weighing of the test tube containing the adsorbent. The development of gas chromatography some 40 years ago led not only to its use in analytical applications but also to the increased investigation of physicochemical processes like adsorption (chapter two). In its simplest form, a gas chromatograph used to measure adsorption isotherms consists of the test tube filled with adsorbent, a detector capable of monitoring the adsorbate concentration, and some means of setting and controlling the temperature. In such a configuration, adsorption isotherms can easily be measured since the test tube does not have to be removed to check the attainment of equilibrium. Instead, a steady detector signal indicates that equilibrium is reached. Dynamic methods suffer from a principal shortcoming: a true equilibrium such as in the case of static measurements (section 1.3.2) is not obtained since by its nature mass and heat transfer resistances are involved in the flow process. The significance of this constraint can be investigated by the use of different flowrates. Today, gas chromatographic methods are widely used to measure adsorption isotherms and in the context of adsorption the terms "dynamic method" and "gas chromatographic method" are used synonymously.

CHAPTER
TWO

The Chromatographic Method

2.1 The Place of Chromatography in Science

2.1.1 History

The earliest reported chromatographic experiments were done by Tswett [43] in 1906. He separated plant pigments by passing their solutions through columns of solid adsorbents and obtained discrete colored bands. The term "chromatography" (from greek, literally: "color writing") was coined by him. Purnell [44] said that Tswett, whose name, in Russian, means color, used the opportunity to show his sense of humor. When applied to current applications and methods, the name is a misnomer. Some 25 years after Tswetts experiments, Kuhn, Lederer and Winterstein [45] rediscovered the technique. From that time on, chromatography became considerably important, particularly in the fields of organic chemistry and biochemistry. The first thorough theoretical work on chromatography was done in 1941 by Martin and Synge [46]. Instead of liquid-solid systems they used a liquid-liquid technique (section 2.1.1) to measure partition coefficients of liquids and were in 1954 awarded the Nobel-Prize for their groundbreaking work. Their finding that paper strips could replace the columns was an astonishing result and lead to the technique of paper chromatography (section

2.1.2). In their original paper, Martin and Synge also pointed out that a gas stream could replace the flowing liquid. In 1947, Glueckauf [47] mentioned the possibility of determining adsorption isotherms from the breakthrough curves of gas-solid chromatography (section 2.1.1). Not much work was done in the field of chromatography until 1952 when James and Martin [48] reported their work on gas-liquid chromatography. This was the beginning of a rapid development of both gas-liquid and gas-solid forms of the technique. Within the next years, chromatography became a powerful method in analytical, physicochemical, and preparative applications (section 2.1.3). James and Phillips [49] were the first who used the chromatographic method to measure gas-solid adsorption isotherms.

2.1.2 Chromatographic Principles

Gas chromatography is a separation process. It can be described as the equilibration of a solute between two immiscible phases, a mobile phase and a stationary phase of large surface area. The mobile phase, either a gas or a liquid, flows over or through the stationary phase which is usually contained in a column. If the stationary phase is a solid, the separation process depends upon its adsorptive properties. Charcoal, molecular sieves, and silica gel are common solid stationary phases. In the case of a liquid stationary phase, it is spread as a thin film over an inert solid. In this case, the different equilibrium concentrations of the sample in the mobile phase and the stationary liquid are the basis for the separation process. Hence, four types of chromatographic combinations are possible. They are shown in Figure 2.1 together with some of their most important characteristics and the researchers who used that combination first.

Three modes of operating a chromatographic system exist. The operation most often carried out in analytical laboratories is the elution technique, also called "differential chromatography": a small load of solute is introduced into the inlet region of the column and its emergence at the column outlet is observed with a suitable detector. The distribution coefficient of the solute between the two phases determines how fast the solute molecules travel through the column. The solute has a higher affinity to the

Gas-Liquid Chromatography (GLC) mobile phase: gas stationary phase: liquid • most versatile and selective of all chromatographic methods (James and Martin [48]) • stationary phases are non volatile solvents on inert particles	**Gas-Solid Chromatography (GSC)** mobile phase: gas stationary phase: solid • provides easy way to determine gas-solid adsorption isotherms (James and Phillips [49]) • stationary phases are adsorbents like charcoal or molecular sieves
Liquid-Liquid Chromatography (LLC) mobile phase: liquid stationary phase: liquid • liquid-liquid systems were investigated by Martin and Synge [46] • practical applications in "paper chromatography"	**Liquid-Solid Chromatography (LSC)** mobile phase: liquid stationary phase: solid • earliest reported form of chromatography [Tswett, 43] • Tswett separated components of plant pigments

Figure 2.1 Chromatographic combinations

stationary phase than to the mobile phase and because of that its velocity will be less than that of the mobile phase. This time difference is called "retention time" and is a characteristic parameter for a given chromatographic system (mobile phase, stationary phase, solute, temperature, column geometry). If the solute is a mixture of different species, each of them migrates independently through the column. The individual bands slowly spread relative to their center of mass, approaching something close to a Gaussian distribution [44]. The different migration velocities are the cause for the separation of the components. If the composition of the sample is not known, the individual retention times can be used to identify the components. This is the basic principle of analytical applications (section 2.1.4).

Another mode of operation is that of frontal analysis (section 2.2.1): the solute concentration in the mobile phase is changed instantaneously to a new value which is provided continuously. This introduces a step-shaped concentration-time profile into the column that travels with a velocity less than that of the mobile phase. If the sample is a mixture of two or more components, the concentration-time profile splits into two or more boundaries which migrate at different velocities. This method differs from the elution operation, because a steady stream of solute has to be provided.

A third chromatographic technique is that of "displacement development". It is a combination of both the elution and frontal analysis method: a small amount of solute is introduced into the mobile phase. It is then pushed along by a third component, a displacer vapor, which is fed to the carrier gas in a constant concentration. The displacer is more strongly adsorbed to the stationary phase than the solute. An advantage of this method is that only the displacer has to be supplied in a continuous stream and a relatively

small amount of solute is sufficient to run an experiment. Also, a mixture of solutes can be investigated, provided that the displacer is more strongly adsorbed than any of the components of the mixture. As elution proceeds the individual solutes are arranged serially in the order of adsorptive strength, and they appear one by one at the column outlet.

One fact is common to all chromatographic techniques: when the solute concentration at the column inlet goes back to zero, eventually all solute molecules will leave the column. This is a direct result of the equilibrium distribution of solute between the two phases. If the stationary phase is a solid, the solute-adsorbent equilibrium distribution is expressed in the form of an adsorption isotherm (section 1.2.1). For a liquid stationary phase, solubility plots of the solute in the liquid phase represent the equilibrium distribution. In both cases, no solute will be adsorbed (or absorbed for the solute-liquid system) if the solute concentration equals zero.

2.1.3 The Chromatographic Apparatus

The basic parts of a gas chromatograph are shown in Figure 2.2. A high pressure gas cylinder serves as the source of carrier gas. A constant rate of gas flow is achieved with a pressure regulator. It assures that the inlet pressure to the column, and hence the flowrate, is uniform. In order to avoid interactions with the solute or the stationary phase, the carrier gas has to be inert. Gases in use are nitrogen, helium, hydrogen, and argon. The carrier gas has to be readily available, pure, and inexpensive.

In elution techniques, the solute is usually introduced with a syringe through a self-sealing septum. Syringes can be used for both gaseous and liquid samples. A careful injection technique is crucial for high reproducibilities [50]. Another method of

introducing the solute is that of sampling valves which have an accurately known volume. They are filled before use and bypassed in the flow system. Upon switching, the carrier gas flows through the sample loop of the valve and the solute is introduced into the system. Concentration step changes for frontal analysis operations are achieved with two-way valves which allow to switch between two continuously provided gas streams. It is essential that those devices create as little upstream flow disturbances as possible.

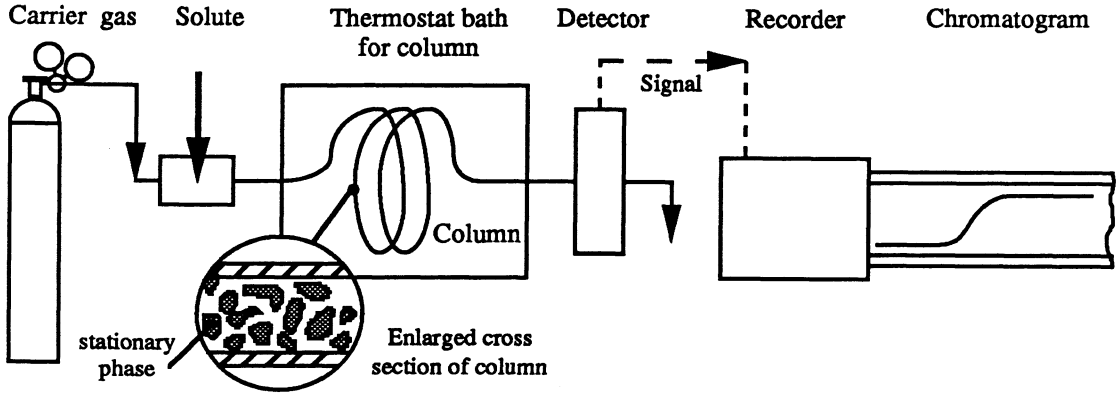

Figure 2.2 Schematic drawing of a gas chromatographic system

The column contains the stationary phase and can be made of glass or metal. In either case, the column material has to be inert. Special procedures to deactivate glass surfaces by use of hexamethyldisilazane and dimethyldichlorosilane have been described [51]. Depending on the amount of stationary phase, the column is either straight or bent in order to fit conveniently into the available thermostated space. In the case of GSC, the solid adsorbent is simply filled into the column and plugs of non-adsorbent glasswool or similar materials ensure that the packed bed is not carried away by the flowing carrier gas. In GLC, the stationary phase is a solvent spread as a thin film over inert particles.

This provides a large contact area and little pressure drop. The solvent has to be non-volatile at the temperatures of the experiment. Special oils with extremely low vapor pressures are used. The packing procedure of columns is very important. A variety of pre-packed columns is commercially available.

The detector indicates and measures the amount of solute components in the column effluent. Several operating principles can be utilized. The most common detectors are the "thermal conductivity cell" (TC) and the "flame ionization detector" (FID). The chromatographic system (solute, carrier gas) and the required characteristics determine the best choice of a detector for an application. In any case, a detector should be linear in its response to solute and insensitive to changes in flow rate of carrier gas and temperature. The detector signal is fed to a strip chart recorder. The resulting paper strips are called chromatograms. They are a permanent record of the experiment and provide the basis for qualitative and quantitative evaluations of the experiment.

Since the chromatographic process is strongly dependent on temperature, the column, the sample introduction device, and the detector have to be maintained at a constant temperature. This is either provided by thermostats baths or by placing the whole apparatus in an oven with some means of setting and controlling the temperature.

2.1.4 Applications

There are three main fields of applications for chromatographic methods:

1) Qualitative and Quantitative Analysis
2) Physicochemical Measurements
3) Preparation and Production

Every day, an innumerable number of chemical analyses is performed in laboratories throughout the world. Applications include analyses of drinking water, food and beverages, human blood, pesticide residue, steroids, petroleum products, and automotive exhausts to name just a few. Gas chromatography is one of the most powerful tools for the analytical chemist. In the field of identifying components this method competes with infrared techniques and mass spectrometry. In quantitative analyses, gas chromatography is the only method that yields extremely accurate results in little time. Furthermore, the technique is relatively simple. The combination of these advantages led to a revolution in analytical chemistry over the last 40 years. It is estimated [52] that over 2000 gas chromatographs exist on the University of Wisconsin-Madison campus alone. A wealth of textbooks and reports have been published on the subject.

Simultaneously with its explosive growth in the area of analytical disciplines, chromatography became a widely used method in physicochemical (nonanalytical) applications. A variety of physical and chemical properties can be determined with the help of chromatography. They are of three types:

1) equilibrium properties
2) kinetic and transport processes
3) miscellaneous

Equilibrium properties of physical systems include gas-solid adsorption isotherms and solubilities of gases in liquids. Phase transition processes such as latent heats and solution interactions such as activity coefficients can also be measured. Furthermore, kinetic and transport processes can be evaluated. They influence the concentration time profile of the migrating peaks and frontal boundaries which leads to the measurement of properties such as diffusivities, reaction rates, and adsorption-desorption rate constants.

A third group of properties is obtained from a variety of chromatographic parameters. Measurements of molecular weights, polymer crystallinity, and surface areas and pore size distribution of porous solid adsorbents fall into this category.

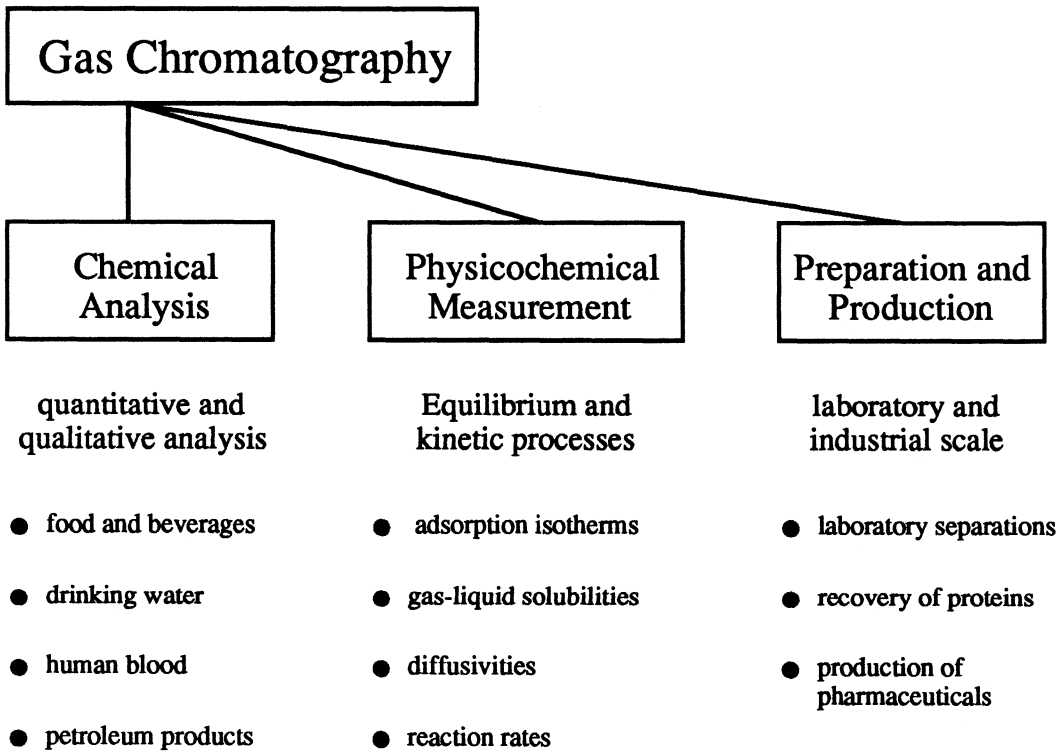

Figure 2.3 Applications of gas chromatography

Gas chromatography can also be used in applications where the separation of a sample with known content is the main objective. This is expressed in the term "preparation and production chromatography". Chromatographic separation processes are particularly attractive in the field of biochemical engineering where classical separation techniques like distillation or absorption can not be applied. A chromatographic separation is very effective but wasteful of both hardware (column) and stationary bed

(the separation agent) because the bulk of the column is free of solute at all stages of the separation. This makes chromatographic separations economically unfeasible from the industrially important standpoints of equipment productivity. On the other hand, adsorptive chromatographic separations are almost ideal at the laboratory scale where equipment productivity is of secondary importance. Figure 2.3 gives a graphical overview of chromatographic applications as outlined in this section.

2.2 Techniques of Measuring Isotherms

2.2.1 Frontal Analysis

A simple method of obtaining gas-solid adsorption isotherms was introduced by James and Phillips [49] in 1954 (section 2.1.1). In this method, pure carrier gas is initially passed through the column. At some time t_0 the carrier gas is replaced by a continuous stream of a mixture of carrier gas and solute vapor at a constant concentration. This leads to a step change in the concentration-time profile of the solute ($dc/dt \rightarrow \infty$), also called "front boundary". The boundary is carried by the mobile phase through the column. Due to the chromatographic principle (section 2.1.2), the solute is held back in the column. The time delay until its emergence at the column outlet, compared to the time pure carrier gas stays in the column, depends on the distribution coefficient of the solute between mobile phase (carrier gas) and stationary phase (solid adsorbent). At a time t_1 the boundary reaches the end of the column. The term "breakthrough" describes this phenomenon. After the breakthrough the solute outlet concentration equals the solute inlet concentration. The time delay of the solute breakthrough, also called retention time, t_R, is obtained by subtracting the travel time of pure carrier gas, t_M from the time the

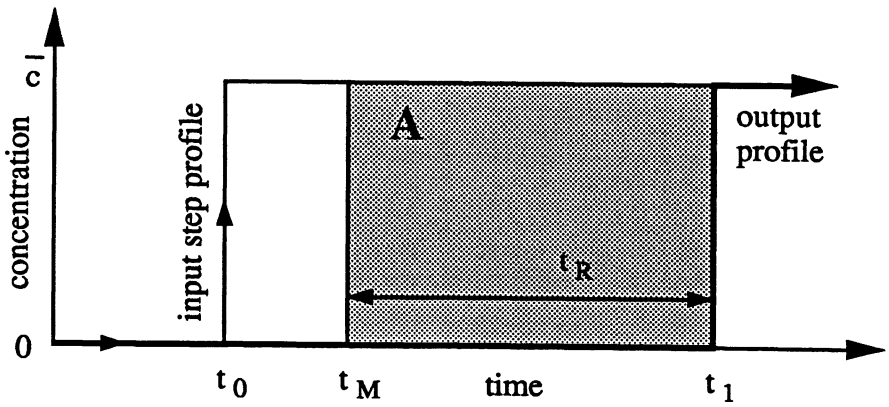

Figure 2.4 Front boundary

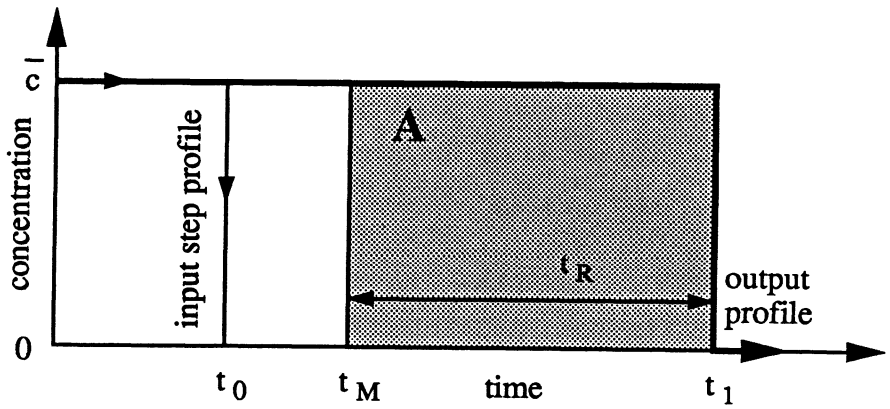

Figure 2.5 Rear boundary

solute stays in the column. Figure 2.4 shows a front boundary for an idealized case where the output is also a step.

When the mixture of carrier gas and solute is replaced by pure carrier gas, a "rear boundary" ($dc/dt \rightarrow -\infty$) is introduced into the system (Figure 2.5). Again, this boundary travels more slowly through the column than pure carrier gas would. At a time t_1, the rear boundary reaches the end of the column and the solute concentration goes back to zero.

The amount of solute adsorbed on the column packing (solid adsorbent) is directly proportional to the shaded areas in Figure 2.4 and 2.5. The total number of moles of solute, n, held by the stationary phase is given by

$$n = \bar{c}\ t_R\ F \tag{2.1}$$

where $\bar{c}$ represents the solute concentration in the mobile phase in units of moles per volume (the bar stands for the "plateau" value), t_R the retention time of solute, and F the volumetric flowrate of the mobile phase. The concentration of solute in the stationary phase in units of moles per mass of adsorbent, q, is obtained by dividing equation 2.1 through the mass of stationary phase, m

$$q = \frac{\bar{c}\ t_R F}{m} \tag{2.2}$$

Since the product of $\bar{c}$ and t_R is identical with the shaded areas A in Figure 2.4 and 2.5, one can also write

$$q = \frac{A F}{m} \tag{2.3}$$

If q is plotted versus $\bar{c}$, one point of the adsorption isotherm is obtained. The complete isotherm is determined by making runs at different solute concentrations, measuring the area A, and calculating q in each case.

The method described so far is an ideal case called "ideal chromatography" where the input concentration-time profile does not change as it migrates through the packed bed. In reality, several physical processes cause the step-shaped input profile to change into a diffuse boundary as it travels along the column (Figure 2.6). These are axial diffusion, non-equilibrium due to resistance to mass transfer between solute and stationary phase, and a non-uniform flow distribution in the packed bed. Figure 2.7 shows a diffuse

frontal boundary developed from a step shaped input profile. A mathematical description of the boundary spreading processes was given by van Deemter [53]. If the diffuse

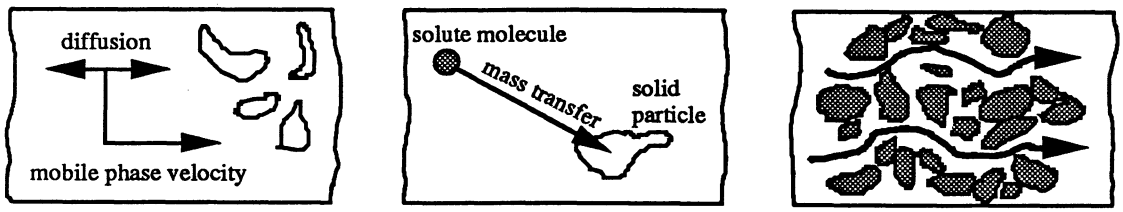

Figure 2.6 Boundary spreading processes

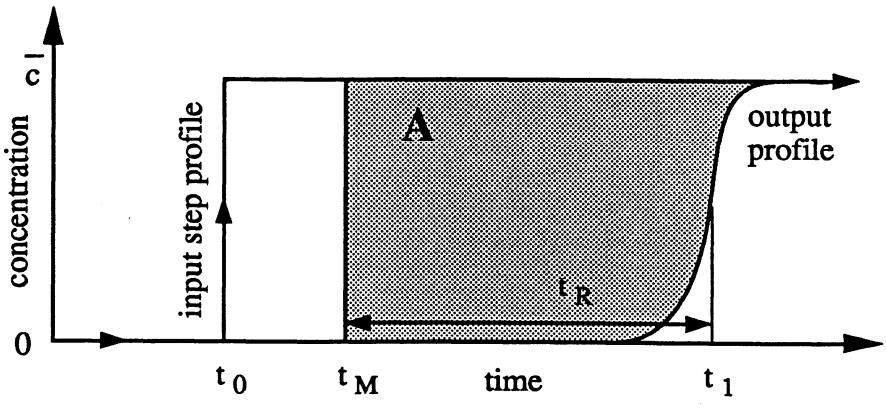

Figure 2.7 Diffuse frontal boundary

boundary is spread symmetrically (this is the case for a first approximation), the retention time of the inflection point can be used to determine t_R in equation 2.2, as shown in Figure 2.7. If the isotherm is obtained by measuring the area A (equation 2.3) no restriction to symmetrically shaped boundaries is given. The area A which has to be used in equation 2.3 is shaded in Figure 2.7.

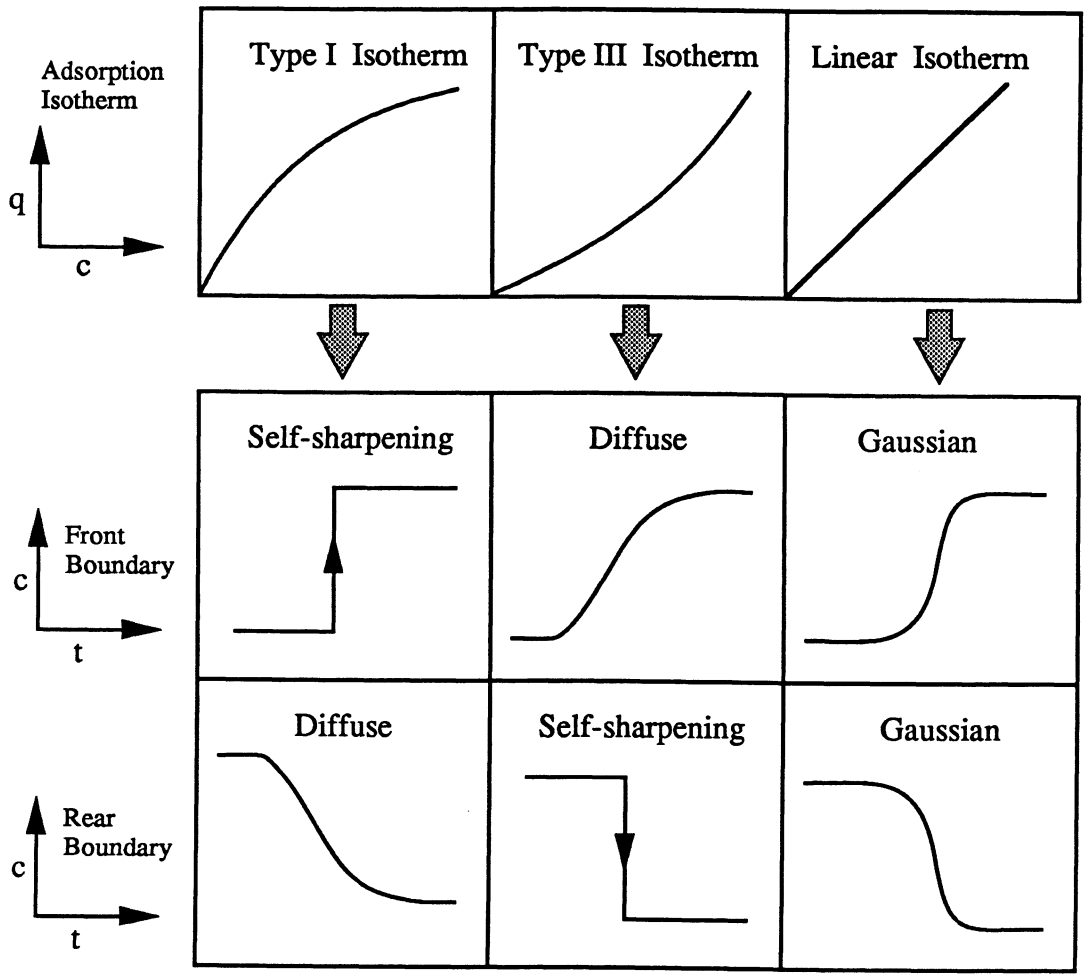

Figure 2.8 Relationship between shape of adsorption isotherm and concentration-time profile at column outlet

The boundary profile depends also (in addition to the boundary spreading processes of axial diffusion, non-equilibrium, and non-uniform flow distribution) on the shape of the adsorption isotherm (section 1.2.3). This relationship is shown in Figure 2.8. In the case of a type I isotherm (Langmuir type, section 1.2.2) front boundaries will have an inherent self-sharpening mechanism. The explanation is as follows: regions of high

solute concentrations tend to be less strongly adsorbed (the slope of the adsorption isotherm decreases with increasing solute concentration). Because of this, regions of strongly adsorbed low solute concentrations diffusing in the flow direction "wait" for the following solute molecules which are less strongly adsorbed. The same mechanism causes rear boundaries of a type I isotherm system to be diffuse. Adsorption systems following type III isotherms exhibit the opposite behavior: front boundaries are diffuse and rear boundaries are self-sharpening.

As stated above, the dependence of the boundary profile on the shape of the adsorption isotherm is independent of the boundary spreading influences of axial diffusion, non-equilibrium, and non-uniform flow distribution. In the case of boundaries with an inherent self sharpening mechanism, the effect competes with the boundary spreading processes. Boundaries that tend to be diffuse will be even more diffuse due to the boundary spreading processes. For linear isotherms, only the boundary spreading processes influence the concentration-time profile of the migrating boundary (Figure 2.8).

2.2.2 Characteristic Point Methods

In this technique, a complete isotherm is derived from the breakthrough curve of one frontal analysis experiment. The method was first described by Conder and Purnell [54] and later reviewed by Conder and Young [55] and Laub and Pecsok [56]. It can only be applied to diffuse boundaries. The main principle of this method is that of so-called "characteristic points". These are points of fixed concentration. Conder and Young [55] describe the idea as " ... (the method) describes the progress of a point of fixed concentration c on a boundary as the boundary moves through the column". Their

thorough mathematical analysis shows that this velocity depends on the slope of the adsorption isotherms at that concentration. Hence, different migration velocities from points of fixed concentration determine the slope of the isotherm. If the method is applied to many characteristic points, a complete isotherm can be constructed from the slopes of individual points. Solute-adsorbent configurations that yield linear adsorption isotherms and experimental techniques that lead to self-sharpening boundaries (section 2.2.1) can not be used for the "frontal analysis by characteristic point" method (FACP) because it is contrary to the basic idea of the technique.

Similar to the FACP method is the "elution by characteristic point" technique (ECP), introduced by Cremer, Huber, and Keulemans [57, 58, 59, 60]. As with FACP, only a single experimental run is required to determine a complete isotherm. In ECP, the diffuse boundary is produced by a large elution peak. The two sides of the peak can be treated as two frontal boundaries. Depending on the isotherm shape, one boundary is diffuse and can be used for calculations based on the FACP method.

2.2.3 Perturbation Techniques

In these methods, the column is first brought into equilibrium with a flowing gas mixture (carrier and solute) at the solute concentration of interest. This creates a steady detector signal and the term "plateau" describes the elevated position of the recorder pen. A small sample of solute is then injected into the column, giving the name to the technique "elution on a plateau". The concentration of the elution peak is infinitesimally greater or smaller than that of the plateau concentration (Figure 2.9). The concentration pulse constitutes a disturbance to the system. Because of that, the method is also called "perturbation technique". Reilley, Hildebrand, and Ashley were the first who suggested

this method [61]. Since the concentration of the pulse is very close to that of the plateau, the peak migrates with nearly constant concentration through the column. A second perturbation technique is the tracer-pulse method. Here it is not a small concentration pulse that disturbs the column but a small sample of detectable isotope of the solute.

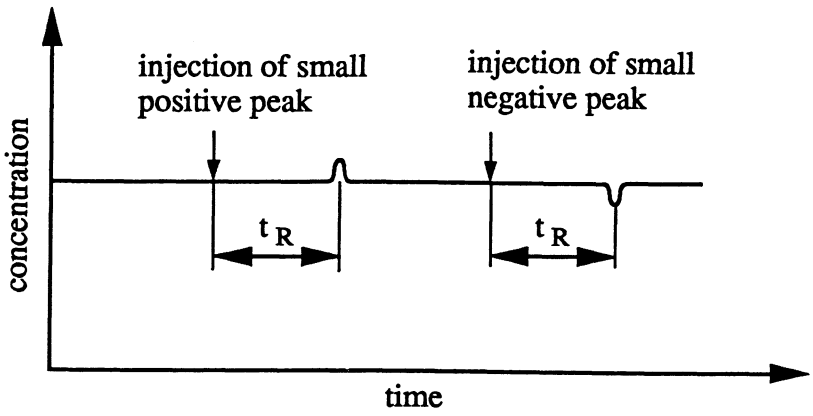

Figure 2.9 Perturbation with small elution peaks

2.2.4 Evaluation of the Different Methods

This study is concerned with the measurement of low concentration adsorption isotherms. The solute concentrations investigated range from approximately 2 to 50 parts per million. At these low surface coverages, Langmuir's model (section 1.2.2) predicts nearly linear adsorption isotherms.

Characteristic point methods (FACP, ECP) are not applicable for solute adsorbent systems that yield linear isotherms. Hence, the time saving potential of these techniques (only one breakthrough curve from a frontal analysis experiment gives a complete isotherm) can not be utilized in this study.

In the low concentration range of solutes, perturbation techniques offer no advantage over frontal analysis methods. The virtue of perturbation methods (where the

boundaries travel with nearly constant concentrations) lies in the fact that the influence of the so-called "sorption effect" diminishes. The sorption effect describes the change of velocity of a migrating boundary due to the flux of solute molecules from the mobile phase to the adsorbent. At the solute concentration of interest in this study, the influence of the sorption effect on the retention time is orders of magnitude smaller than the expected experimental error.

For the objective of this study, frontal analysis techniques are the methods of choice to experimentally obtain adsorption isotherms.

CHAPTER
THREE

Experimental

3.1 The Experimental Apparatus

Figure 3.1 shows a schematic drawing of the flow system used in this study. This section gives a brief overview of the operating principle. Sections 3.1.1 to 3.1.9 will discuss the individual parts in detail. The frontal analysis measurement procedure is described in section 3.2.

The main parts of the experimental equipment are a Hewlett-Packard 5890 SERIES II (hereafter referred to as HP 5890) gas chromatograph (19), a Hewlett-Packard 3396A electronic integrator (22), an analog to digital converter (20), and an Apple IIe personal computer (21). The solute-nitrogen mixture of constant concentration is contained in a high pressure gas cylinder (4). A two stage pressure regulator (7) with a stainless steel diaphragm reduces the very high source pressure (above 2000 psi) to the pressure used by the instruments and provides a constant outlet pressure as the pressure in the cylinder decreases. Two pressure gauges indicate the cylinder pressure and the delivery pressure to the flow system respectively. The pressure regulator also incorporates an on/off valve. All other gas cylinders use the same type of pressure regulator described above. The solute-nitrogen mixture is diluted with a stream of pure nitrogen (3). Hence, lower solute

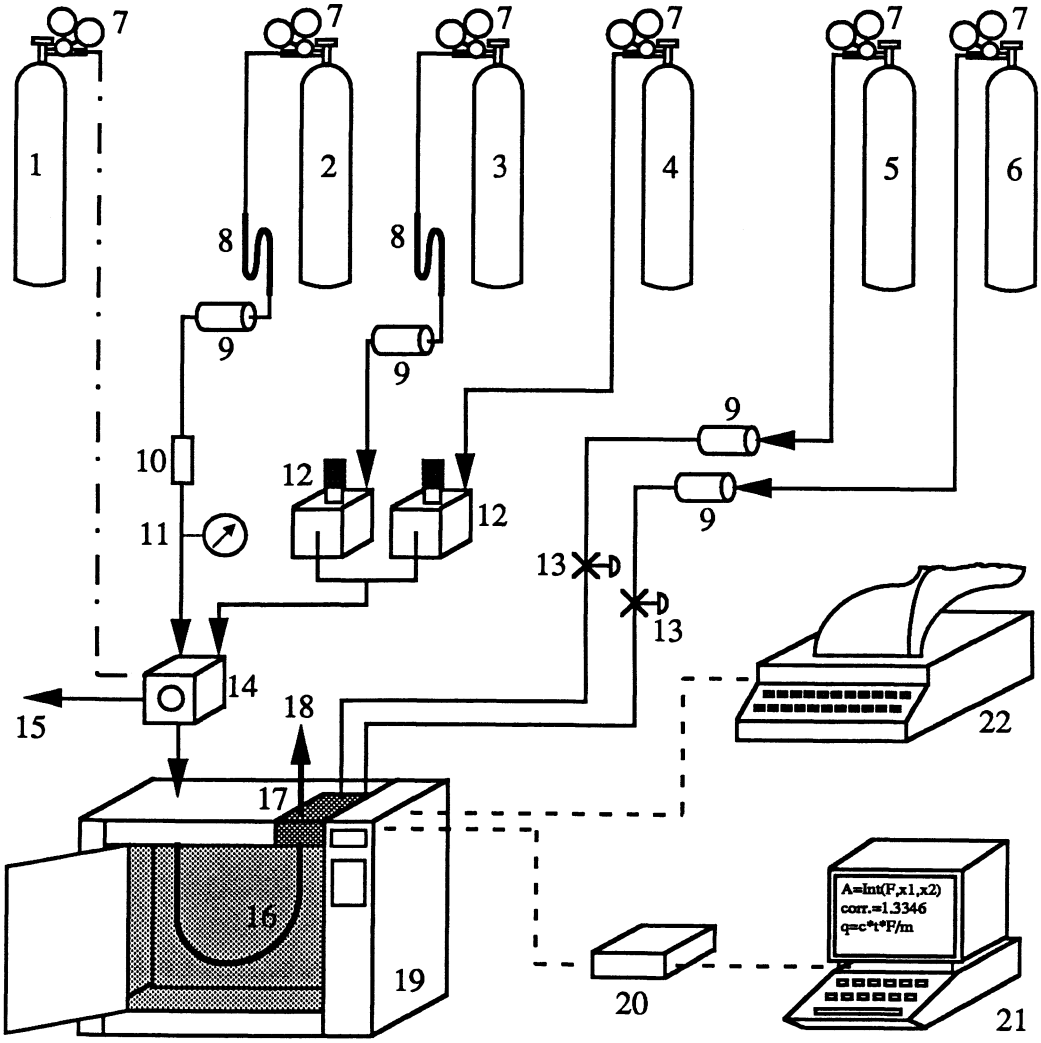

1. compressed air
2. carrier gas
3. nitrogen diluent
4. solute-nitrogen mixture
5. compressed air
6. hydrogen
7. pressure regulator
8. hydrocarbon filter
9. moisture trap
10. hydrocarbon trap
11. pressure gauge
12. flow controller
13. on/off valves
14. two-stream selection valve
15. vent to atmosphere
16. glass column
17. flame ionization detector
18. detector exhaust
19. gas chromatograph
20. A/D converter
21. personal computer
22. electronic integrator

Figure 3.1 Flow system

concentrations than that in the solute-nitrogen cylinder can be achieved, depending on the ratio of the two flowrates. A second gas cylinder with pure nitrogen serves as the source of carrier gas (2). Both nitrogen sources have a purity of 99.996+% by volume as reported on the cylinder.

After flowing out of the gas cylinders, both nitrogen diluent and nitrogen carrier gas are passed through a hydrocarbon filter (8) and a moisture trap (9). The s-shaped hydrocarbon filter contains 30/60 mesh activated charcoal in a metal casing and purges residue organics from the nitrogen. The moisture traps remove water vapor from the gas streams. The color of the adsorbing particles inside the transparent casing of the moisture traps indicate the degree of saturation. The nitrogen carrier gas flows through an additional hydrocarbon trap (10).

The flowrates of the solute-nitrogen mixture and the nitrogen diluent are set with two flow controllers (12) designed to give constant volumetric flowrates even if the upstream pressure changes slightly. A pneumatically driven two-stream selection valve (14) allows the operator to select between the two continuously provided gas streams of nitrogen carrier gas and solute-nitrogen mixture respectively. One gas stream is directed towards the column, the other is vented to the atmosphere (15). The adsorbent bed is contained in a glass column (16) which is mounted inside a temperature controlled zone in the HP 5890 gas chromatograph (19). The hydrocarbon filter (10), the pressure gauge (11), and the two-stream selection valve (14) are also located in the HP 5890 gas chromatograph but for clarity purposes, they are drawn separately in Figure 3.1.

The solute concentration in the column effluent is monitored and measured with a flame ionization detector (FID) (17). This detector burns the emerging gases in a hydrogen-air flame. Hydrogen and air are provided from high pressure steel cylinders

(5, 6). Moisture traps identical with those used for the nitrogen streams dehumidify the hydrogen and air streams. The FID response is a voltage which is proportional to the solute concentration in the column effluent. This detector signal is fed to an analog to digital converter (A/D converter) (20) and, independently, to an electronic integrator (22). The analog to digital converter translates the analog detector signal into a digital signal which can be processed by and stored on the disk drive of a personal computer.

Standard 1/8 inch outer diameter copper tubing is used for the flow connections between gas cylinders, hydrocarbon and moisture traps, and the flow controller. The two-stream selection valve and the column inlet inside the gas chromatograph are connected via 1/16 inch outer diameter stainless steel tubing. The connections between the individual parts are sealed with teflon tape and checked for leaks. The pneumatically driven two-stream selection valve is connected with the compressed air cylinder via a tygon hose.

3.1.1 Adsorbate Supply

The solute-nitrogen mixtures studied in this work were custom made from Matheson, a commercial gas products company. The mixtures were contained in standard full-sized steel or aluminum cylinders at pressures above 2000 psi. The manufacturer reported the solute concentration and its tolerance in parts per million (ppm) by volume on the cylinder. A typical label is shown in Figure 3.2. The gas products company called the mixtures "certified standards" and described the preparation process as follows: "certified standards are calibration gas mixtures prepared by a variety of gravimetric, partial pressure, and volumetric techniques. Component certification is provided through the use of NBS standard reference materials, primary standards, certified weights, or wet

chemical methods.". In this study, the reported concentrations and its tolerances were assumed to be correct. No verification was done.

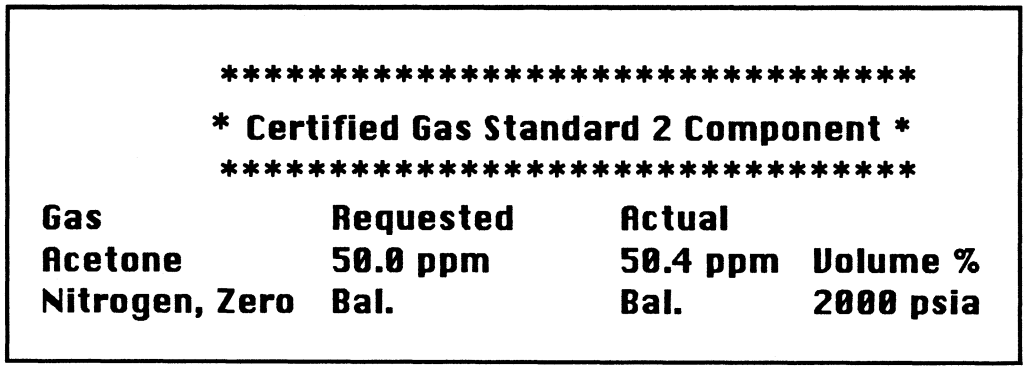

Figure 3.2 Typical label on the gas cylinder of an acetone-nitrogen mixture

3.1.2 The Gas Chromatograph

The HP 5890 gas chromatograph is the central part of the flow system. Its main function is the temperature control of the column which is mounted inside an oven-like compartment. Figure 3.3 shows a sketch of the device. The gas chromatograph also contains the flame ionization detector and several other parts of the flow system. These are the two-stream selection valve, the hydrocarbon trap, flow controller and pressure gauge for carrier gas, and on/off valves for the hydrogen and air supply to the flame ionization detector.

Originally, the oven temperature could be set from room temperature up to 450°C in increments of 1°C (an optional cryogenic cooling using liquid nitrogen allows subambient control down to -80°C). The two-stream selection valve which was used in this study (an optional feature) limits the available temperature range from room

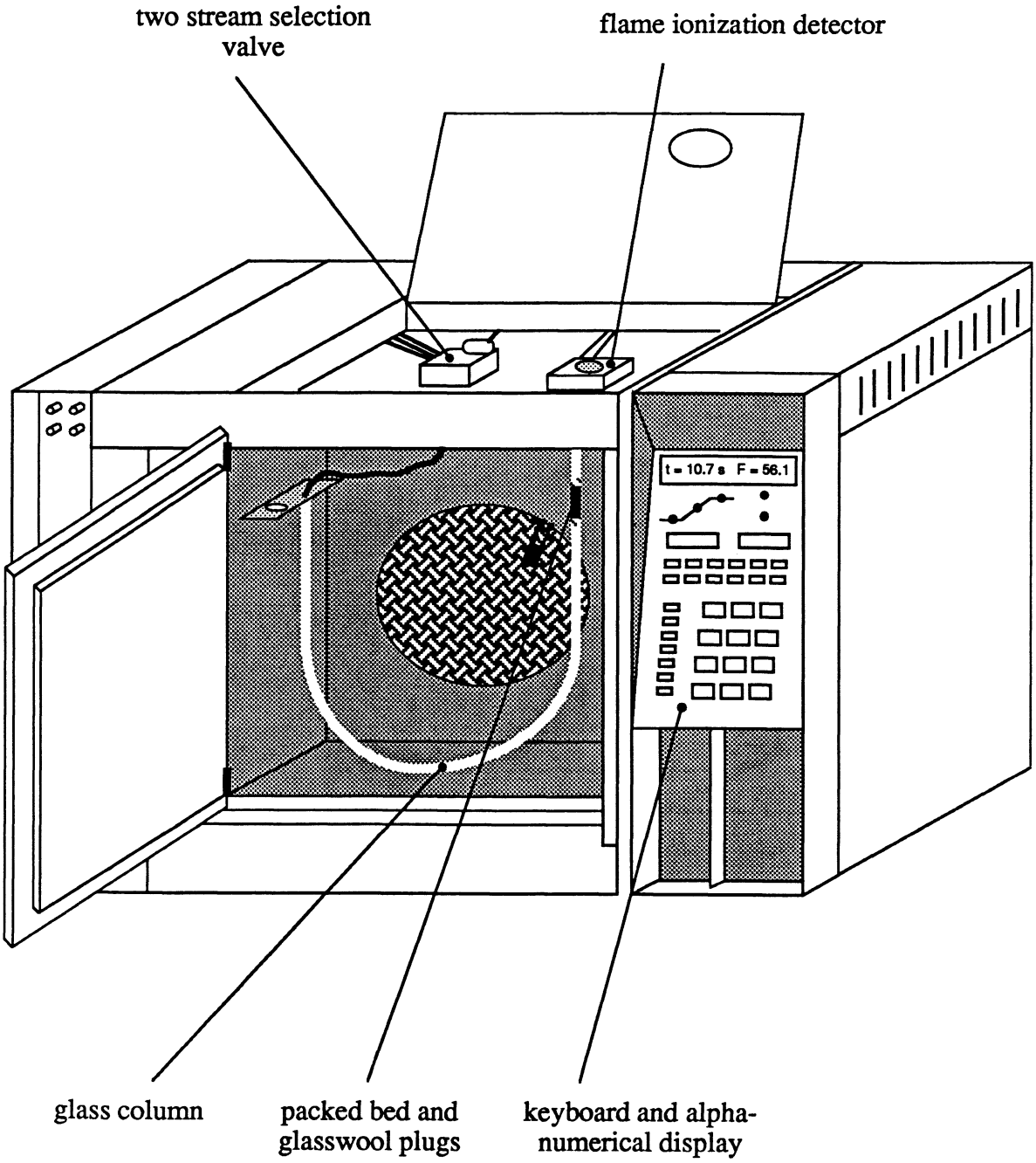

Figure 3.3 HP 5890 gas chromatograph

temperature to 175°C. The detector temperature can be controlled independently from the oven temperature from room temperature to 400°C.

An equilibrium time feature for both temperature controlled zones (oven and detector) indicates the elapsed time from the moment the actual temperature comes within 1°C of the temperature setting. It does not account for actual heat transfer mechanisms inside the temperature controlled zone (e.g., the column temperature compared to the oven temperature) but after a sufficiently long equilibrium time it can be assumed that the temperature of the adsorbent bed is equal with the temperature in the oven-like compartment.

A keyboard together with an alphanumerical display is used to control all functions of the apparatus such as the temperatures of the oven and detector, the detector signal, and the position of the two-stream selection valve. The alphanumerical display and the keyboard can also be used as a stopwatch for the measurement of flowrates with a soap film flowmeter (section 3.1.8).

3.1.3 Column and Column Packing

The columns used in this study were made of glass with an outer diameter of 1/4 inch and an inner diameter of approximately 1/8 inch. They were custom made from a scientific glass apparatus company. A tight connection to the fittings inside the gas chromatograph was provided with ferrules (Figure 3.4a). Two different ferrule materials were used in this study, teflon and graphite. The teflon ferrules were relatively soft and could not be reused after a connection was made. The graphite ferrules were more durable than the teflon ferrules and were used two or three times.

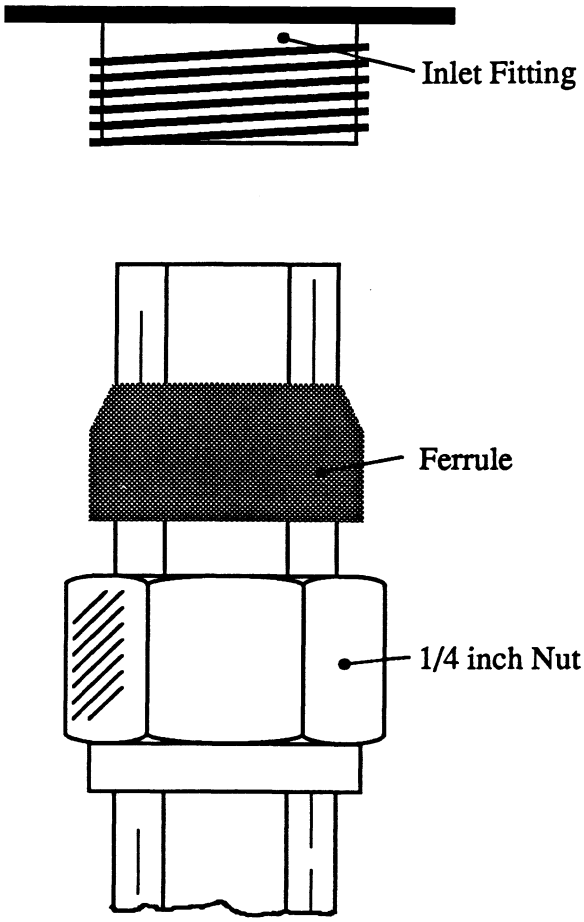

Figure 3.4a column connection to inlet fitting

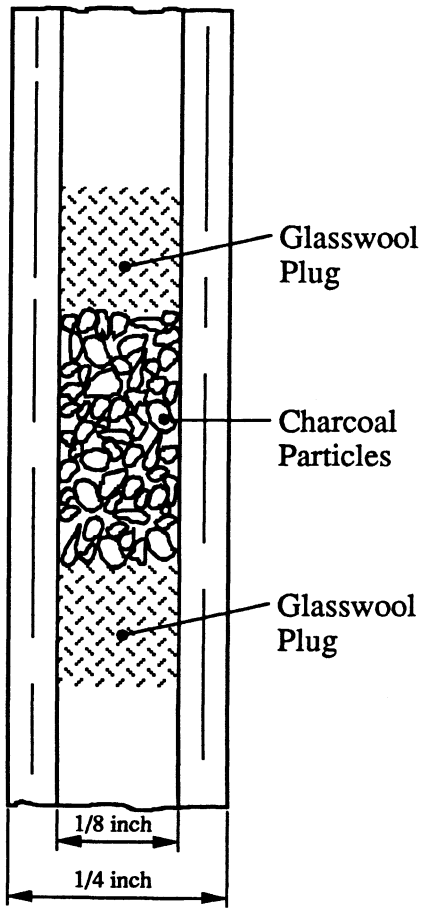

Figure 3.4b part of glass column containing packed be

Figure 3.4b shows the part of a glass column containing the packed bed. The glasswool plugs are used to conserve the shape of the packed bed and to prevent the charcoal particles from being carried away by the flowing gas. The glasswool used in this study was deactivated with silane (Hewlett Packard, #5080-8764). Before packing, the empty column was thoroughly rinsed with acetone and allowed to dry over night. The mass of charcoal was weighed with an analytical balance which had an accuracy of 1 milligram. Non-adhesive weighing paper was used. After the filling process, the

columns were sealed with end caps to ensure that no adsorption of atmospheric gases took place.

3.1.4 The Flame Ionization Detector

The flame ionization detector (FID) monitors and measures the concentration of solute in the column effluent. A schematic drawing of the device is shown in Figure 3.5. The FID responds with an electrical signal to compounds that contain CH-groups and produce ions when burned in a hydrogen-air flame [62]. Some molecules in the flame

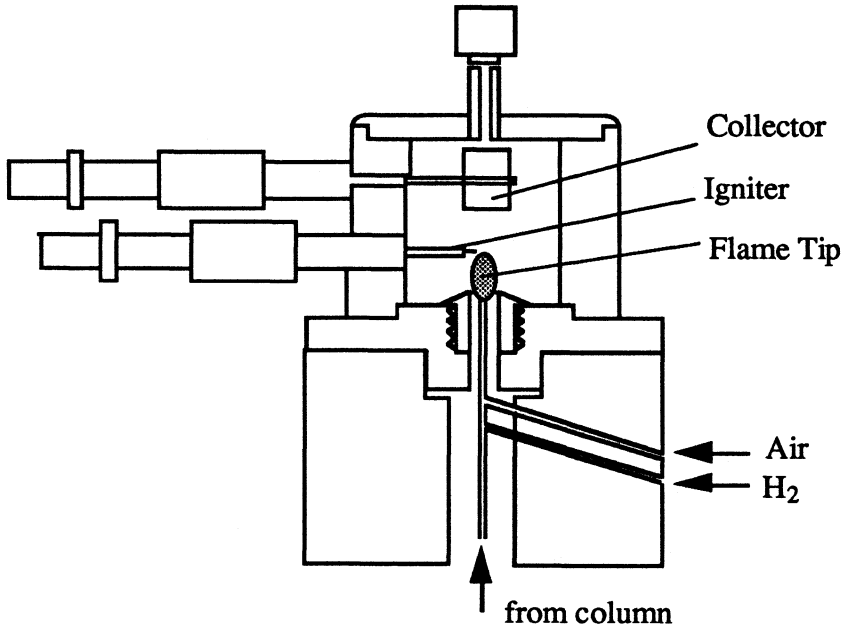

Figure 3.5 Flame ionization detector

acquire sufficient energy to ionize. Because of this, the conductivity of the flame increases and the change is a direct measure for the solute concentration. All organic compounds produce a signal, although a few (e.g., formic acid, acetaldehyde,

formaldehyde) exhibit poor sensitivity. Inorganic compounds producing little or no response include nitrogen, carbon dioxide, helium, and water (Table 3.1). This insensitivity to gases such as nitrogen and helium leads to their use as carrier gases in chromatographic systems with flame ionization detectors.

Table 3.1 Inorganic compounds producing little or no response in a flame ionization detector

He	CS_2	NH_3
Ar	COS	CO
Kr	H_2S	CO_2
Ne	SO_2	H_2O
Xe	NO	$SiCl_4$
O_2	N_2O	$SiHCl_3$
N_2	NO_2	SiF_4

The output signal is directly proportional to the concentration of the organic compound. A flame ionization detector has the widest linear range of any detector used in gas chromatography. It reaches from the minimum detectable limit through concentrations greater than 10^7 times the minimum detectable limit [50]. The linearity of the detector used in this study was tested by plotting its signal versus the concentration of solute (Figure 3.6).

A high detector sensitivity is desired in a chromatographic system designed for low concentration measurements. In addition to the detector geometry, the FID sensitivity depends upon the temperature and the flow rates of air, hydrogen, and the inert

component in which the solute is diluted (nitrogen). For maximum sensitivity, a standard sample of solute of interest in the concentration range expected is analyzed. By experimenting with different flowrates, the settings giving maximum response can be determined. This procedure has been described as "peaking the burner" [50]. The detector used in this study was very sensitive to the hydrogen flowrate. Figure 3.7 shows the detector signal for different hydrogen flowrates. A clear maximum is given for flowrates of approximately 60 ml/min. This setting was used for the measurements in this study.

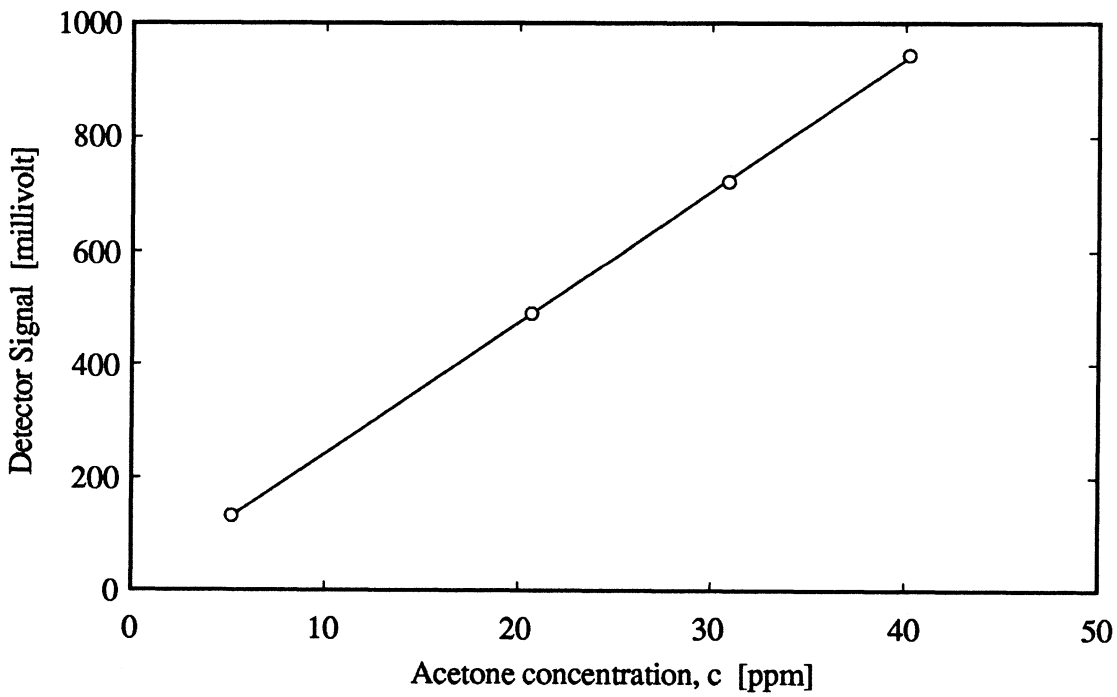

Figure 3.6 Linearity of the detector signal

A change in the air flowrate had very little influence on the detector signal (provided the air flowrates were greater than approximately 300 ml/min). After this optimizing

procedure, the flowrates of hydrogen and air were simply controlled by setting their respective pressures at the pressure regulators. The linear characteristic of a flame ionization detector is not constrained to its operation at maximum sensitivity.

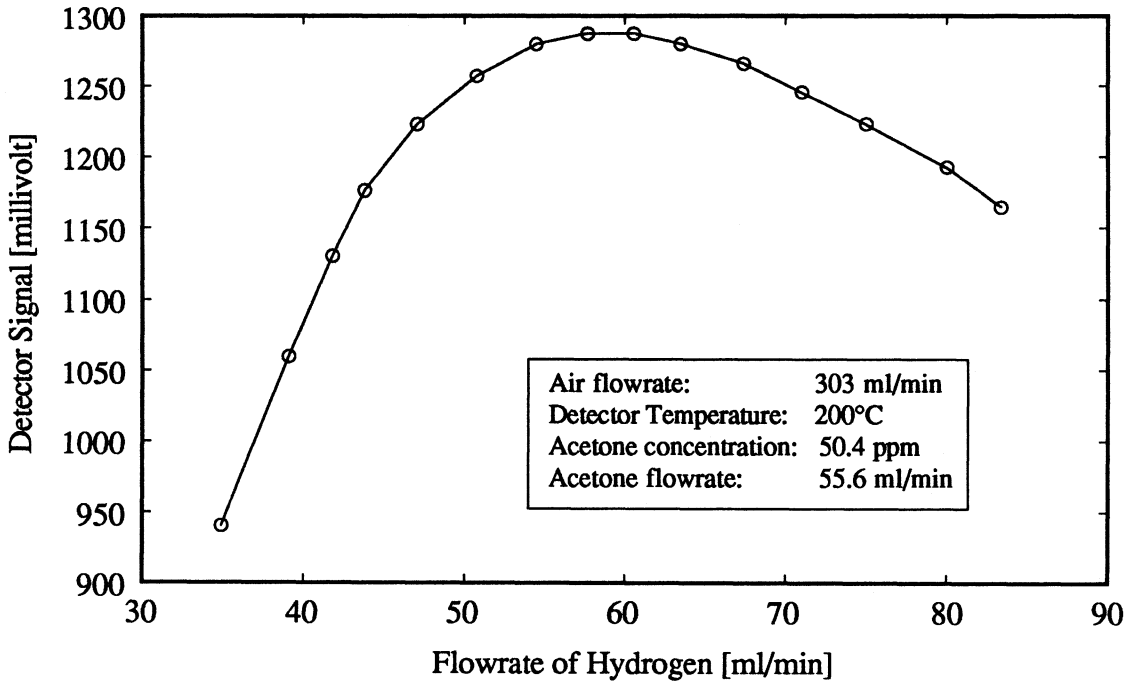

Figure 3.7 Detector sensitivity as a function of the hydrogen flowrate

The flow rates of the solute-nitrogen mixtures were limited to approximately 60 ml/min, otherwise the flame was blown out. The flame was ignited with an electrical resistance element. The ignition of the flame can be checked by the displayed detector signal (on the alphanumerical display of the HP 5890 gas chromatograph) or by holding a blank metal surface (e.g., a wrench) over the detector exhaust. The water vapor (from the combustion of hydrogen and oxygen) condenses upon the surface and indicates a burning flame.

3.1.5 Data Acquisition

An eight channel 14 bit analog to digital converter (A/D converter), manufactured by Strawberry Tree Computers, was used to change the (analog) detector output into a digital signal by changing the analog signal into a series of 0's and 1's that approximate the number. The number of bits in the approximation determines how accurate the translation process is. The 14 bit converter used in this study resolves one count out of two raised to the 14th power. Hence, the resolution of the device is 1/16384 or 0.006%. One channel of the analog to digital converter was connected to one detector output cable (the other detector output cable was connected to the electronic integrator), the other seven channels were not used.

The converted data was displayed on the screen of the Apple IIe personal computer and stored on a disk in the disk drive of it. The data logging intervals could be set from 10 seconds on up to any desired value. Two columns of data were recorded on the disk, the time and the corresponding digital signal. In its original version, all eight channels were recorded on the disk at each data logging interval even though only one channel was used. In order to fully utilize the limited disk space, a change in the source code of the software controlling the data logging process was made to ensure that only the signal of the connected channel and the corresponding time was stored on the disk.

As mentioned earlier, two separate analog output signals are provided by the flame ionization detector, one of which is sent to the electronic integrator (section 3.1.6) the other to the A/D converter. For both connections, the analog output level ranges from 0 to 1 volt. All detector signals from one experiment have to be translated into an output signal between 0 and 1 volt, also called "dynamic range". A signal attenuation option

allows sizing the signal output so that the largest signal of interest during a run does not exceed 1 volt. Fourteen different attenuation setpoints are possible. A setpoint of "0" means that the detector signal is not adjusted before it is sent to the analog to digital converter. In this case, a detector signal of 800 mV (0.8 V) will be sent as 800 mV to the A/D converter. If the detector signal goes up to 1600 mV (1.6 V) parts of the information are lost because the signal sent to the A/D converter can not exceed 1 volt. Each step to a higher attenuation setpoint value decreases the output signal level by a factor of two.

$$\text{signal sent to ADC} = \frac{\text{detector signal}}{2^{\text{attenuation}}} \tag{3.1}$$

To minimize the operational error for the A/D converter, the attenuation should be set to the lowest value possible, provided the largest occuring signal does not exceed 1 volt.

3.1.6 The Electronic Integrator

A Hewlett-Packard 3396A electronic integrator was used to obtain concentration versus time plots (breakthrough curves) of the frontal analysis experiments. When purchased, this device was thought to be capable of obtaining the composite area A of chromatograms as described in section 2.2.1. Since the integrator is specifically designed for applications in analytical chemistry where the elution chromatographic technique is predominant, the integrator was not able to determine the area A as shown in Figure 2.4 and 2.7. Because of this, the analog to digital converter was added to the experimental equipment and the area A was determined by means of numerical integration. The integrator served only as a x-y plotter.

3.1.7 Flow Control

Two adjustable flow controllers were used to set the flowrates of the solute-nitrogen mixture and the nitrogen diluent gas respectively. These flow controller are continuously adjustable from flowrates of a few ml/min to over 1000 ml/min. They have a linear characteristic of the stem position versus flow what permits a direct reading of the flow adjustment by use of conventional turns counting. The release of volatile chemicals is eliminated by the use of stainless steel diaphragms. Both flow controllers are mounted into an aluminum chassis.

3.1.8 The Soap Film Flow Meter

The flow rates of gases were measured with a soap film meter (Figure 3.8). It is an absolute instrument and requires no calibration. The flow rate is measured as follows: the rubber hose is attached to the outlet of the detector. A specifically designed adapter with a silicone O-ring ensures a sealed connection. The rubber bulb is filled with a soap solution. This is either pure water with a small amount of detergent or commercially available "Snoop" leak detection solution. Upon squeezing of the rubber bulb the soap solution covers the side inlet and a soap bubble forms and is carried up in the instrument. A stopwatch is used to determine the time it takes to travel a distance representing a calibrated volume. The flowrate is calculated by dividing the volume by the measured time. The soap film meter used in this study had three calibrated volume marks, 1 ml, 10 ml, and 100 ml. The tube had to be wetted thoroughly before a measurement. The accuracy of the flow-measurements is described in the uncertainty analysis (appendix A.1).

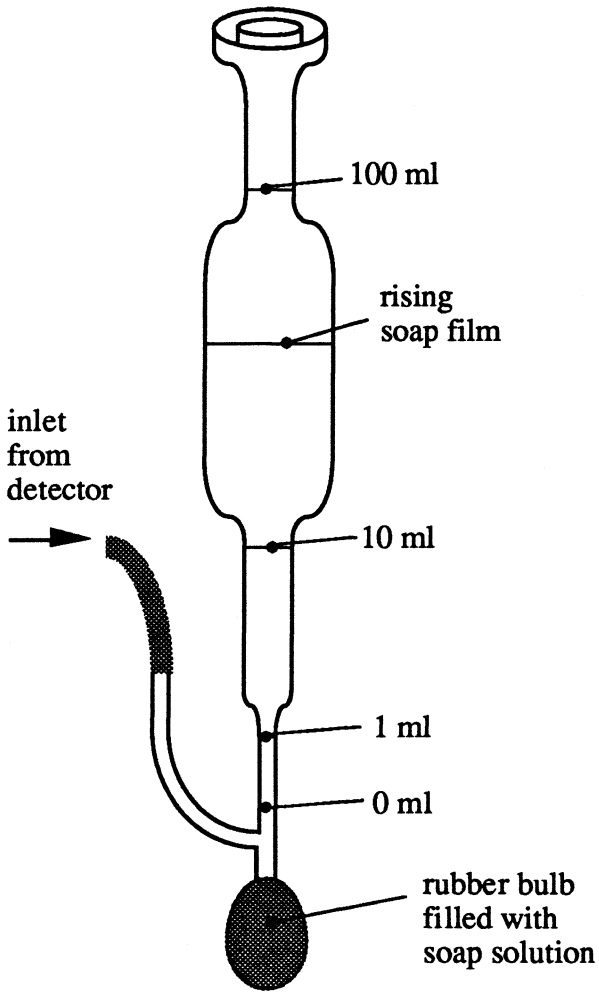

Figure 3.8 Soap film flowmeter

3.1.9 The Two-Stream Selection Valve

The switching valve is located at the top part of the gas chromatograph. It allows to switch between two continuously provided gas streams, one of which is the solute-nitrogen mixture, the other the carrier gas. The operating principle is shown in Figure 3.9. The valve is driven pneumatically. In the "off" -position, carrier gas flows to the column and the solute-nitrogen stream is vented. If the valve is in the "on"-position, the

solute-nitrogen mixture is directed towards the column and the carrier gas is vented. The desired position can be controlled from the keyboard of the gas chromatograph.

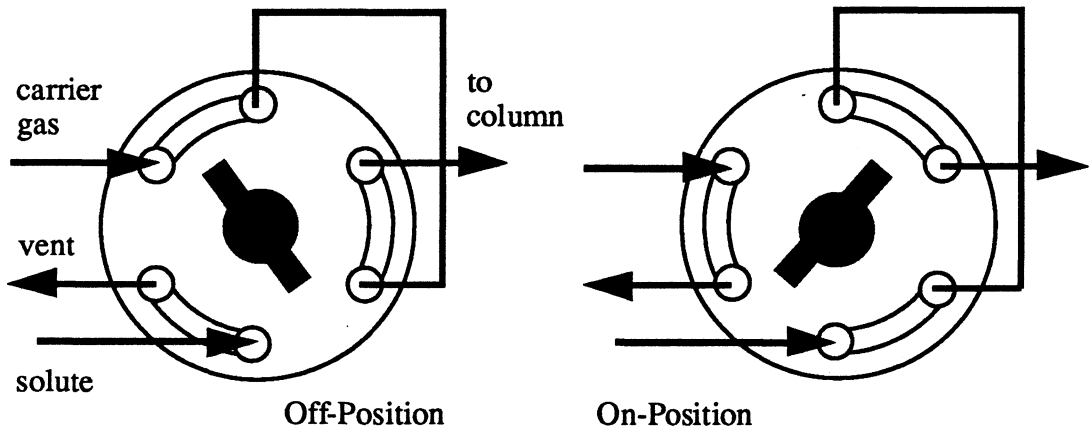

Figure 3.9 Two-stream selection valve

3.2 Experimental Procedure

This section describes the procedure of a frontal analysis experiment in detail. Section 3.2.1 summarizes the process in form of an "operating manual". The calculation of adsorption isotherms from the A/D converter data, including theoretical aspects such as pressure and temperature corrections, is described in section 3.3.

3.2.1 An "Operating Manual"

1) Slowly open the main valves at all high pressure gas cylinders (carrier gas, solute-nitrogen mixture, nitrogen diluent, air, and hydrogen)

2) Turn HP 5890 gas chromatograph, electronic integrator, and data acquisition equipment (analog to digital converter and personal computer) on

3) Open the on/off needle valves (at the pressure regulators) on the carrier gas, air, and hydrogen cylinders

4) Check the position of the two-stream selection valve. It should be in the "off" position (this can be controlled from the keyboard of the gas chromatograph)

5) Set the oven temperature to the desired value (the temperature at which the following experiment is performed)

6) Wait until the chosen oven temperature is reached (any temperature not at setpoint causes the red "NOT READY" light to be lit

7) Open the needle valves at the pressure regulators on the solute-nitrogen mixture and the nitrogen diluent gas cylinders

8) Turn the two-stream selection valve into the "on" position and wait two to three minutes (to let the gas streams flow through the system)

9) Set the solute-nitrogen mixture flowrate to the desired value (with the flow controller) and measure it with the soap film flowmeter (trial and error process)

10) Set the nitrogen diluent flowrate (with the corresponding flow controller) and measure the combined flowrate of solute-nitrogen mixture and nitrogen diluent

11) Turn the two-stream selection valve into the "off" position and shut the needle valve (at the pressure regulator) on the solute-nitrogen gas cylinder

12) Open the on/off valves for the hydrogen and air supply to the FID (those at the gas chromatograph) and ignite the detector

13) Set the oven temperature to the desorption temperature of 175°C and wait until the desorption process is finished (usually 30 minutes)

14) Reduce the temperature to the desired value (the temperature of the experiment)

15) Set the data logging equipment to the desired data logging intervals and insert a new disk into the disk drive

16) Prepare the electronic integrator, e.g. set the proper signal attenuation factor, forward the paper to a new page, and report important parameters of the experiment on the paper (flowrates, temperatures)

17) Open the needle valve (at the pressure regulator) on the solute-nitrogen mixture gas cylinder

18) Turn the two-stream selection valve into the "on" position and start the electronic integrator

19) Start the data logging process. The time gap between turning the two-stream selection valve into the "on" position and starting the data logging process has to be identical with the gas holdup time

3.2.2 The Desorption Process

The adsorbent beds were desorbed prior to initial use and after each experimental run. The desorption process was performed at temperatures of 175 °C and carrier gas (pure nitrogen) flow rates of approximately 50 ml/min. The desorption time between experimental runs was typically 30 minutes. Prior to initial use of an adsorbent bed, the desorption time was two hours. In any case, the desorption time and temperature were considered to be important experimental parameters and were reported with obtained results. The desorption process was monitored with the flame ionization detector and a low detector signal was taken as an indicator that the desorption process was successful.

3.2.3 The Mixing Process of Solute and Nitrogen

The solute concentration of the solute-nitrogen mixtures were reported on the gas cylinders as reported in section 3.1.1. It was assumed to be constant during the time of the experiments. Lower solute concentrations were achieved by diluting the solute-

nitrogen mixture with a stream of pure nitrogen (section 3.1). The resulting (lower) concentration were computed from the ratio of the flowrates of the solute-nitrogen mixture and nitrogen diluent respectively

$$c_{res} = c_{sm} \frac{F_{sm}}{F_{total}} \tag{3.2}$$

where c_{res} is the resulting concentration and c_{sm} is the solute concentration in the solute-nitrogen mixture. F_{sm} is the flowrate of the solute-nitrogen mixture and F_{total} the combined flowrate of solute-nitrogen mixture and nitrogen diluent.

3.2.4 The Input Profile

So far, the input concentration-time profiles of the solute were assumed to be ideally step-shaped as described in section 2.2.1 and shown in Figures 2.4, 2.5, and 2.7. The calculation of the adsorption isotherms (described in the next section, 3.3) is based on step-shaped input concentration-time profiles. There are two ways to determine the actual shape of the input profiles.

A second detector could be placed at the column inlet and be used to monitor the solute concentration. This method is exact but has the disadvantage that it needs an (expensive) second detector. When the input profile is in fact ideally step shaped, the second detector loses its function.

A simpler way to determine the shape of the input profiles was used in this study: a frontal analysis experiment was conducted with an empty column. It was assumed that diffusional processes did not change the boundary as it migrated through the empty column. Hence, the detector at the column outlet monitored the inlet concentration-time profile (which was identical with the outlet concentration-time profile). The detected

concentration-time profiles were step-shaped. It was concluded that the two-stream selection valve was suited for frontal analysis experiments.

3.3 Calculation of Isotherms from ADC Data

The data recorded by the analog to digital converter on the disk drive of the personal computer is used to calculate the adsorption-isotherms. The recorded data consists of two columns, the time and the corresponding digital signal. This is shown in Table 3.2. The first row in Table 3.2 corresponds to the instant when the data acquisition equipment is turned on. At the beginning of a frontal analysis experiment, the solute is held back in the adsorbent bed (section 2.2.1). Because of this, the digital signal recorded in the first rows of Table 3.2 (0.01126) is not caused by detected solute molecules but by a (steady) background signal from the flame ionization detector.

Table 3.2 Parts of a typical set of (digital) data as recorded by the A/D converter

time [sec]	Digital signal from A/D conv.
0.00	0.01126
17.00	0.01126
.	.
182.00	0.02586
198.00	0.03128
.	.
1416.00	0.59857
1432.00	0.60148
.	.
1566.00	0.60440
.	.
1717.00	0.60732
1734.00	0.60732

There are two ways to eliminate this zero offset. It can be done either at the HP 5890 gas chromatograph before the signal is sent to the ADC or it can be done after the data is recorded. The second approach was chosen in this study: the background signal is subtracted from all data points. The third column in Table 3.3 shows the data after the subtraction is done.

In a subsequent step, the data is transformed from voltage units into units of concentration: the third data column in Table 3.3 is multiplied with the ratio of the input solute concentration of the experiment and the final signal as recorded on the disk. The results of this conversion are shown in column four of Table 3.3.

Table 3.3 Data after elimination of zero offset and change into ppm-units

time [sec]	Digital signal from A/D conv.	Eliminated zero-shift	signal in ppm-units
0.00	0.01126	0.00000	0.00000
17.00	0.01126	0.00000	0.00000
.	.	.	.
182.00	0.02586	0.01460	1.23528
198.00	0.03128	0.02002	1.69410
.	.	.	.
1416.00	0.59857	0.58730	49.69373
1432.00	0.60148	0.59022	49.94078
.	.	.	.
1566.00	0.60440	0.59314	50.18784
.	.	.	.
1717.00	0.60732	0.59606	50.40000
1734.00	0.60732	0.59606	50.40000

A plot of the time (column 1) versus the signal (column 4) represents the chromatogram as obtained with the electronic integrator (which was just used as a x-y

plotter, section 3.1.6). The fundamental difference is that the digital data allows further manipulation with the help of a personal computer.

A numerical integration procedure was used to determine the area under the time versus signal curve. The area A as needed in equation 2.3 was obtained by subtracting the result of the numerical integration from the rectangular area which results from a multiplication of the duration of the experiment and the solute concentration.

3.3.1 Flowmeter Corrections

A correction for the vapor pressure of the soap solution is necessary. The vapor pressure of the soap solution is little affected by the presence of detergent in the water

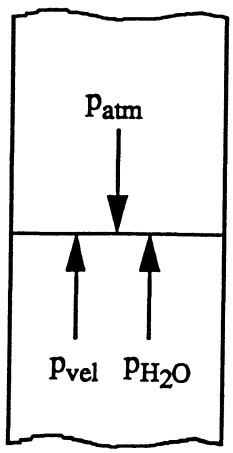

Figure 3.10 Force balance on soap film

[55] and for the present purpose the soap solution can be treated as pure water. A force balance on a soap film (Figure 3.10) and dividing by the constant soap film area yields

$$p_{atm} = p_{vel} + p_{H_2O} \tag{3.3}$$

where p_{atm} is the atmospheric pressure, p_{vel} the velocity pressure of the column effluent, and p_{H_2O} the vapor pressure of the soap solution which is a relatively strong function of the temperature. The introduction of a correction factor c_{vp} eliminates the influence of the vapor pressure of the soapy water

$$c_{vp} = \frac{p_{atm} - p_{H_2O}}{p_{atm}} \tag{3.4}$$

The measured flowrate has to be multiplied with c_{vp} in order to get a corrected value. Figure 3.11 shows a plot of the correction factor c_{vp} for a temperature range usually encountered in a laboratory. The atmospheric pressure was assumed to be 760 mmHg. It has little affect on equation 3.4.

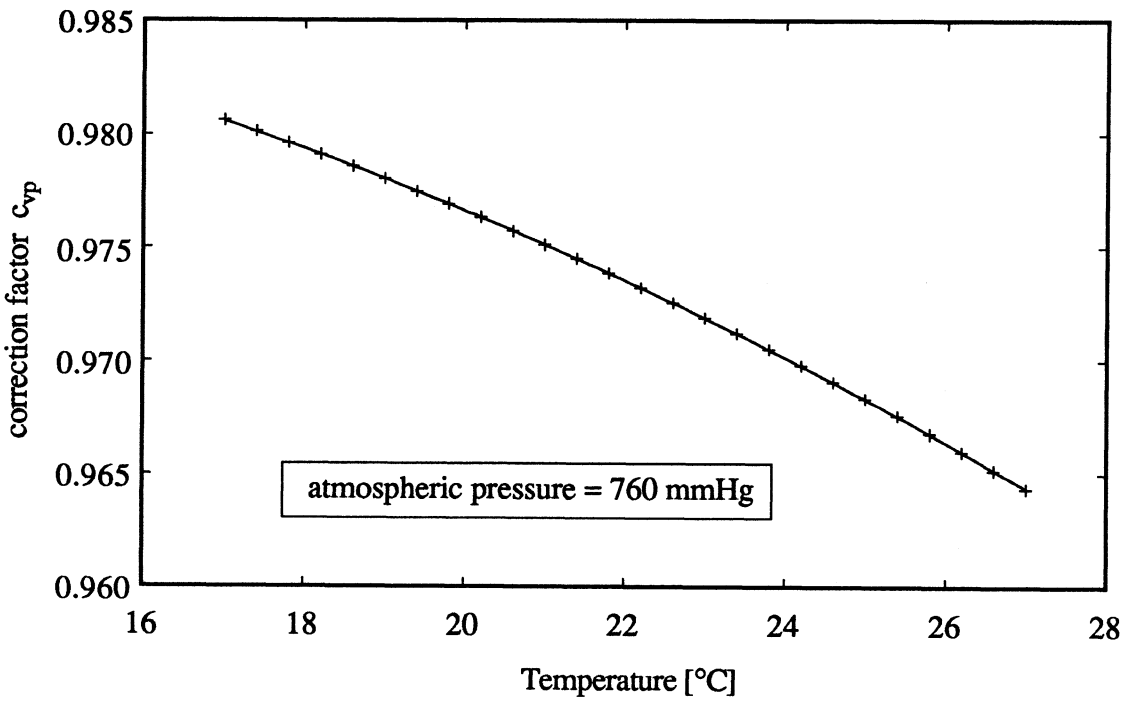

Figure 3.11 Flowmeter correction factor

A correction for the measured volumetric flowrate due to different temperatures of packed bed and flowmeter was not necessary, because the measured (volumetric) flowrate was transformed into a mass flowrate.

3.3.2 Pressure Correction

The narrow interstices between the charcoal particles of the packed bed offer some resistance to flow, and thus, there is a pressure gradient along the length of the column. Since a real gas is compressible and the number of molecules per time flowing past a given cross section must be the same at any point inside the packed bed (law of continuity), it follows that the volumetric flowrate is greater at the end than at the beginning of the packed bed. The flowrate is measured at the column outlet (section 3.1.8). Because of this, the measured flowrate is greater than the flow rate at any other point in the column. James and Martin [48] introduced a correction factor j to convert the measured volumetric flowrate into an average flowrate inside the packed bed

$$j = \frac{3}{2}\frac{(p_i/p_o)^2 - 1}{(p_i/p_o)^3 - 1} \tag{3.5}$$

where p_i is the inlet pressure (of the packed bed) and p_o the pressure at the outlet of the packed bed which is equal to the atmospheric pressure. The inlet pressure could be measured with a pressure gauge at the column inlet. In fact, this is done in most chromatographic systems [52]. The packed beds under investigation in this study were relatively short compared to the total length of the glass column. A pressure gauge at the column inlet would therefore not accurately measure the pressure at the beginning of the packed bed because of the additional pressure drop in the empty column.

To determine the pressure ratio in equation 3.5 and hence the correction factor j, the pressure drop across the packed bed was evaluated by means of the semi-empirical Blake-Kozeny equation [63] (appendix A.2). The resulting j-factors were very close to unity and were hence not accounted for in this study.

3.3.3 The Gas Holdup Time

A correction for the retention time of a non-adsorbed component, such as air, was done in each experiment. The retention time t_h of a non-adsorbed component can be obtained from introducing an elution peak (or a step-change concentration profile) into the column and measuring the time t_h until it breaks through at the detector (assuming that the non-adsorbed component is detected by the detector). This method is usually used in analytical applications of chromatography (chapter two).

In this study, the gas holdup time t_h was 20 seconds. It was determined from a frontal analysis run with an empty column. In an actual experimental run with activated carbon in the column, most of the column volume was still empty (because so little carbon was used, compared to the column volume) and it was assumed that the measured time t_h was not affected by the small packed bed of activated carbon. In the experimental runs, the gas holdup time t_h was accounted for by starting the data acquisition equipment (analog to digital converter) a time t_h after the two-stream selection valve was switched into the "on" position.

CHAPTER
FOUR

Experimental Results and Analysis

4.1 Experimental Data

4.1.1 Isotherms from 40°C to 130°C

Adsorption isotherms of acetone on Calgon OL 20/50 activated carbon were measured at temperatures ranging from 40°C to 130°C (Figure 4.1). A summary of the physical properties and specifications of the activated carbon is given in appendix A.4. The error bars in Figure 4.1 result from an uncertainty analysis (appendix A.1). The

Table 4.1 Experimental data for adsorption of acetone on Calgon OL 20/50 carbon; concentration, c, in ppm; amount adsorbed, q, in mg/g

130°C	c	50.4	40.2	30.9	20.7	10.35	5.11	2.02
	q	0.586	0.481	0.366	0.258	0.115	0.066	0.028
115°C	c	50.4	40.2	30.7	20.4	10.35	5.11	2.02
	q	0.990	0.852	0.683	0.466	0.246	0.128	0.058
100°C	c	50.4	40.2	31.0	20.4	10.35	5.2	2.02
	q	1.822	1.540	1.210	0.891	0.482	0.253	0.116
85°C	c	50.4	40.7	30.5	20.5	10.35	5.04	2.07
	q	3.205	2.777	2.195	1.596	0.977	0.534	0.273
70°C	c	50.4	40.2	30.5	20.5	10.35	5.04	2.07
	q	5.885	5.030	4.065	3.095	1.972	1.124	0.589
55°C	c	50.4	39.6	33.0	20.7	10.35	5.19	2.66
	q	9.873	8.616	7.606	5.554	3.522	2.122	1.353
40°C	c	50.4	37.56	24.68	10.35	2.41		
	q	15.89	13.92	11.28	6.88	2.57		

datapoints are connected by straight lines. As expected theoretically (chapter one), the amount of adsorbed acetone, q, increases with decreasing temperature. All isotherms curve towards the origin and do not follow the straight line shape as suggested from the

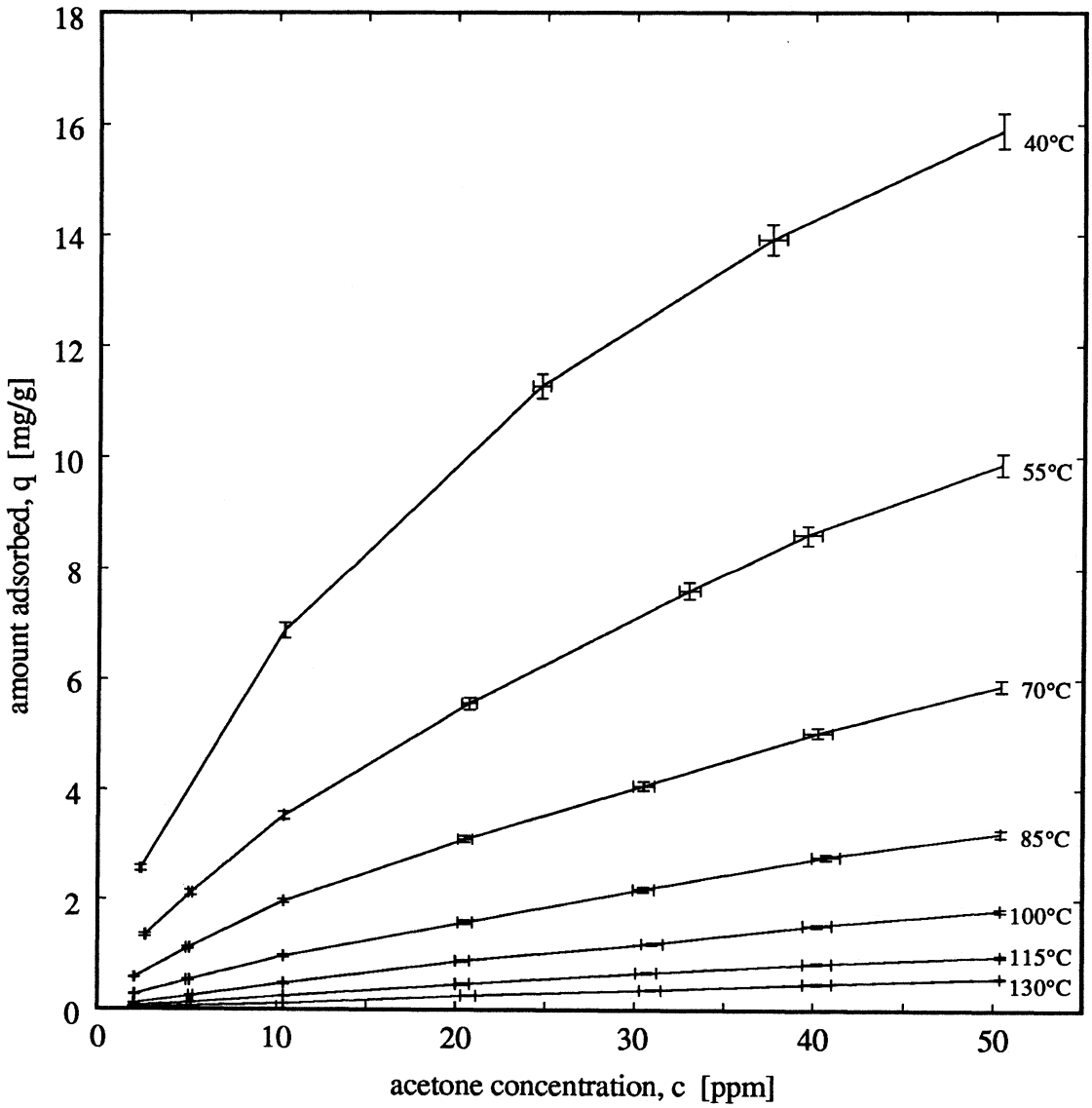

Figure 4.1 Isotherms of acetone on Calgon OL 20/50 activated carbon

Henry type equation for low adsorbate concentration. In Figure 4.1, this trend is obvious for the lower temperatures (40°C to 85°C) and, also due to the scale of plotting, somewhat less apparent for isotherms ranging from 100°C to 130°C. Table 4.1 contains the data plotted in Figure 4.1.

4.1.2 Data from two Source Cylinders

As described in chapter three, lower acetone concentrations than those contained in the source cylinder (50.4 parts per million) were obtained by diluting this acetone

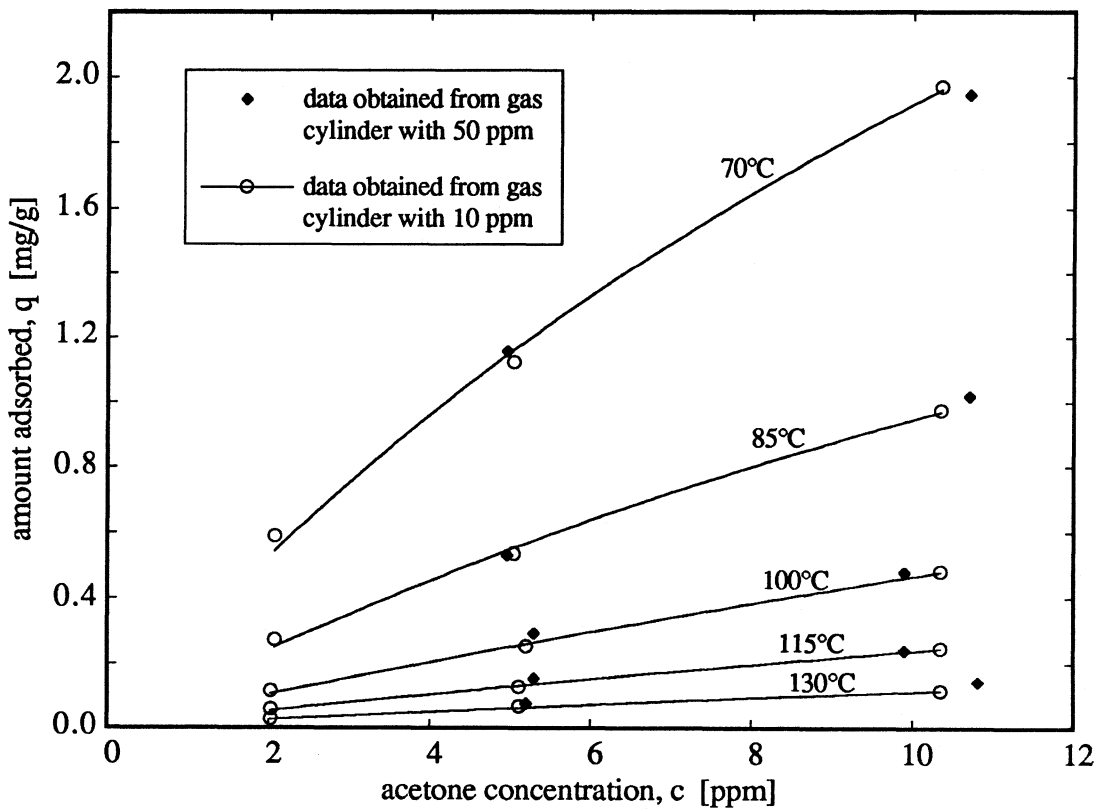

Figure 4.2 Comparison of data from two source cylinders

concentration with a stream of pure nitrogen. Concentrations down to approximately five parts per million (ppm) were obtained by this method. In order to check the accuracy of the mixing process and the obtained lower concentrations (the resulting concentrations are a function of the flowrates of acetone-nitrogen mixture and nitrogen diluent) additional data points at 10.35 ppm and approximately 5 ppm and 2 ppm were measured with a second source cylinder. This second cylinder contained an acetone concentration of 10.35 ppm. Figure 4.2 shows data points obtained from both cylinders. The slight deviations in Figure 4.2 for the amount adsorbed, q, result from inaccuracies in the determination of the concentration of the (diluted) acetone streams. This is due to the limited accuracy of the flowrate measurements (see uncertainty analysis, appendix A.1). In Figure 4.1 the data points representing acetone concentrations from approximately 20 ppm to 50.4 ppm were obtained from the gas tank containing 50.4 ppm, the data entries from approximately 2 ppm to 10.35 ppm were obtained with the cylinder containing 10.35 ppm.

4.1.3 Adsorption-Desorption Measurements

A main concern in the engineering of regenerative adsorptive equipment is the change of the adsorptive capacity after many adsorption-desorption cycles. Eight consecutive adsorption runs with acetone at 100°C were made with the same type of activated carbon (Calgon OL 20/50) described in section 4.1. These measurements were done with an acetone concentration of 50.4 ppm. A glass column was filled with fresh charcoal. "Fresh" in this context means that the sample was taken out of a sealed storage container. Although no information about the history of the sample was available, it was assumed that this specimen was new and unused.

Before the first adsorption-desorption cycle, the sample was desorbed for eight hours at 175°C. After each adsorption run, the specimen was desorbed for 30 minutes at 175°C. The following adsorption measurement was executed after the column was allowed to cool down to 100°C. This took approximately 5 minutes. The resulting adsorptive capacities (the amount adsorbed) are plotted in Figure 4.3 versus the run number. There seems to be an overall decrease in the adsorption capacity with increasing number of adsorption desorption cycles. The adsorptive capacity for the eighth run in

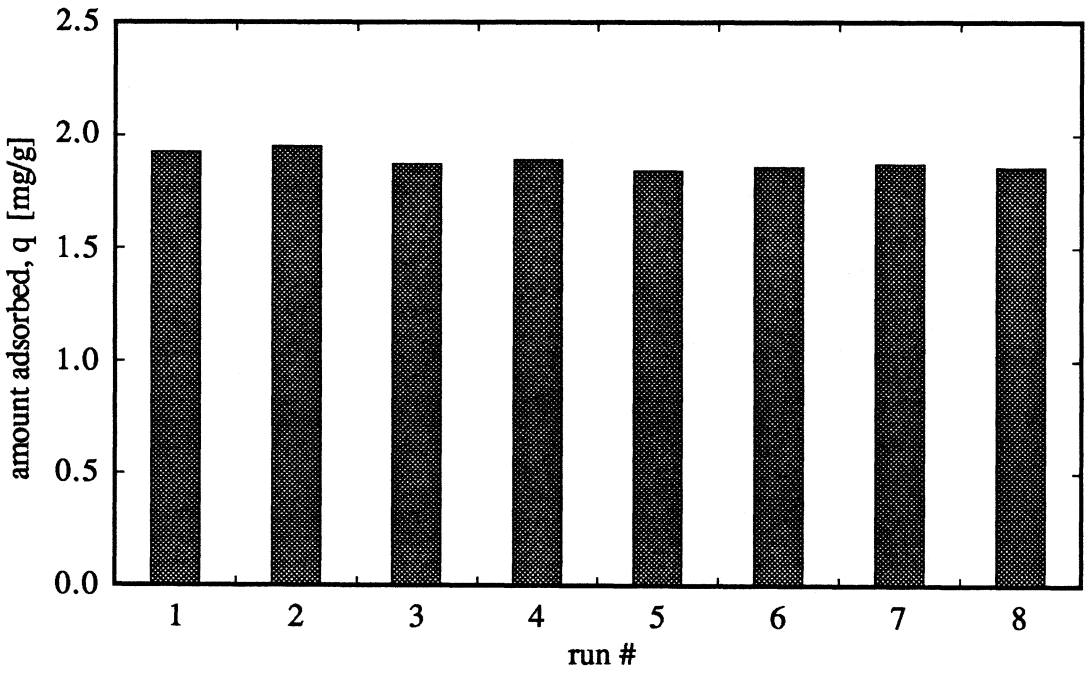

Figure 4.3 Adsorption-desorption runs on Calgon OL 20/50 carbon

Figure 4.3 amounts to 1.882 mg/g. In section 4.1, the reported result for an acetone concentration of 50.4 ppm at 100°C was 1.822 mg/g. This difference indicates that the adsorptive capacity would further decrease if more adsorption-desorption cycles were continuously done. The measurements in section 4.1 were done with a different sample

(of the same kind) and at least 50 adsorption - desorption runs were carried out for calibration and testing purposes of the equipment before the first isotherms were measured and reported in section 4.1.

4.1.4 Measurements with Crushed Charcoal

Eight adsorption-desorption cycles at 100°C and an acetone concentration of 50.4 ppm were measured on crushed Calgon OL 20/50 activated carbon. The methodology of these measurements was identical with that described in section 4.1.3. The crushing

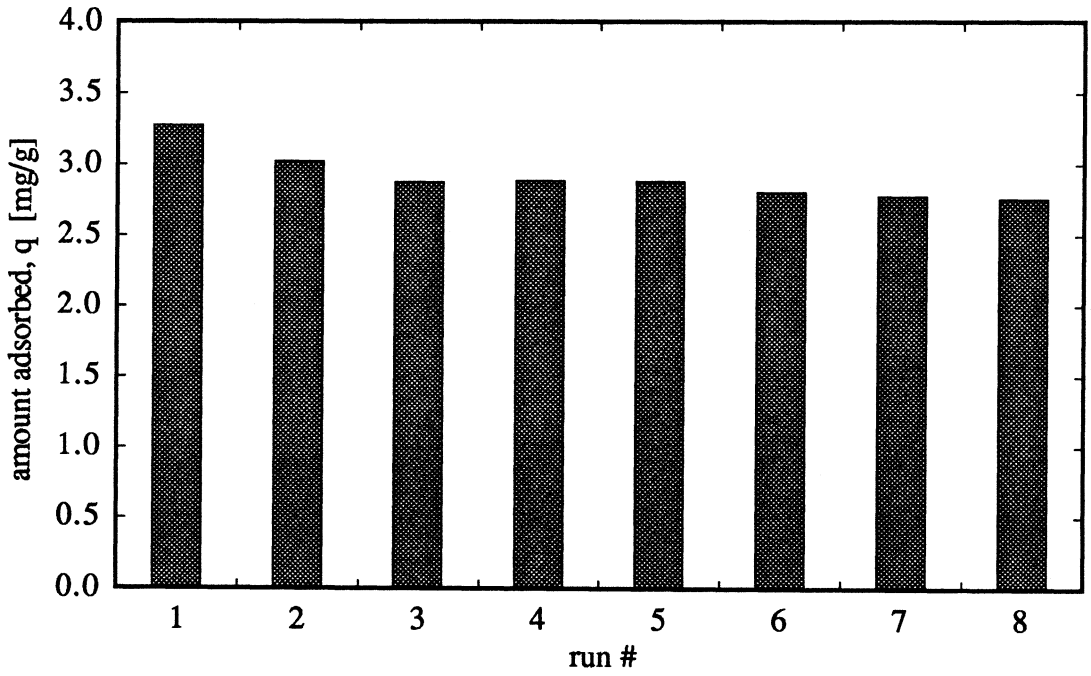

Figure 4.4 Adsorption-desorption runs on crushed Calgon OL 20/50 carbon

process was performed with a mortar and pestle. The grinding process was carried out for approximately 5 minutes. No excessive force was used. No attempt was made to evaluate the size distribution of the crushed material. The adsorptive capacity of the

activated carbon is plotted in Figure 4.4 as a function of the run number. Similar to the measurements with uncrushed charcoal (section 4.1.3), the amount adsorbed, q, clearly decreases with increasing run number.

In general, the adsorptive capacity of the crushed charcoal is substantially higher than that of the uncrushed condition. After eight adsorption-desorption cycles, the uncrushed charcoal gives a value of 1.882 mg/g (Figure 4.3) whereas the crushed version yields an adsorptive capacity of 2.761 mg/g (Figure 4.4). This is a difference of 46.7 percent. Most likely, the higher specific surface area of the crushed charcoal is the reason for the higher adsorptive capacity.

4.1.5 Unit System

The acetone concentrations in Table 4.1 and Figure 4.1 and 4.2 are reported in units of ppm (by volume). Other units often used in the literature to describe solute concentrations are the solute partial pressure and the molar concentration in units of moles per volume of gas phase. The first two (ppm and partial pressure) are independent of temperature. Parts per million can be directly converted in partial pressure by dividing with the total atmospheric pressure. This yields a conversion factor of 0.101325 to convert parts per million into partial pressure (in Pascal) if an atmospheric pressure of 101.325 kPa is assumed.

The ideal gas law can be employed to compute the solute concentration in units of moles per volume of gas phase. It follows that one mole of ideal gas occupies a volume of 0.022414 m^3 (for standard conditions at 0°C and 101.325 kPa). At room temperature (22°C, the condition where the measurements of this study were performed), this value changes to 0.024218 m^3. Furthermore, for ideal gases, the volume fraction is equal to

the mole fraction. Hence, a mole fraction of 0.0000504 (which corresponds to 50.4 ppm) is identical with an acetone concentration of 2.081E-9 mole/cm^3 of gas phase (or 2.081 nanomole/cm^3). For calculations it is convenient to note that 1 ppm equals 0.0413 nanomole/cm^3 at 22°C and a total pressure of 101.325 kPa.

The mass fraction ξ_s of solute can be computed from the solute mole fraction y_s by

$$\xi_s = \frac{M_s}{M} y_s \tag{4.1}$$

where M_s is the molecular weight (or molar mass) of the solute and M is the molecular weight of the mixture which is obtained from

Table 4.2 Acetone concentration of acetone-nitrogen mixture in different units

Component	Volume analysis [%]	partial pressure [Pa]	Mole fraction [-]	Mass fraction [-]	Molar conc. (at 22°C) [mole/cm^3]
Acetone MW=58.08	0.00504	5.107	0.0000504	0.000105	2.081E-9
Nitrogen MW=28.01	99.99496	101319.893	0.9999496	0.999895	4.1289E-5
Total	100.00	101325.000	1.00	1.00	4.129E-5

$$M = \sum_i M_i y_i \tag{4.2}$$

where the i's indicate all components of the mixture. Table 4.2 shows the acetone concentration of one source cylinder in different units.

The amount of adsorbed solute has so far been reported in units of milligrams of adsorbed acetone per gram of activated carbon (mg/g). Other units which could be used

are the number of moles of adsorbed acetone and the volume of adsorbed solute per mass of charcoal. If the density of the adsorbent is known, the amount of adsorbed acetone could also be related to the volume of adsorbent. Since density measurements would involve an additional experimental uncertainty, the mass of adsorbent was considered to be more suited to report the amount adsorbed.

4.2 Heat of Adsorption

Adsorbed molecules are more stabilized on the adsorbent surface than they were prior to adsorption in the gas phase. Because of this loss of kinetic energy, the adsorption process is exothermic in nature (chapter one). Adsorption is also accompanied by a phase change and the amount of heat evolution depends on the choice of the system. The two most important definitions of heat of adsorption are the "differential heat of adsorption" and "isosteric heat of adsorption" [64]. The differential heat of adsorption, Q_{diff}, is defined when the adsorption process takes place in an isolated system. The isosteric heat of adsorption, Q_{st}, is the heat Q released in a constant temperature calorimeter when a differential amount of gas is adsorbed at constant pressure

$$Q_{st} = \left[\frac{\partial Q}{\partial n_S}\right]_{T,p} \tag{4.3}$$

where n_S are the number of moles of gas adsorbed, T is the absolute temperature and p is the partial pressure of the adsorbate in the gas phase. The van't Hoff isobar equation relates Q_{st} to adsorption isotherms at different temperatures. It is derived from equating the chemical potential of the adsorbed phase and the gas phase, applying the Gibbs-Helmholtz relation, and assuming that the vapor phase behaves like an ideal gas.

$$\frac{d\,\ln p}{dT} = \frac{Q_{st}}{RT^2} \tag{4.4}$$

$$\frac{d\,\ln p}{d\,(1/T)} = -\frac{Q_{st}}{R} \tag{4.5}$$

If Q_{st} is assumed to be independent of the temperature, integration of equation (4.5) yields

$$\ln p = -\frac{Q_{st}}{R}\frac{1}{T} \tag{4.6}$$

Equation (4.6) represents the equation of a straight line. Plots of lnp versus 1/T are called van't Hoff plots and are used to determine Q_{st}. From experimentally obtained isotherms at a constant amount adsorbed and two different temperatures T_1 and T_2, Q_{st} is obtained by

$$Q_{st} = R\,\frac{(\ln p_1 - \ln p_2)}{(1/T_1 - 1/T_2)} \tag{4.7}$$

If the van't Hoff plot yields a straight line, the assumption of a temperature independent Q_{st} was justified. If lines for different amounts adsorbed have the same slope, it can be assumed that Q_{st} is also independent of the fractional coverage (the amount adsorbed). Figure 4.5 shows the natural logarithm of p versus the reciprocal temperature for five values of the amount adsorbed. The p-values for a given amount adsorbed were calculated from the Radke and Prausnitz curve fit equations as described in section 4.3 of this chapter. The isosteric heat of adsorption Q_{st} is obtained from the slope of the lines (equation 4.7). These lines are fitted through the data with a least square error curve fit. The isosteric heat of adsorption Q_{st} decreases with increasing amount adsorbed (Figure 4.6). The scale of the ordinate in Figure 4.6 is chosen to clearly show this relation. At

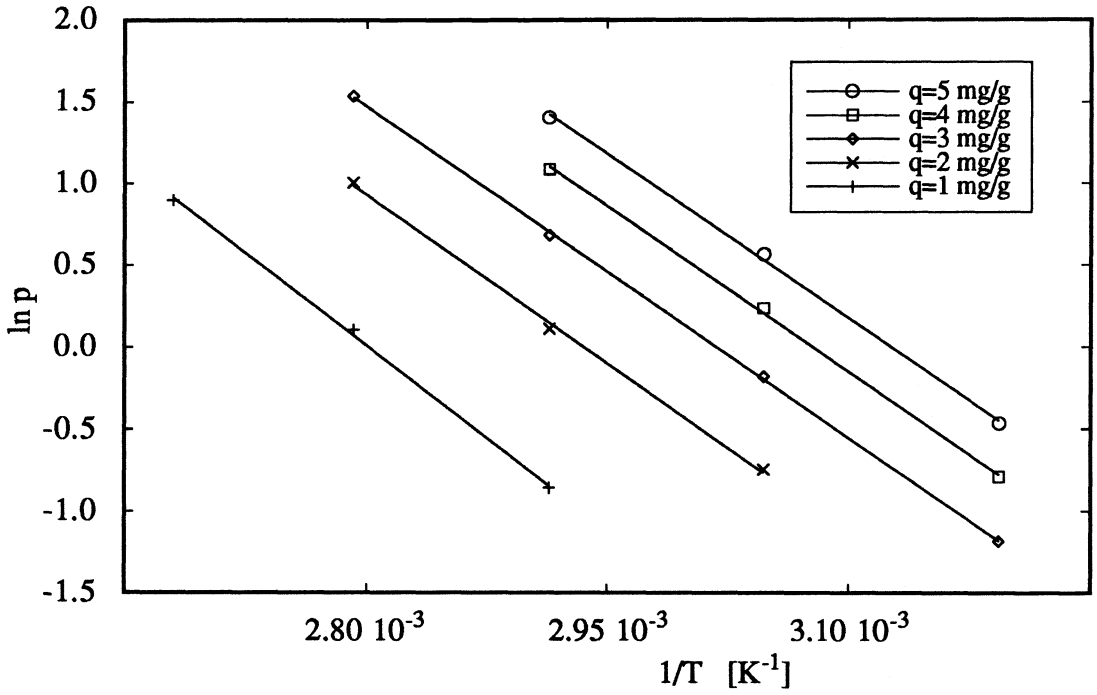

Figure 4.5 Van't Hoff Plot

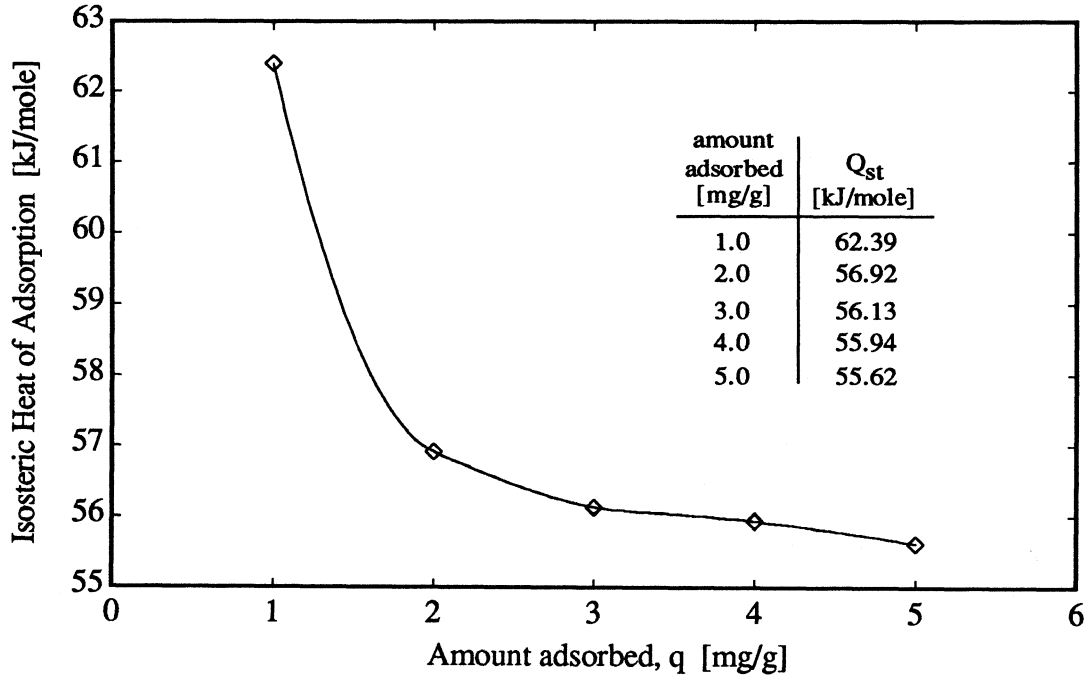

Figure 4.6 Heat of adsorption as a function of the amount adsorbed

atmospheric pressure, acetone has a heat of vaporization of 29.14 kJ/mole. As described in chapter one, the heat of adsorption and the heat of vaporization should be, for most adsorbate-adsorbent systems, in the same order of magnitude. Clearly, the acetone-activated carbon system under investigation in this study exhibits this behaviour.

4.3 Fit of Adsorption Models to Isotherm Data

Adsorption models can be fitted to experimentally obtained isotherms. In this case, a set of coefficients is computed to the specified function representing the model. These coefficients are determined in a way to minimize the square of the difference between the original data (the experimental data) and the calculated value from the predicting function (the equation representing the model). This gives the name to the method, "least squares error curve fit".

The accuracy of curve fits is usually expressed by the "sum of squares". As the name indicates, the deviations of the model to the experimentally obtained data are squared and summed up. In this study, a "modified" sum of squares, called root-mean-square (RMS) error, was used to evaluate the deviations between model and experimental data

$$\text{RMS} = \sqrt{\frac{\text{Sum of Squares}}{\text{N}}} \tag{4.8}$$

where N is the number of data points for a given isotherm (temperature). This was done to compare fits with different numbers of experimental data points. The square root is taken from this ratio in order to get a value that represents the real deviations (the differences were squared in the first place to avoid that positive and negative deviations cancel out).

The least squares error curve fit can be done for linear and nonlinear models. A linear model (a linear predictive function) is a model that can be expressed in linear form. This is the case when the derivatives with respect to the parameters do not contain other

Table 4.3 Adsorption models

Name	original form	linearized form
Langmuir	$\frac{q}{q_0} = \theta = \frac{K p}{1 + Kp}$	$\frac{p}{q} = \left(\frac{1}{q_0 K}\right) + \left(\frac{1}{q_0}\right) p$
Freundlich	$q = k_F c^{(1/n_F)}$	$\ln q = \ln k_F + \frac{1}{n_F} \ln c$
Radke and Prausnitz	$q = \left[\frac{1}{K_H p} + \frac{1}{k_F p^{(1/n_F)}}\right]^{-1}$	none
Toth	$\frac{q}{q_0} = \left[\frac{1}{(K p)^t} + 1\right]^{-1/t}$	none
Dubinin-Radushkevich	$W = W_0 \exp(-kA^2)$	$\ln W = \ln W_0 - kA^2$
Dubinin-Astakhov	$W = W_0 \exp\left[-\left(\frac{A}{E}\right)^n\right]$	none

parameters (it has nothing to do with "straight lines"). The set of parameters of a linear model can be obtained in a straightforward fashion whereas the nature of a nonlinear

curve fit involves an iteration process. Many software packages incorporate linear curve fit models but only few allow nonlinear data analysis. The nonlinear fits in this chapter were performed with Kaleidagraph [65], a data analysis and graphics presentation application for Macintosh personal computers.

Table 4.3 shows the mathematical form of the models most often used in the literature. These six models will be used in the remainder of this chapter to correlate the experimental data.

4.3.1 The Langmuir and the Freundlich Model

The simplest model of adsorption is that of Langmuir (chapter one) in which adsorption takes place on a uniform surface and without any interaction between adsorbed molecules. A purely empirical adsorption model is that by Freundlich [64]. By its mathematical form it is obvious that this model does not hold for high solute concentrations because it gives no limit of the adsorption capacity q. The amount adsorbed goes to infinity when the concentration increases. The Langmuir and the Freundlich model require a different set of parameters for each temperature (for each isotherm fit).

Both the Langmuir and the Freundlich isotherm equation can be rewritten in linearized form. If plotted in this linearized form, the mathematical equation takes the form of a straight line. The experimental data points (which will not be exactly on a straight line because the model is only an approximation for the experimentally obtained data) can be curve fitted with a straight line following the least squares error curve fit method described above (Figure 4.7 and 4.8). The parameters of the model are then obtained from the slope and the y-axis intercept of the straight line. The linearized Langmuir plot

of p/q and p is somewhat insensitive to small deviations from the model since the acetone concentration occurs in both variables.

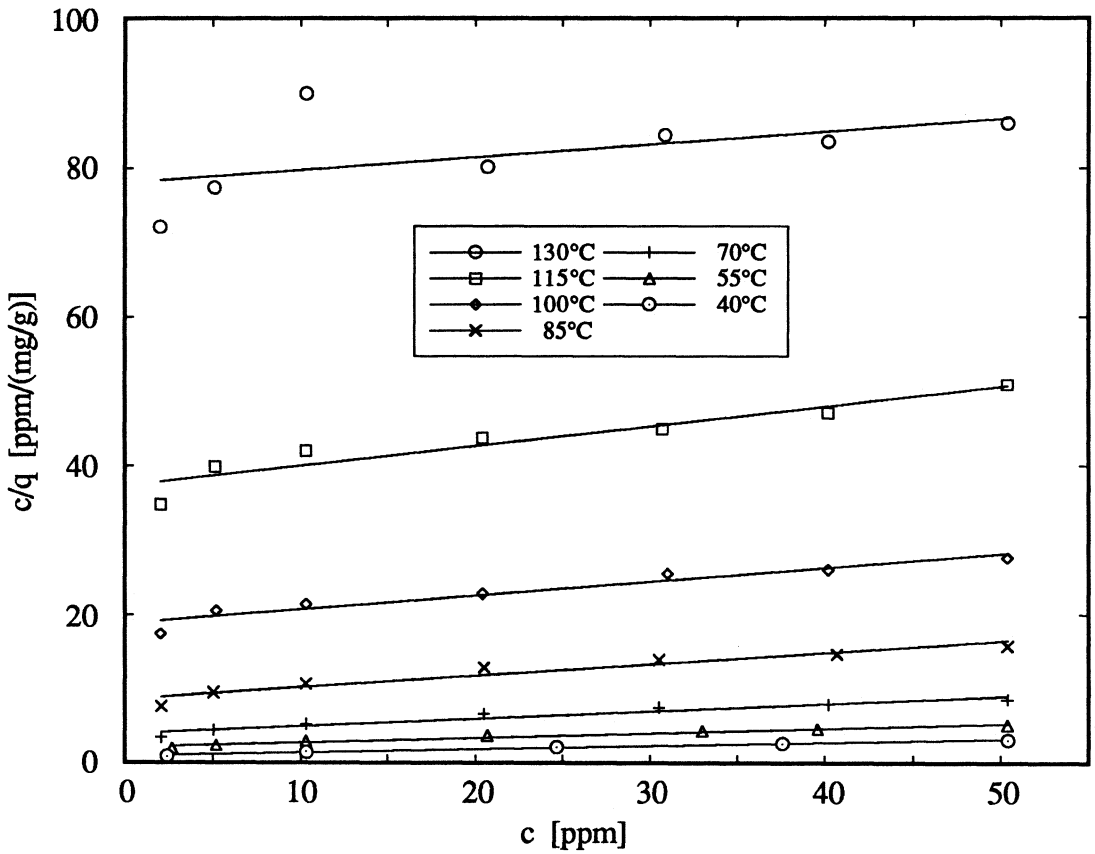

Figure 4.7 Linearized Langmuir plot

Figure 4.9 and 4.10 show resulting Langmuir and Freundlich curve fits obtained from both a nonlinear fit (Kaleidagraph, solid lines) and from the linearized approach (dashed lines). Table 4.4 and 4.5 contain the data plotted in Figure 4.7 and 4.8. For the Langmuir model, the nonlinear fit generally correlates the data better. The linear fit overestimates the experimental data in the low concentration range (2 - 35 ppm) and

underestimates the data for higher acetone concentrations (35 - 50 ppm). The Freundlich model shows a reversed trend: low concentration data is underestimated and high concentration data is overestimated. As a precise means of comparison of the quality of the curve fits, the root-mean-square (RMS) error is calculated for both models (Langmuir and Freundlich) and for each temperature and is reported in the last two columns of Table 4.4 and 4.5. In every case, the nonlinear fit approximates the experimental data better, expressed in smaller values for RMS.

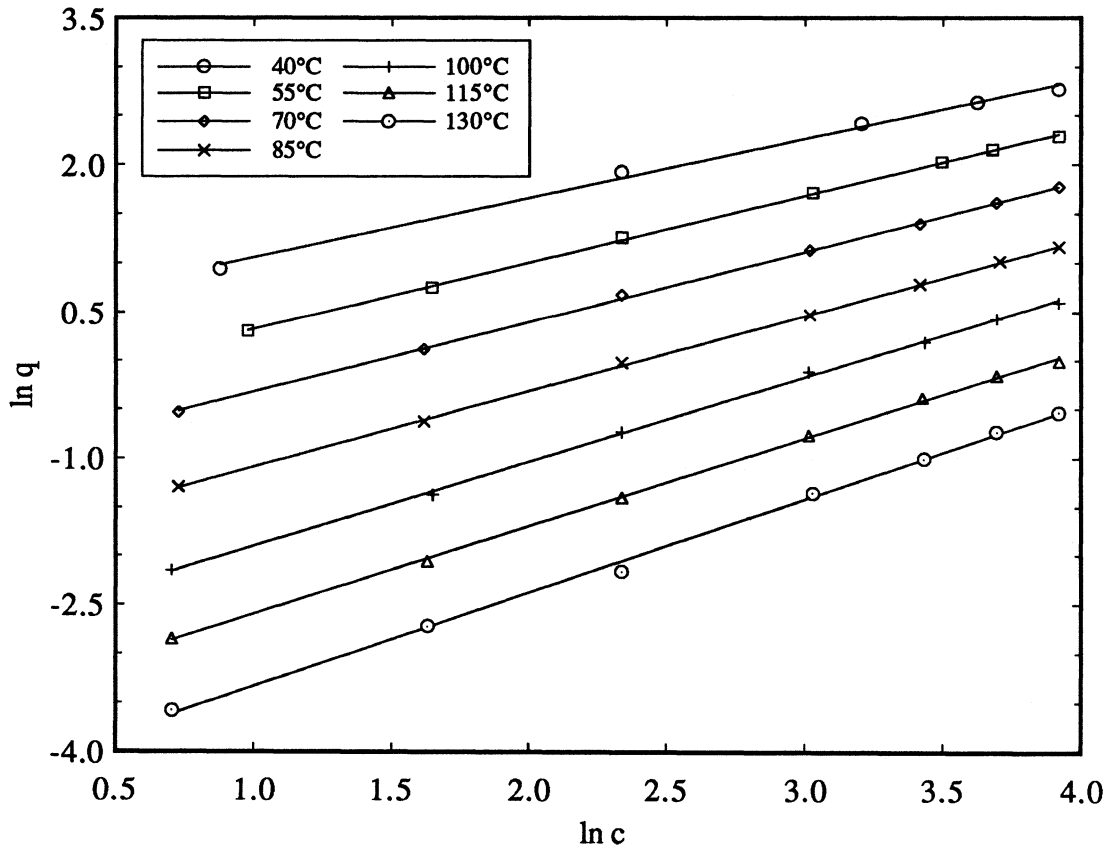

Figure 4.8 Linearized Freundlich plot

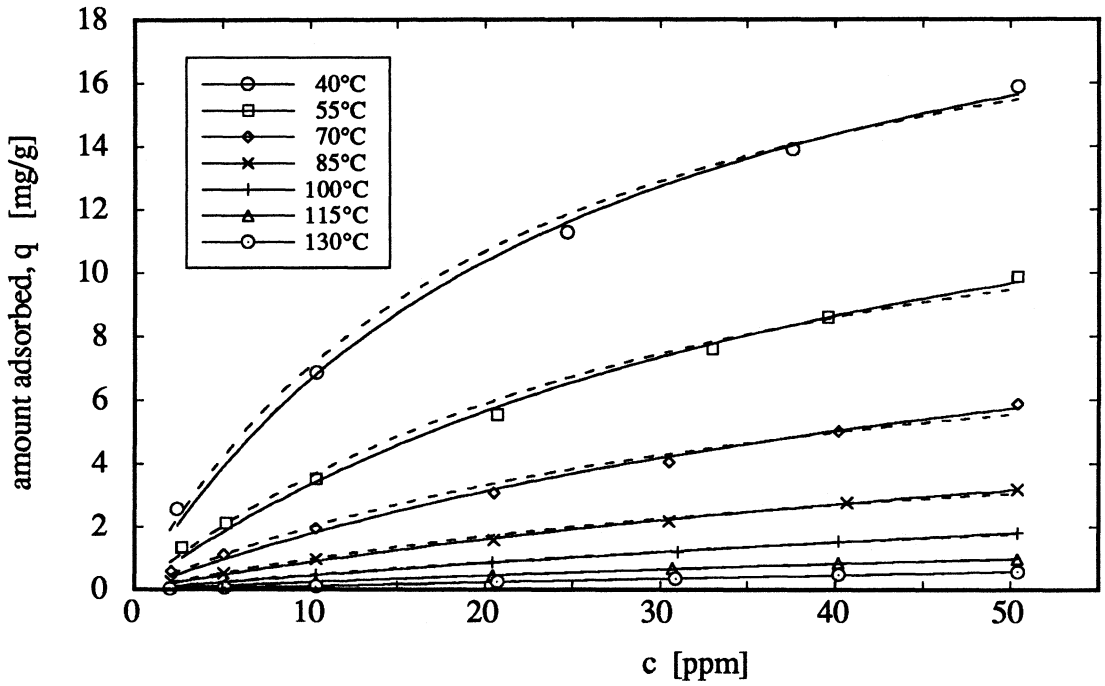

Figure 4.9 Langmuir curve fit

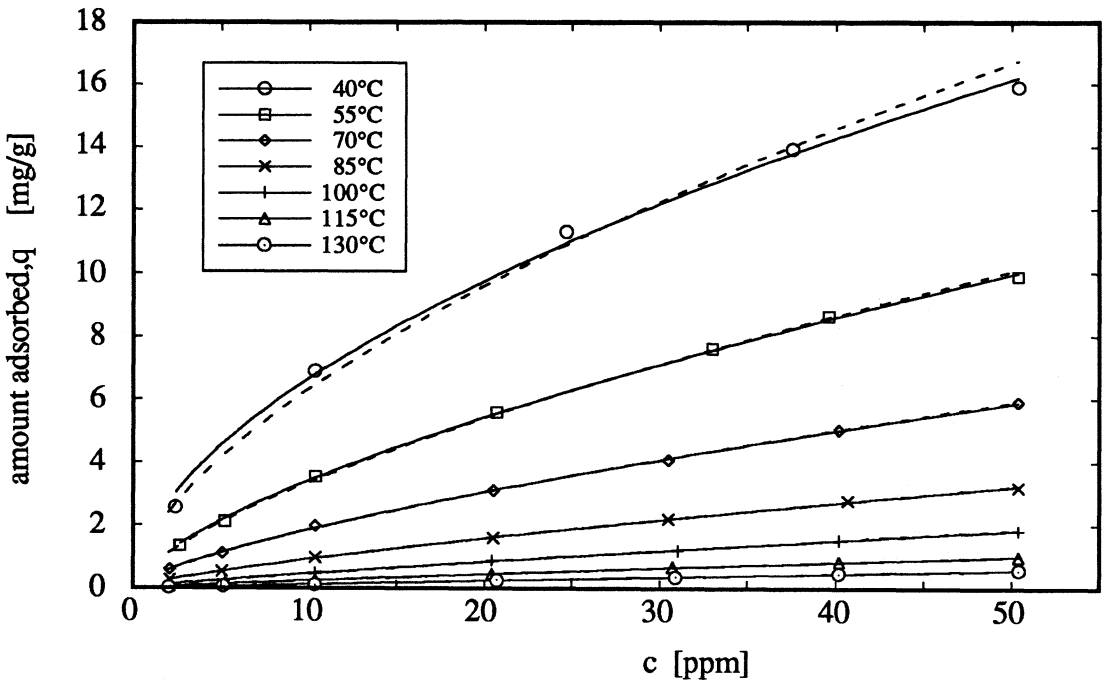

Figure 4.10 Freundlich curve fit

Table 4.4 Data from Langmuir curve fit

T	linearized curve fit		non linear curve fit		error estimation RMS	
[°C]	q_0 [mg/g]	K [1/ppm]	q_0 [mg/g]	K [1/ppm]	linear	non linear
130	5.8531	0.002188	9.5272	0.001307	0.006997	0.006157
115	3.7597	0.007125	4.0868	0.006432	0.009348	0.008690
100	5.3169	0.009996	6.7004	0.007371	0.02611	0.01716
85	6.4450	0.01811	8.6980	0.01144	0.08754	0.05187
70	9.9701	0.02510	12.785	0.01626	0.1960	0.1352
55	15.921	0.02941	18.348	0.02230	0.2647	0.1982
40	21.940	0.04759	23.479	0.03956	0.3857	0.3019

Table 4.5 Data from Freundlich curve fit; $[k_F]$ = mg/(g ppm^(1/n_F))

T	linearized curve fit		non linear curve fit		error estimation RMS	
[°C]	n_F [-]	k_F	n_F [-]	k_F	linear	non linear
130	1.04675	0.013781	1.03296	0.013286	0.007538	0.006564
115	1.11242	0.030400	1.16108	0.034643	0.01855	0.01568
100	1.15626	0.062850	1.19451	0.069026	0.02294	0.01779
85	1.28954	0.155082	1.30032	0.158449	0.02209	0.02111
70	1.39136	0.353561	1.40712	0.362666	0.03822	0.03353
55	1.46852	0.699954	1.50407	0.738000	0.09638	0.07692
40	1.65761	1.572898	1.81601	1.870620	0.4667	0.3054

4.3.2 The Radke and Prausnitz and the Toth Model

The Radke and Prausnitz equation [64] combines the Freundlich equation with the Henry type equation (chapter three). The Henry type equation is the limiting case of the Langmuir isotherm when the amount adsorbed, q, is far smaller compared with the adsorptive capacity of the adsorbent. The Radke and Prausnitz equation contains three parameters.

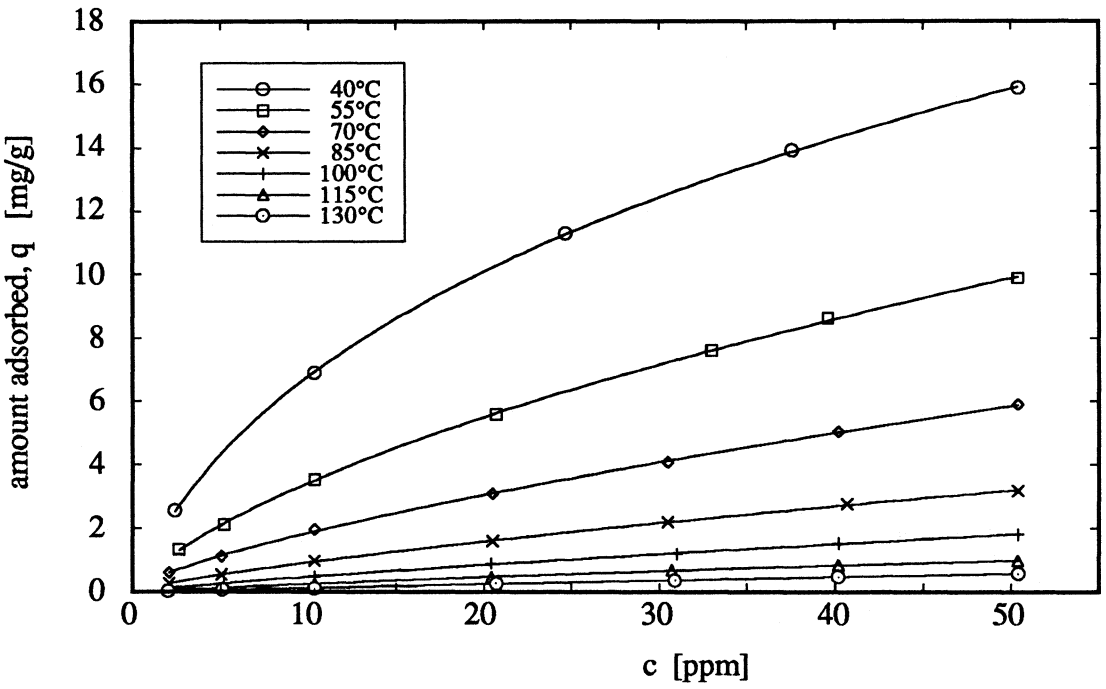

Figure 4.11 Radke and Prausnitz curve fit

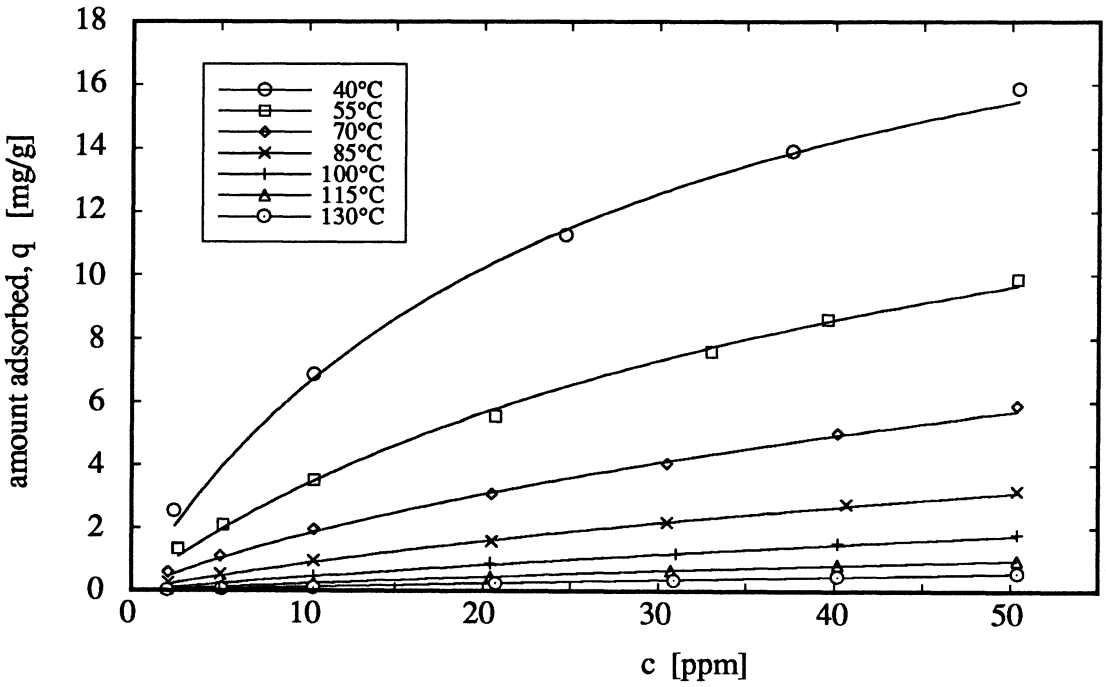

Figure 4.12 Toth curve fit

Another isotherm expression is the Toth equation [64]. It also contains three parameters. When the parameter t is equal to unity, the Toth equation is identical to the Langmuir expression. For low concentrations (partial pressures) the Toth equation reduces to the Henry type expression. The parameters for the Radke and Prausnitz and the Toth equation were obtained for each temperature with a nonlinear curve fit. The results are shown in Figure 4.11 and 4.12. The root-mean-square (RMS) errors were computed for both models for each temperature and are shown in Table 4.6, together with the error estimation of the other four models described in this chapter. The Radke and Prausnitz equation gives the lowest RMS for each temperature. Hence, it can be said that this equation correlates the experimental data best.

4.3.3 Dubinin-Polanyi Theory

A general approach to the correlation of adsorption equilibria was developed by Dubinin [66] based on ideas from Polanyi [66] and Berenyi [66]. The adsorbed molecules within the microporous adsorbent are considered to behave as a liquid with properties different from those of the bulk liquid at the same temperature. For an ideal gas (the fugacities are replaced with partial pressures) the adsorption potential

$$A = - R T \ln\left(\frac{p}{p_s}\right) \tag{4.9}$$

gives the difference in free energy between the adsorbed phase and the saturated liquid sorbate at the same temperature. The adsorption potential A is calculated directly from the ratio of the equilibrium partial pressure of the solute, p, and the saturation vapor pressure p_s for that temperature. The major difference of the Dubinin-Polanyi theory compared to the other four adsorption models described above (Langmuir, Freundlich, Radke and

Prausnitz, and Toth) is that the adsorption equilibrium relation for a given adsorbate-adsorbent system can be expressed independent of temperature by using the adsorption potential

$$W = q/\rho = W(A) \tag{4.10}$$

In equation (4.10), W is the volume of micropores filled by the adsorbate, q is the amount adsorbed and ρ is the density of the adsorbed phase. The relation between the volume of fluid adsorbed and the adsorption potential as expressed in equation (4.9) and

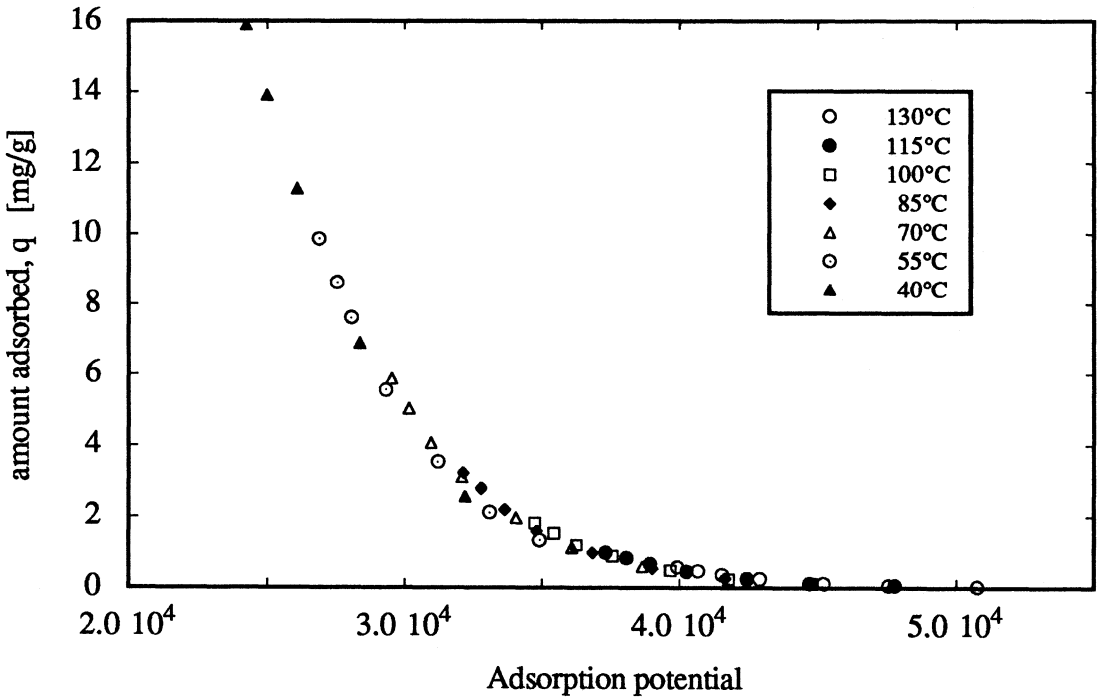

Figure 4.13 Characteristic curve for the acetone-activated carbon system investigated in this study

(4.10) is called the characteristic curve. Figure 4.13 shows the characteristic curve for the acetone-activated carbon system under investigation in this study. In Figure 4.13, the

density of the adsorbed phase was assumed to be a constant (independent of temperature) and hence the amount adsorbed, q, instead of W, is plotted versus the adsorption potential.

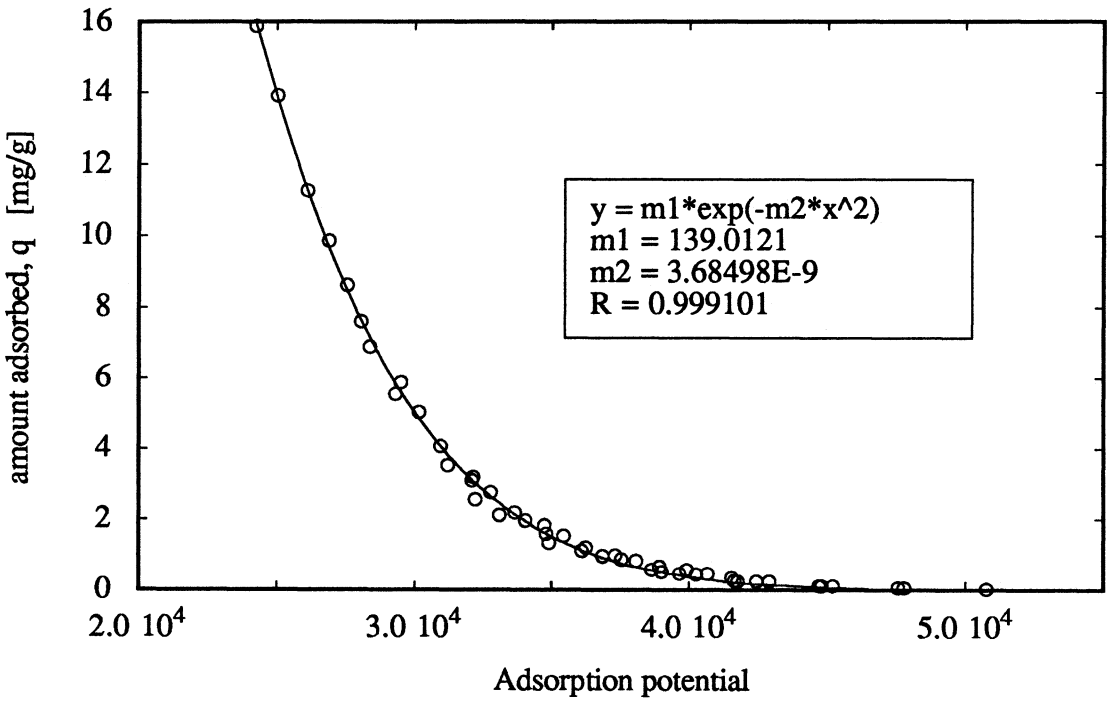

Figure 4.14 Dubinin-Radushkevich curve fit of characteristic curve

Dubinin [64] derived an equation which describes the characteristic curve. It is called the Dubinin-Radushkevich equation

$$W = W_0 \exp(-kA^2) \tag{4.11}$$

Dubinin and Astakhov [64] generalized the Dubinin-Radushkevich equation to the following form

$$W = W_0 \exp[-(A/E)^n] \tag{4.12}$$

Figure 4.14 and 4.15 show the characteristic curve fitted with the Dubinin-Radushkevich equation and the Dubinin-Astakhov equation, respectively. The parameters of the equation are given within the graphs.

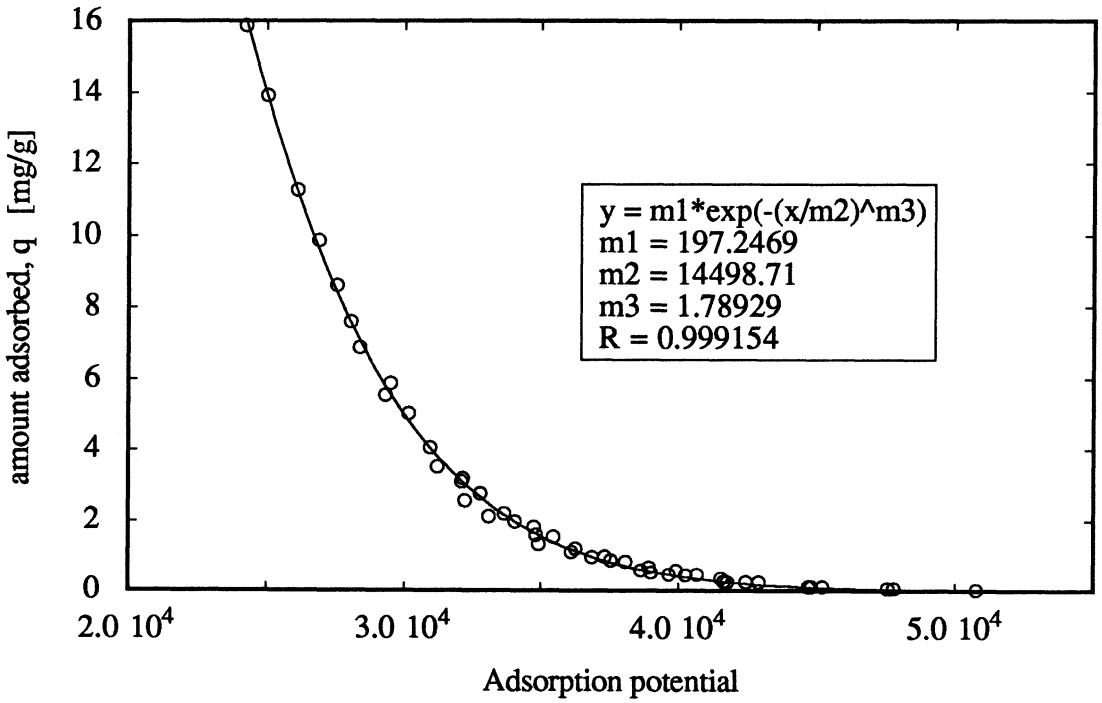

Figure 4.15 Dubinin-Astakhov curve fit of characteristic curve

If W is replaced by q and the adsorption potential (equation 4.9) is substituted into equations 4.11 and 4.12, one obtains

$$q = q_0 \exp\left[-k \left(-R\,T \ln\left(\frac{p}{p_{sat}}\right)\right)^2\right] \tag{4.13}$$

$$q = q_0 \exp\left[-\left(\left(-R\,T \ln\left(\frac{p}{p_{sat}}\right)\right)/E\right)^2\right] \tag{4.14}$$

Equations 4.13 and 4.14 can be used to plot the curve fits in a q versus p (or c) graph for each temperature T in order to compare the fits with the experimentally obtained data (Figure 4.16 and 4.17). Again, the quality of the curve fits is expressed by the RMS error of the deviations between predicting function and experimental data. These data are shown in Table 4.6. Compared to the Dubinin-Radushkevich model, the Dubinin-Astakhov approach results in smaller RMS's (except for 55°C and 70°C). Both the Dubinin-Radushkevich and the Dubinin-Astakhov model can not be directly compared to the four other models described in this chapter (Langmuir, Freundlich, Radke and Prausnitz, and Toth) because the former correlate the experimental data over the whole temperature range. This is an advantage in terms of simplicity but results in higher deviations of the predicted data from the experimental results as can be seen in Table 4.6.

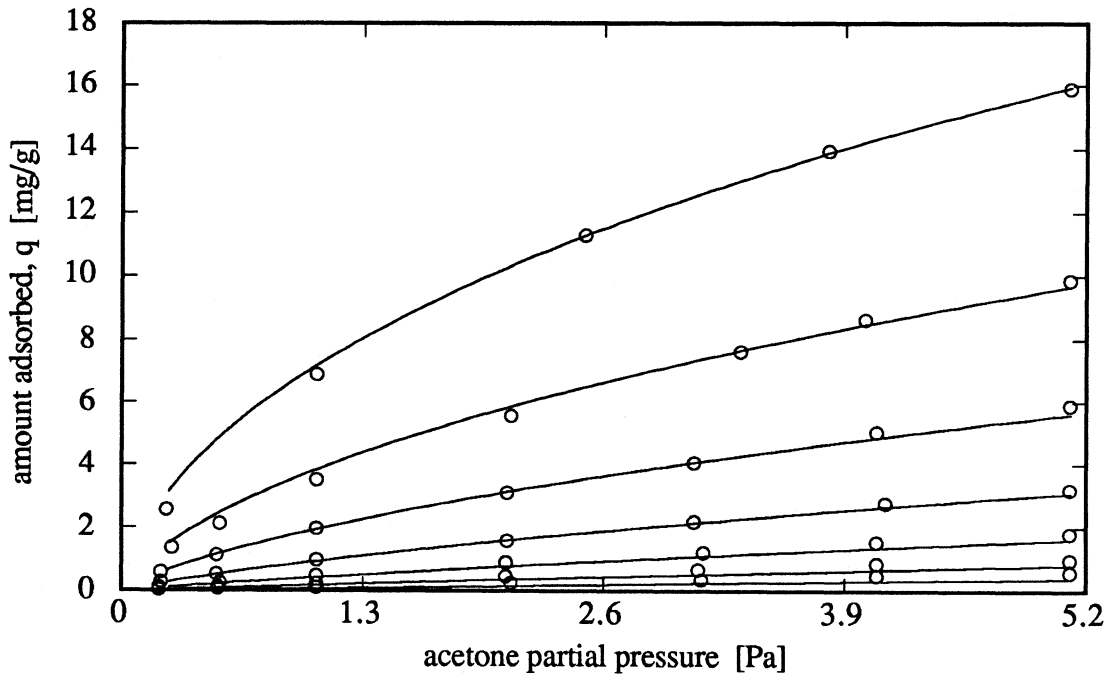

Figure 4.16 Dubinin-Radushkevich curve fit

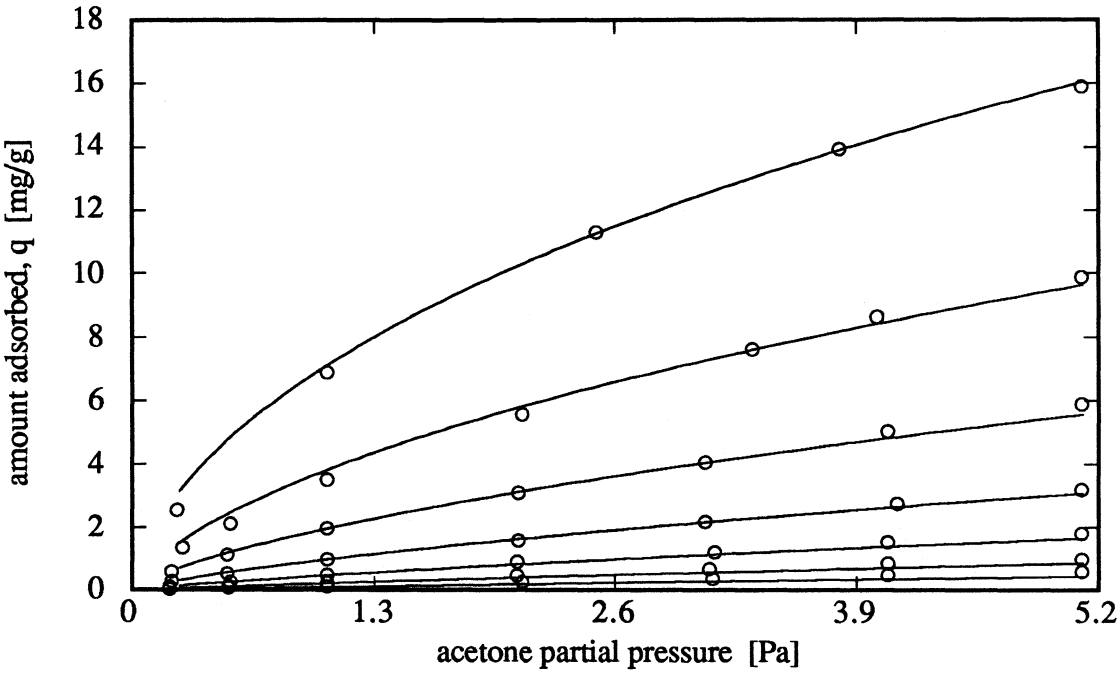

Figure 4.17 Dubinin-Astakhov curve fit

Table 4.6 Error estimation (root-mean square (RMS) error) for the six adsorption models investigated in this study

T [°C]	Langmuir	Freundlich	Radke/Pr.	Toth	Dub./Rad.	Dub./Asta.
130	0.006157	0.006564	0.006157	0.009905	0.1160	0.08834
115	0.008690	0.01568	0.008691	0.009377	0.1235	0.08887
100	0.01716	0.01779	0.01530	0.03147	0.1202	0.08855
85	0.05187	0.02111	0.02050	0.05260	0.06902	0.06079
70	0.1352	0.03353	0.03345	0.09786	0.1278	0.1490
55	0.1982	0.07692	0.04861	0.1688	0.2423	0.2540
40	0.3019	0.3054	0.03467	0.3103	0.2502	0.2476

4.4 Prediction of Isotherms

The Dubinin-Radushkevich model (Equation 4.13) was used to calculate isotherms in the temperature range from 40°C to 130°C in increments of 5°C (Figure 4.18). It has to be noted that the mathematical form of the Dubinin-Radushkevich model (equation 4.13) does not allow zero solute concentrations or partial pressures. The range of partial pressures plotted in Figure 4.18 goes from 0.0001 Pa to 5.2 Pa. In section 4.3.3, the same procedure was used to compare the calculated isotherms with experimentally obtained data (temperature increments of 15°C). Since the correlation of the data was reasonably good (Figure 4.16), also expressed by the error estimation RMS in Table 4.6, it was assumed that the model can also be used to predict isotherms at temperatures between those which were experimentally obtained.

The virtue of the Dubinin-Radushkevich model (and the Dubinin-Astakhov model) lies in the fact that the predictive function (equation 4.13) is simple in nature. The curve fit to the characteristic curve yields one set of parameters which is valid for the whole temperature range.

Isotherms could also be calculated with the Langmuir, Freundlich, Radke and Prausnitz, and Toth models. To do so, the temperature dependent sets of coefficients had to be described by suitable mathematical functions which could then be substituted into the predictive function as given in Table 4.3. Four all four models, the functions describing the temperature dependence of the coefficients were rather complicated. Approximating the temperature dependence with linear functions gave no satisfactory results.

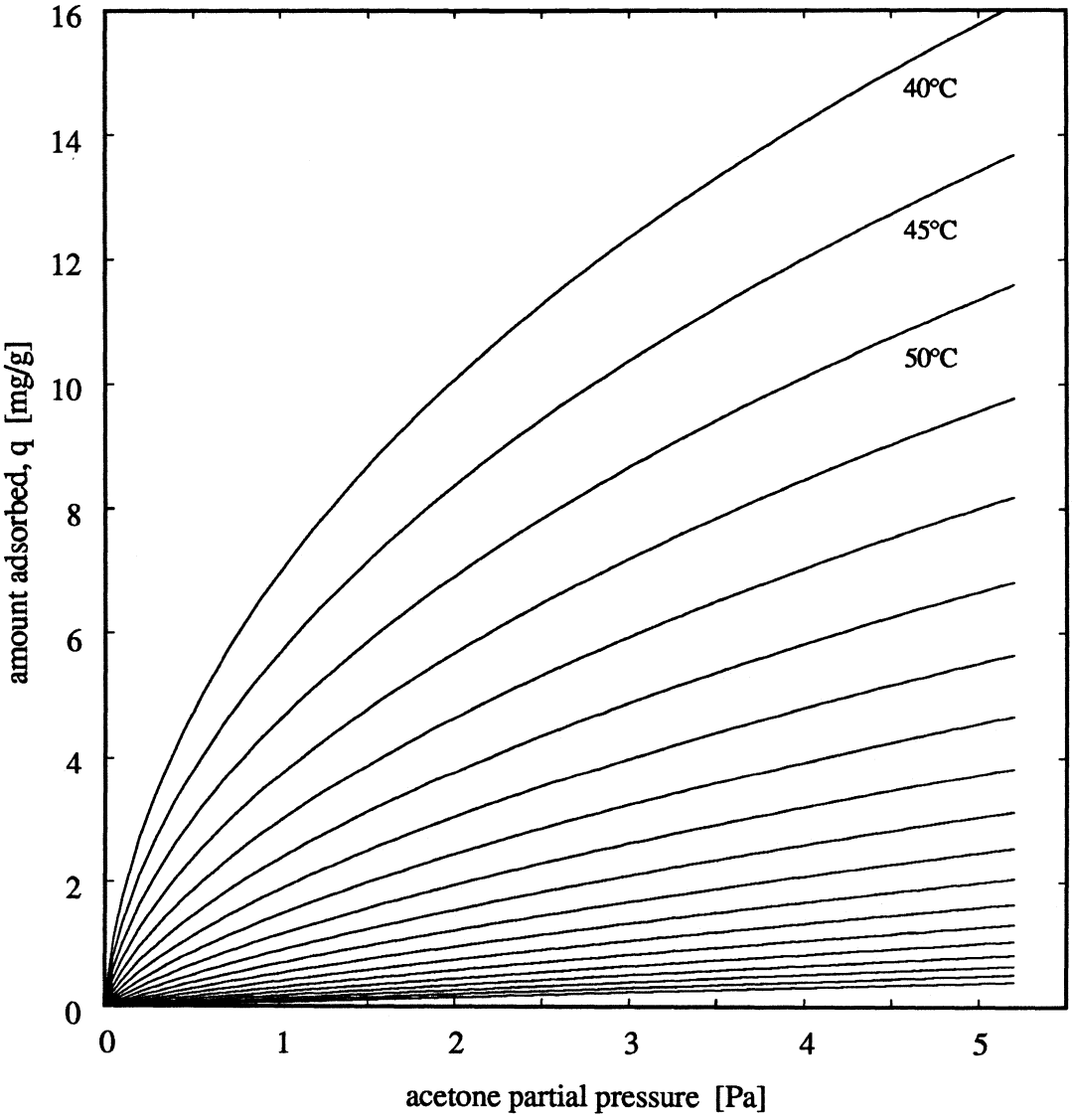

Figure 4.18 Calculated isotherms from the Dubinin-Radushkevich model for temperatures from 40°C to 130°C in 5°C increments

The coefficients for the Dubinin-Radushkevich and the Dubinin-Astakhov model were predicted from experimentally obtained data between 40°C and 130°C. As shown above (Figure 4.18), the resulting predictive function can be used to calculate isotherms

within this temperature range. At the end of this work, an isotherm was measured at 27°C. These data are not included in any of the Figures and Tables above. Instead, it was tried to extrapolate the predictive functions from the Dubinin-Radushkevich and the Dubinin-Astakhov model to this temperature. The results are shown in Figure 4.19. The Dubinin-Astakhov model predicts the data slightly better for higher acetone partial pressures, but in general, both models give only a poor approximation of the data.

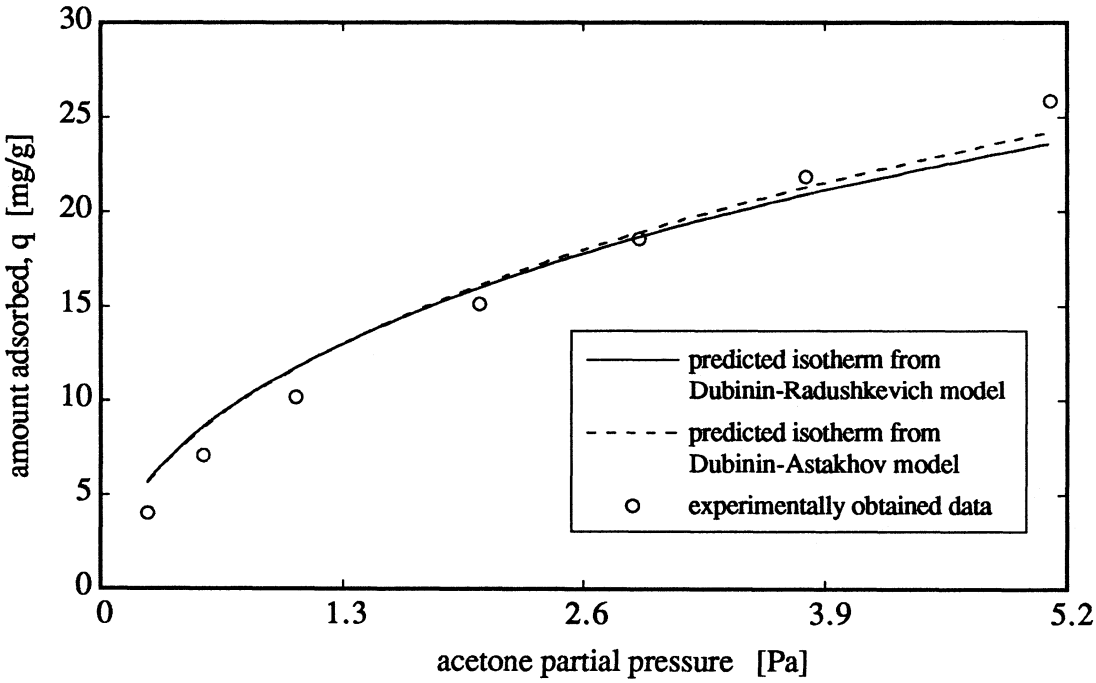

Figure 4.19 Measured and calculated isotherms for 27°C

4.5 Comparison with Acetone Data published in Literature

An innumerable number of reports dealing with adsorption of organic compounds on activated carbon has been published in the literature. However, most of these

experiments did not cover the very low concentration range of interest to indoor air quality (ppm-ppb) and to this thesis. Those studies which were conducted for this low concentration range used different types of activated carbon than the type used in this study (Calgon OL 20/50). In addition, the direct comparison of data is constrained by the use of different temperatures. As mentioned in section 4.4, an isotherm at 27°C was measured at the end of this study. These data is not included in sections 4.1 to 4.3. Because of the experimental equipment used for this study (no cooling), a lower temperature could not be obtained. In Figure 4.20, the isotherm at 27°C, together with data at 40°C, is compared with data from Forsythe [32] taken at 25°C. Forsythe used a Columbia 4LXC 12/28 activated carbon. No detailed specifications about this carbon type are given in Forsythe's report.

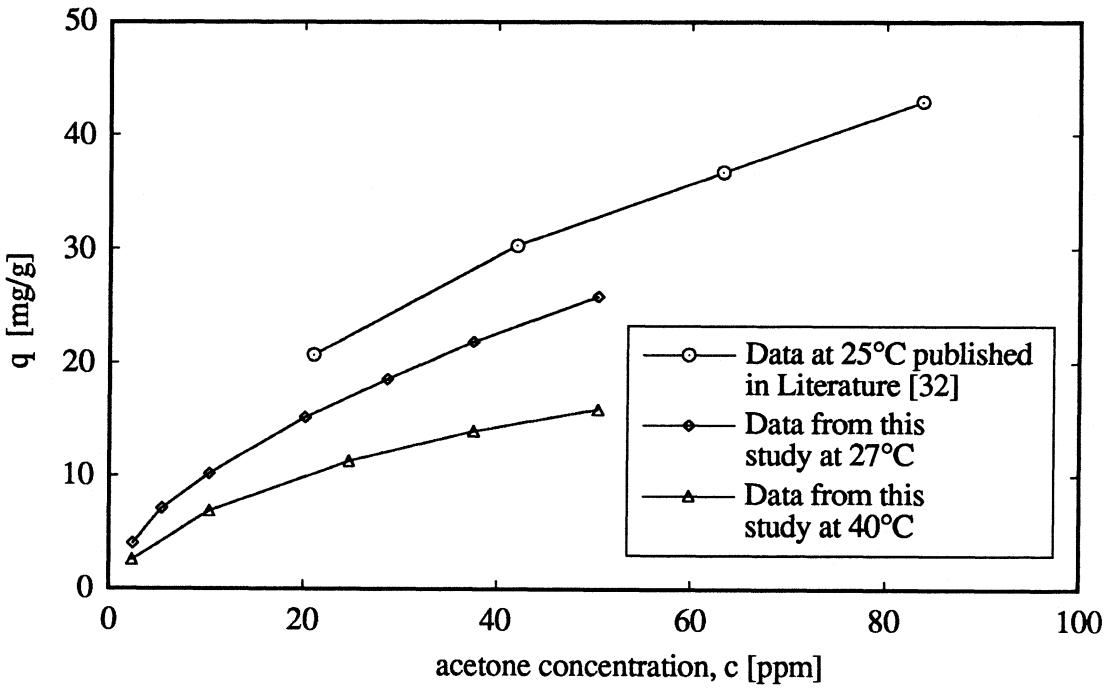

Figure 4.20 Comparison of data with results published in literature

CHAPTER
FIVE

Conclusions and Recommendations for Future Work

5.1 Conclusions

There were two primary objectives of this thesis. The first objective was to investigate whether a chromatographic flow method can be used to determine low concentration adsorption isotherms of organic vapors on activated carbon. This task included the design of an apparatus and the selection of the best measurement technique. Adsorption equilibrium data in the low concentration range (parts per million down to parts per billion) is of interest to indoor air quality research. The designed apparatus, as well as the measurement technique, a frontal analysis methodology, were described in chapter three of this thesis.

The main parts of the experimental equipment were a Hewlett Packard 5890 gas chromatograph with a flame ionization detector, an analog to digital converter, and a personal computer. The data acquisition equipment was used to obtain digital concentration-time plots for numerical analyses of the data. A detailed operating manual for the operation of the apparatus was given in section 3.2. These instructions described

the various steps of preparing the equipment and the sequence of a frontal analysis experiment.

The second objective of this work was to use the apparatus for the measurement of some single component adsorption isotherms of organic vapors on activated carbon. Acetone was chosen for this purpose because it is a common indoor air pollutant and has a relatively high affinity to activated carbon. Isotherms were measured in the temperature range from 27°C to 130°C and acetone concentrations ranging from approximately 2 ppm to 50.4 ppm. All experiments were done on Calgon OL 20/50 activated carbon. At 40°C, the amount of adsorbed acetone ranged from 2.57 milligram per gram carbon at an acetone concentration of 2.41 ppm to 15.9 milligram per gram at 50.4 ppm. Different acetone concentrations were obtained by diluting an acetone-nitrogen mixture of known composition with a stream of pure nitrogen. This method was proven to be accurate and simple.

The resulting isotherms curved towards the concentration axis and did not follow the straight line shape as suggested by the Henry equation for low adsorbate concentrations. Six adsorption models were fitted to the experimental data. Out of these, the Radke and Prausnitz model fitted the data best. An error estimation ε was introduced to compare the quality of different fits. A correlation following the Dubinin-Polanyi theory yielded a single equation which correlated the experimental data over the whole temperature and concentration range. The isosteric heat of adsorption was found to be a function of the amount adsorbed. For two milligrams acetone adsorbed per gram of carbon, the value was 57 kJ per mole of acetone. A thorough uncertainty analysis showed that the obtained data was accurate within approximately two percent of the values reported in chapter four. Adsorption measurements on crushed Calgon OL 20/50 activated carbon yielded

adsorption capacities which were 46% higher than those obtained from the uncrushed carbon.

5.2 Recommendations for Future Work

In order to provide a broader basis for the modeling of regenerative adsorptive air filters, more adsorption equilibrium data should be measured. This includes both single component and multicomponent systems where several organic compounds are present at the same time. Furthermore, the adsorption of organics depends on the type of carbon used. The adsorptive capacities of several different carbon types should be measured. In order to limit the experimental work, all remaining experiments could then be conducted with the carbon that yields the highest affinity towards the organic species of interest.

Since adsorptive air filters in an actual building application operate with polluted moist air, it has to be investigated how the adsorption properties of activated carbon are influenced by the presence of water vapor. Also, the adsorptive capacities of crushed carbons were found to be substantially higher than those of the regular, uncrushed condition. It should be carefully investigated whether this increase could be utilized in practical operation, taking the increased pressure drop of packed beds containing small particles into account.

The frontal analysis technique used in this study was found to be reliable and accurate. However, the flowrates through the flame ionization detector were limited to approximately 55 ml/min. This resulted in time consuming experiments. The time until complete saturation of the carbon beds was reached ranged from hours to days, depending on the temperature and the acetone concentration of the experiment. Since the

mass of activated carbon inside the glass column can not be further decreased, a split flow technique would allow higher flowrates and hence faster experiments. The column effluent would be split into two streams, a small one that is directed through the detector and a large one that is vented to the atmosphere. An improved fume hood system should be installed in the laboratory, because most of the adsorbate would not be burned in the flame ionization detector.

The investigation of water vapor can not be done with the flame ionization detector presently in use because water is not detected by it. A different detector, such as a thermal conductivity cell, could overcome this constraint. In addition, some organics that are of main concern to indoor air quality research, such as formaldehyde, exhibit only poor sensitivity in a flame ionization detector but are easily detected by a thermal conductivity cell.

Appendix A.1

Uncertainty Analysis

In chapter four, the amounts of adsorbed acetone, q, were calculated using the equation

$$q = b\frac{F\,A}{m} \tag{A.1.1}$$

where F is the measured flowrate, A is the composite area of the chromatogram as described in chapter two, and m is the mass of activated carbon in the glass column. A unit conversion constant, b, is used to obtain q in units of milligram acetone per gram of activated carbon. Written in a more general form, the result q is a function of the independent variables, F, A, and m

$$q = q(F, A, m) \tag{A.1.2}$$

If w_F, w_A, and w_m are the uncertainties in the independent variables, the uncertainty in the result, w_q, can be expressed by

$$w_q = \left[\left(\frac{\partial q}{\partial F} w_F\right)^2 + \left(\frac{\partial q}{\partial A} w_A\right)^2 + \left(\frac{\partial q}{\partial m} w_m\right)^2\right]^{1/2} \tag{A.1.3}$$

This method of determining uncertainties in experimental results has been presented by Kline and McClintock [67]. The partial derivatives of the governing equation (A.1.1) are given by

$$\frac{\partial q}{\partial F} = \frac{b\,A}{m}, \quad \frac{\partial q}{\partial A} = \frac{b\,F}{m}, \quad \frac{\partial q}{\partial m} = -\frac{b\,F\,A}{m^2} \tag{A.1.4}$$

The uncertainties in the independent variables, w_F, w_A, and w_m, have to be evaluated from statistical means or from known uncertainties in the corresponding measurement procedures.

The uncertainty in the flowrate, w_F, was determined from repeated readings of a flowrate that was assumed to be constant. Furthermore, it was assumed that the used technique to measure the flowrate involved no bias error (other than those accounted for as described in chapter three). The digital stopwatch which was used in these measurements had a resolution of 1/10 of a second. The conversion into flowrates (the procedure is described in chapter three), gave results that fluctuated around a mean value (e.g., all readings were either 55 ml/min, 55.5 ml/min, or 56 ml/min). A Gaussian error distribution was not applicable to these tests. Based on this experiment, the uncertainty in the flowrate was set to be 1 ml/min.

The overall uncertainty in the composite area A (described in chapter two) involved uncertainties in the analog to digital converter, the numerical integration process, and the determination of acetone concentrations if those were obtained by diluting the acetone-nitrogen mixture with pure nitrogen. In these cases, the resulting (lower) acetone concentrations were calculated from the ratio of the flowrates of acetone-nitrogen mixture and nitrogen diluent plus acetone-nitrogen mixture, respectively. Due to the uncertainties in the flowrate measurements, the calculated resulting (lower) acetone concentrations had also an uncertainty which was evaluated to be two percent. The overall uncertainty in the area A was three percent, taking the additional uncertainty caused by the data acquisition equipment (A/D converter) into account.

The resolution of the balance which was used to weigh the activated carbon was 0.5 milligram or 0.0005 gram. Summarized, the single uncertainties are given by

$$w_F = 1 \text{ ml/min}, \quad w_A = 0.03 \text{ A}, \quad w_m = 0.0005 \text{ gram} \qquad \text{(A.1.5)}$$

The resulting uncertainty in q, w_q, is shown in Table A.1.1 for each measured data point of the isotherms between 40°C and 130°C. As described above, there is also an uncertainty in the acetone concentration, w_C, where those are obtained by diluting the acetone-nitrogen mixture with pure nitrogen (Table A.1.1). Since the isotherms are plotted as q versus c, the uncertainty in the amount adsorbed, q extends in the y-direction and the uncertainty in the acetone concentration (where applicable) extends in the x-direction of the isotherm plot.

Table A.1.1 Uncertainties for isotherms from 40°C to 130°C

T [°C]	m [gram]	F [ml/min]	Area, A [ppm*sec]	q [mg/g]	w_q [%]	w_c [%]
130	0.0993	55.6	26921	0.586	**2.00**	**0.0**
130	0.0993	55.6	22071	0.481	**1.87**	**2.0**
130	0.0993	55.0	17007	0.366	**1.89**	**2.0**
130	0.0993	55.0	11956	0.258	**1.88**	**2.0**
130	0.0993	56.1	5248	0.115	**1.86**	**0.0**
130	0.0993	50.8	3293	0.0660	**2.02**	**2.0**
130	0.0993	51.2	1390	0.0280	**2.01**	**2.0**
115	0.0993	55.6	45462	0.990	**1.87**	**0.0**
115	0.0993	55.6	39118	0.852	**1.87**	**2.0**
115	0.0993	55.0	31719	0.683	**1.89**	**2.0**
115	0.0993	55.6	21379	0.466	**1.87**	**2.0**
115	0.0993	56.1	11185	0.246	**1.85**	**0.0**
115	0.0993	50.8	6446	0.128	**2.04**	**2.0**
115	0.0993	51.2	2918	0.0580	**2.04**	**2.0**
100	0.0993	55.0	84569	1.82	**1.89**	**0.0**
100	0.0993	55.6	70725	1.54	**1.87**	**2.0**
100	0.0993	54.5	56675	1.21	**1.90**	**2.0**
100	0.0993	55.6	40893	0.891	**1.87**	**2.0**
100	0.0993	56.1	21940	0.482	**1.85**	**0.0**

Table A.1.1 continued

100	0.0993	48.4	13346	0.253	**2.13**	**2.0**
100	0.0993	51.2	5791	0.116	**2.02**	**2.0**
85	0.0993	55.6	147169	3.20	**1.87**	**0.0**
85	0.0993	55.0	128899	2.78	**1.89**	**2.0**
85	0.0993	55.0	101875	2.19	**1.89**	**2.0**
85	0.0993	55.0	74059	1.60	**1.89**	**2.0**
85	0.0993	56.1	44446	0.977	**1.85**	**0.0**
85	0.0993	55.0	24804	0.534	**1.89**	**2.0**
85	0.0993	54.5	12810	0.273	**1.91**	**2.0**
70	0.0993	55.6	270191	5.89	**1.87**	**0.0**
70	0.0993	55.6	230961	5.03	**1.87**	**2.0**
70	0.0993	55.0	188651	4.07	**1.89**	**2.0**
70	0.0993	55.0	143638	3.10	**1.89**	**2.0**
70	0.0993	56.1	89730	1.97	**1.85**	**0.0**
70	0.0993	55.0	52147	1.12	**1.89**	**2.0**
70	0.0993	54.5	27606	0.589	**1.90**	**2.0**
55	0.0471	54.5	219347	9.87	**2.12**	**0.0**
55	0.0471	56.1	185960	8.62	**2.08**	**2.0**
55	0.0471	54.5	168978	7.61	**2.12**	**2.0**
55	0.0471	54.1	124307	5.55	**2.13**	**2.0**
55	0.0471	55.3	77114	3.52	**2.10**	**0.0**
55	0.0471	55.6	46220	2.12	**2.09**	**2.0**
55	0.0471	55.5	29513	1.35	**2.09**	**2.0**
40	0.0471	54.5	353034	15.9	**2.12**	**0.0**
40	0.0471	52.6	320370	13.9	**2.18**	**2.0**
40	0.0471	53.1	257169	11.3	**2.16**	**2.0**
40	0.0471	56.1	148385	6.87	**2.08**	**0.0**
40	0.0471	57.1	54385	2.57	**2.05**	**2.0**

Appendix A.2

Determination of the Pressure Correction factor j

Known: Geometry of packed bed, velocity of flowing gas phase

Find: Pressure drop (p_i - p_o), pressure ratio p_i/p_o, pressure correction factor j

Schematic:

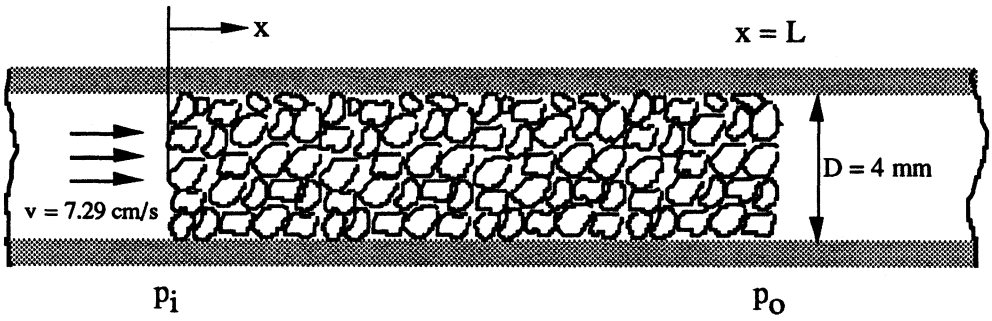

Figure A.2.1 Activated carbon particles in glass column

Assumptions:

1) The semi-empirical Blake-Kozeny equation [63] holds in this case
2) All particles in the packed bed are of spherical form and there is no size distribution
3) The flowing gas phase consists of pure nitrogen
4) The properties of the gas phase are independent of pressure

Properties:

$\rho_{,N2}$ = 1.162 kg/m^3

$\mu_{,N2}$ = 0.0175 cp = 17.5E-6 kg/m sec

Analysis:

Reynolds Number (Re) = D v ρ / μ = 4E-3 m × 7.29E-2 m/sec × 1.162 kg/m^3 / 0.0175E-3 kg/m sec = 19.36 (laminar flow)

The Blake Kozeny equation (semi empirical, [63]) describes the pressure drop in a packed column for laminar flow and isothermal conditions

$$(p_o - p_L) = \frac{150\, v\, L\, \mu}{D_p^2} \frac{(1-\varepsilon)^2}{\varepsilon^3} \qquad \text{(A.2.1)}$$

The void fraction ε is the ratio of the "void volume" over the bed volume. The particle diameter is expressed by D_p and the velocity v in equation (A.2.1) is the superficial velocity (7.29 cm/sec, in this case). The void fraction ε of the packed beds used in this study were not known. Even though this parameter could be measured, no attempt was done to do so. The following calculations were done for a bed length of 2 cm.

The particle diameter D_p is directly related to the mesh size of the activated carbon particles. A mesh size of "20/50" translates into sieve openings of 0.8 mm and 0.3 mm respectively. Since it was assumed earlier that there is no size distribution, a suitable mean for D_p has to be substituted into equation (A.2.1). Figure A.2.2 shows resulting pressure drops across the packed bed as a function of the particle diameter for several void fractions.

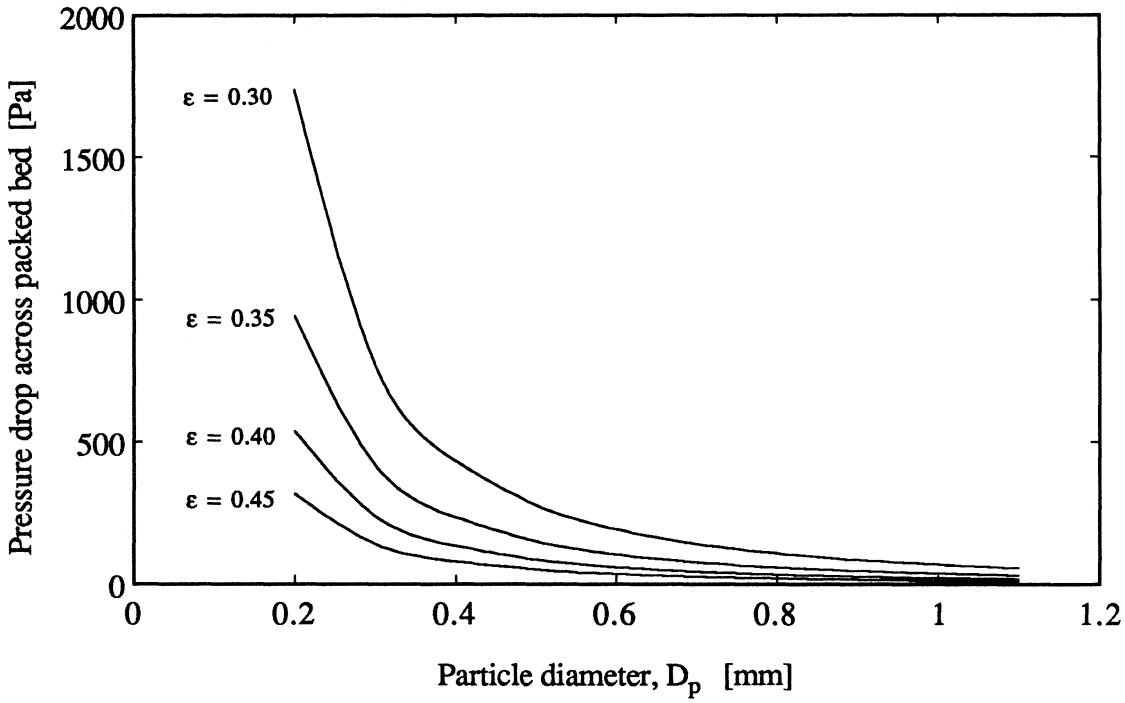

Figure A.2.2 Pressure drop as a function of the particle diameter for several void fractions

The pressure drop is highly dependent on the particle diameter and, somewhat less crucial, on the void fraction. Nevertheless, for the particle diameters of interest to this study, the resulting pressure drops are relatively small. For some of the calculated pressure drops (Figure A.2.2), Table A.2.1 shows the corresponding inlet to outlet pressure ratio p_i/p_o and the resulting pressure correction factor j (as described in chapter 3). In these calculations, the outlet pressure p_o was assumed to be atmospheric (101.325 kPa). The resulting j-values are very close to unity and hence there was no pressure correction made for the results presented in chapter four.

Table A.2.1 Inlet/outlet ratios p_i/p_o and correction factors j for several values of the pressure drop $(p_i - p_o)$

Pressure Drop $(p_i - p_o)$ [Pa]	Inlet/Outlet Ratio p_i/p_o [-]	Correction factor j [-]
200	1.00197	0.99901
300	1.00296	0.99852
400	1.00395	0.99803
500	1.00493	0.99754
600	1.00592	0.99705
700	1.00790	0.99655
800	1.00790	0.99606
900	1.00888	0.99557
1000	1.00987	0.99508
1200	1.01184	0.99410
1400	1.01382	0.99312
1600	1.01579	0.99215
1800	1.01776	0.99117
2000	1.01974	0.99020

Appendix A.3

Heat Transfer Considerations inside the glass column

Known: Geometry of column, velocity and inlet temperature of flowing gas phase

Find: Temperature of the flowing gas stream (nitrogen-acetone mixture) as a function of the axial position in the column if the gas enters the column with a temperature of 25°C

Schematic:

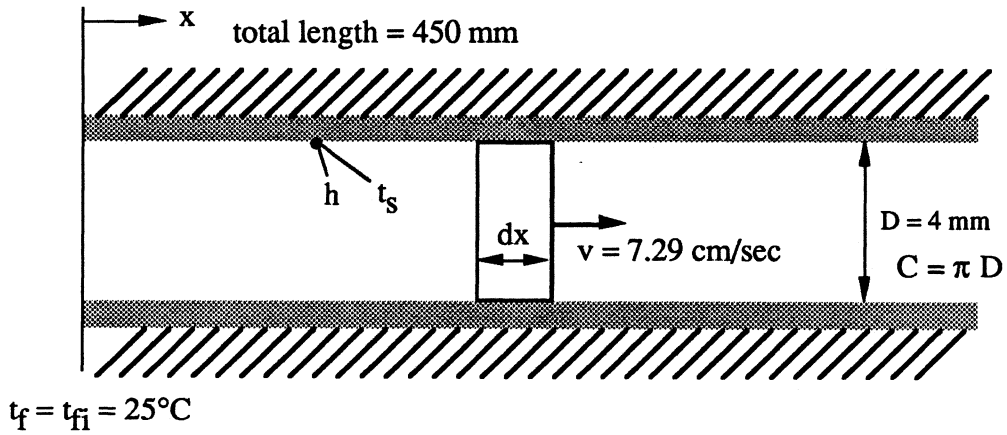

Figure A.3.1 Migrating fluid element in the glass column

Assumptions:

1) Constant temperature of the glass surface
2) No velocity distribution (plug flow)
3) The flowing gas phase consists of pure nitrogen
4) Properties of the gas phase are independent of temperature

Properties:

$Pr_{,N2}$ (at 50°C) = 0.7131

$c_{p,N2}$ = 1041 J/kg K

$k_{,N2}$ = 27.6E-3 W/m K,

$\mu_{,N2}$ (at 50°C) = 17.5E-6 kg/m sec

$\rho_{,N2}$ = 1.162 kgm^3

Analysis:

Reynolds Number (Re) = D v ρ / μ = 4E-3 m × 7.29E-2 m/sec × 1.162 kg/m^3 / 0.0175E-3 kg/m sec = 19.36 (laminar flow)

A heat balance on the fluid element of length dx in Figure A.3.1 and an equation describing the heat exchange between the fluid element and the glass surface yield

$$dq = \dot{m}\, c_p\, dt_f \tag{A.3.1}$$

$$dq = h\, C\, dx\, (t_s - t_f) \tag{A.3.2}$$

$$\frac{h\, C}{\dot{m}\, c_p} dx = \frac{dt_f}{(t_s - t_f)} \tag{A.3.3}$$

where equation (A.3.3) is obtained from equating (A.3.1) and (A.3.2). Since t_s is assumed to be constant, equation (A.3.3) can be rewritten as

$$-\frac{h\, C}{\dot{m}\, c_p} dx = \frac{d(t_f - t_s)}{(t_f - t_s)} \tag{A.3.4}$$

Integration between x=0 to x=x and $t_f = t_{fi}$ to $t_f = t_f$ yields

$$-\frac{h\, C}{\dot{m}\, c_p} x = \ln\left(\frac{t_f - t_s}{t_{fi} - t_s}\right) \tag{A.3.5}$$

$$\left(\frac{t_f - t_s}{t_{fi} - t_s}\right) = \exp\left(-\frac{h\,C}{\dot{m}\,c_p}x\right) \tag{A.3.6}$$

$$t_f = \exp\left(-\frac{h\,C}{\dot{m}\,c_p}x\right)(t_{fi} - t_s) + t_s \tag{A.3.7}$$

Equation (A.3.7) can be used to determine the temperature of the fluid element at any length x. This equation makes sense in a physical way: the exponent term varies between zero and unity. If, for a given x, it is close to zero (what corresponds to high convective heat transfer coefficients, large contact areas, and small mass flowrates and heat capacities), the temperature of the fluid element will be close to that of the surface. The other physical extreme is given when the exponential term approaches unity. In this case, the fluid temperature t_f does not change and $t_f = t_{fi}$.

The convective heat transfer coefficient h is obtained from a Nusselt correlation. Hausen [68] developed the following semi-empirical relation for fully developed laminar flow

$$Nu = 3.66 + \frac{0.0668\,(D/L)\,Re\,Pr}{1 + 0.4\,[(D/L)\,Re\,Pr]^{2/3}} \tag{A.3.8}$$

Substituting the values for D/L, Re, and Pr into equation (A.3.8) yields a result of Nu=3.67 which is very close to Nusselt's original value of 3.66 (first term on the right hand side of equation (A.3.8)). This indicates that the column is sufficiently long and the thermal starting length has only a minor influence on the Nusselt number.

The convective heat transfer coefficient h is now easily obtained from the definition of the Nusselt number

$$Nu = \frac{h\,D}{k} = 3.67 \tag{A.3.9}$$

$$h = \frac{3.67\ k}{D} = 25.3\ W/m^2\ K \qquad (A.3.10)$$

With a known convective heat transfer coefficient h, a circumference of 12.57E-3 m, a mass flowrate of 1.065E-6 kg/sec, and a known specific heat capacity c_p, the exponential factor

$$\exp\left(-\frac{h\,C}{\dot{m}\,c_p}x\right)$$

in equation (A.3.7) takes values very close to zero, as shown in Table A.3.1 for several length of x. This indicates that the temperature t_f of the fluid element is, (after a short length of travelling down the column, compared to the total column length of 450 mm), very close to the temperature of the glass surface.

Table A.3.1 Fluid temperatures and values of the exponent term for several lengths of x

x [mm]	$\exp\left(-\frac{h\,C}{\dot{m}\,c_p}x\right)$	t_f [°C]
1	0.75062	62.41
5	0.23829	139.26
10	0.05678	166.48
20	3.224E-3	174.52
30	1.831E-4	174.97
100	3.485E-13	175.00
200	1.215E-25	175.00
450	8.712E-57	175.00

This quantitative relationship holds for any surface temperature. Hence, at equilibrium conditions, it is reasonable to assume that the inner surface temperature of the column equals the outer surface temperature (since there is no driving force) and that the temperature of the flowing gas stream equals that of the glass surface. Figure A.2.2 shows this behavior: for x = 2 cm the temperature of the flowing gas equals that of the glass surface (a surface temperature of 175 °C was assumed). The total column length is 45 cm.

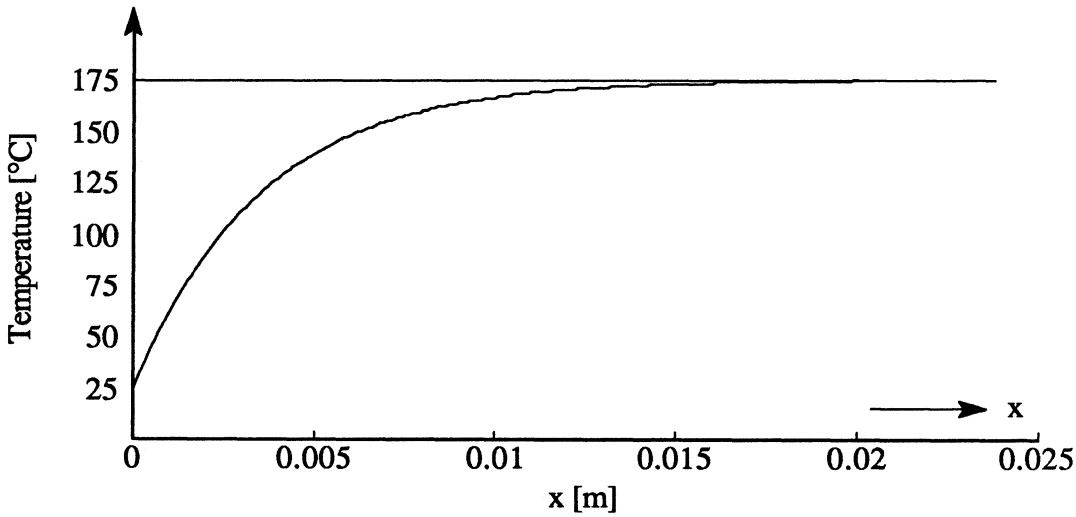

Figure A.3.2 Temperature of the flowing gas stream as a function of the axial position for the first 25 mm in the column

Appendix A.4

Physical Properties and Specifications of Calgon Activated Carbon OL 20/50

Calgon type OL carbon is made from selected grades of bituminous coal combined with binders to give hardness. The following is a list of the physical properties and specifications of the product as provided from the manufacturer (Calgon):

Physical properties:

Total Surface Area (N_2-Adsorption method)	1000-1100 m^2/g
Apparent Density (Bulk Density)	0.48 g/cm^3
Particle Density (Hg Displacement)	0.75 g/cm^3
Real Density (He Displacement)	2.2 g/cm^3
Pore Volume (Within Particle)	0.88 cm^3/g

Specifications:

Mesh Size, US Sieve Series	20 x 50
Larger than 20 mesh, Maximum	3%
Smaller than 50 mesh, Maximum	1%
Iodine Number, Minimum	1050
Molasses Number, Minimum	200
Ash, Maximum	8%
Moisture as packed, Maximum	2%
Abrasion Number, Minimum	70

Surface area measurements with the same N_2-adsorption method were conducted to verify the specifications of the manufacturer. These measurements yielded a total surface area of 1116 m^2/g.

Appendix A.5

A typical frontal analysis chromatogram

The following is a reduced chromatogram as obtained from the electronic integrator for a frontal analysis run at 130°C and an acetone concentration of 40.2 ppm. The chart speed was set to 1cm per minute. The experiment took approximately 30 minutes.

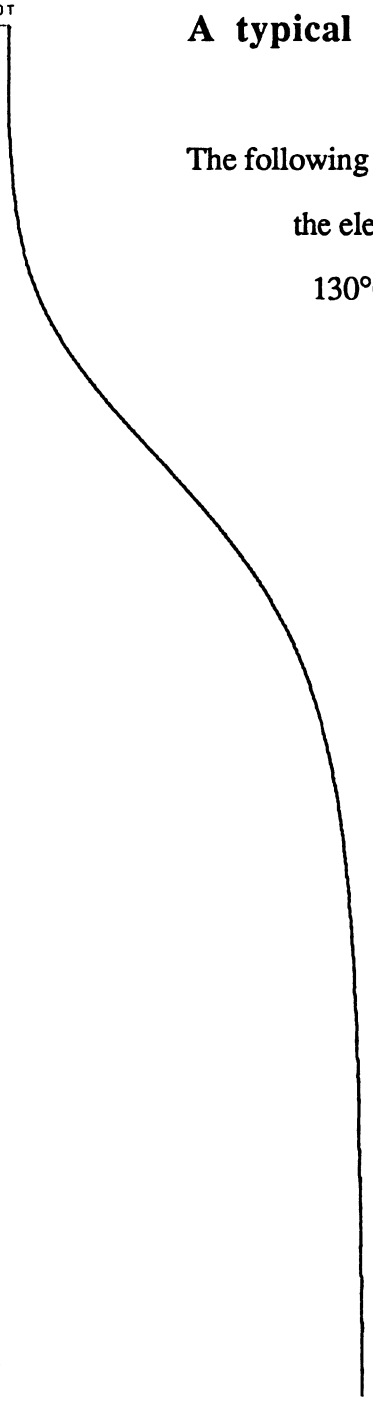

References

1 Treybal, R.E., *Mass-Transfer Operations*, McGraw-Hill, London, 1981

2 Scheele, C.W., *Chemical Observations on Air and Fire*, 182 (1780)

3 Fontana, F., *Memorie Mat. Fis. Soc. ital. Sci.*, **1**, 679 (1777)

4 London, *F., Z. Physik.*, **63**, 245 (1930)

5 London, F., *Z. Physik. Chem.*, **11**, 222 (1930)

6 Born, M., Mayer, J.E., *Z Physik.*, **75**, 1 (1932)

7 Gregg, S.J., Sing, K.S.W., *Adsorption, Surface Area and Porosity*, Academic Press, New York, 1967

8 Habgood, H.W., Hanlan, J.F., *Can. J. Chem.*, **37**, 843 (1959)

9 Boucher, E.A., Everett, D.H., *Trans. Faraday Soc.*, **67**, 2720 (1971)

10 Philips, C.S.G., *Discuss. Faraday Soc.*, **7**, 241 (1949)

11 Basmadjian, D., *Can. J. Chem.*, **38**, 141 (1960)

12 Josefewitz, Othmer, *Ind. Eng. Chem.*, **40**, 739 (1948)

13 Dubinin, M.M., *Zhur. Phys. Chem.*, **34**, 959 (1960)

14 Dubinin, M.M., *Chem. Rev.*, **60**, 235 (1960)

15 Lewis, W.K., Gilliland, E.R., Chirtrow, B., Cadogan, W.B., *Ind. Eng. Chem.*, **42**, 1319 (1950)

16 Nelsen, F.M., Eggertsen, F.T., *Analy. Chem.*, **30**, 1387 (1958)

17 Atkins, J.H., *Analy. Chem.*, **36**, 579 (1964)

18 Daeschner, H.W., Stross, F.H., *Analy. Chem.*, **34**, 1150 (1962)

19 Labofina, S.A., *Analy. Chem.*, **35**, 259 (1963)

20 Masamune, S., Smith, R.J., *AIChE Journal*, **10**, 246 (1964)

21 Weber, T.W., Chakravorti, R.K., *AIChE Journal*, **20**, 228 (1974)

22 Smisek, M., Cerny S., *Active Carbon: Manufacture, Properties and Applications*, Elsevier Publishing Company, New York, 1970

23 Kyle, B.G., Eckhoff, N.D., *Odor Removal from Air by Adsorption on Charcoal*, Techn, Rep. Prep. for the Nat. Environmental Research Center, EPA-650/2-74-084, PB-236-928

24 Fan, L.T., *Mathematical Simulation of an Adsorber for Pollutant Removal*, Techn, Rep. Prep. for the Nat. Environmental Research Center, EPA-650/2-74-110, PB-239-331

25 Cooney, D.O., *Ind. Eng. Chem. Proc. Des. Dev.*, **13**, 368 (1974)

26 Schneider, P., Smith, J.M., *AIChE Journal*, **14**, 886 (1968)

27 Langmuir, I., *J. Chem. Soc.*, **40**, 1361 (1918)

28 Fowler, R.H., Guggenheim, E.A., *Statistical Thermodynamics*, Cambridge University Press, Cambridge, 1939

29 Suwanayuen, S., Danner, R.P., *AIChE Journal*, **26**, 68 (1980)

30 Brunauer, S., Deming, L.S., Deming, W.S., Teller, E., *J. Amer. Chem. Soc.*, **62**, 1723 (1940)

31 Brunauer, S., Emmett, P.H., Teller, E., *J. Amer. Chem. Soc.*, **60**, 309 (1938)

32 Forsythe, R.K., *Adsorption and Dispersion of selected organic gases flowing through activated carbon adsorber beds*, Ph.D. Thesis, Kent State University, 1988

33 Ramanathan, K., Debber, V.L., Environmental Progress, **7**, 230 (1988)

34 James, D.H., Phillips, C.S.G., J. Chem. Soc., 1066 (1954)

35 Harris, M.R., Sing, K.S.W., J. appl. Chem., **5**, 223 (1955)

36 Kiri, K.A., Walker, P.C., J. Sci. Instr., **42**, 821 (1965)

37 Gregg, S.J., Sing, K.S.W., J. phys. Chem., **56**, 388 (1952)

38 Foster, A.G., Proc. roy. Soc. **147**, 128 (1934)

39 Gregg, S.J., J. chem. Soc., 1438 (1955)

40 Bickley, R.I., Ph.D. Thesis, Exeter University (1963)

41 Gulbranson, E.A., Rev. sci. Instrum., **15**, 201 (1944)

42 Davies, R.G., Chem. & Ind., 160 (1952)

43 Tswett, M., Ber. deut. botan. Ges., **24**, 316 (1906)

44 Purnell, H., *Gas Chromatography*, John Wiley &Sons, New York, 1962

45 Kuhn, R., Winterstein, A., Lederer, E., Hoppe-Seyler's Z. physiol. Chem., **197**, 141 (1931)

46 Martin, A.J.P., Synge, R.L.M., Biochem. J., **35**, 1358 (1941)

47 Glueckauf, E., J. chem. Soc., 1302 (1947)

48 James, A.T., Martin, A.J.P., Biochem. J., **50**, 679 (1952)

49 James, D.H., Phillips, C.S.G., J. chem. Soc., 1066 (1954)

50 McNair, H.M., Bonelli, E.J., *Basic Gas Chromatography*, Varian, Palo Alto, 1968

51 Perry, J.A., *Introduction to Analytical Gas Chromatography*, Volume 14, Marcel Dekker, New York, 1981

52 Langer, S.H., Lecture Notes, Dept. of Chem. Eng., University of Wisconsin-Madison, 1991

53 Van Deemter, J.J., Zuiderweg, F.J., Klinkenberg, A., Chem. Eng. Sci., **5**, 271 (1956)

54 Conder, J.R., Purnell, J.H., Trans. Faraday Soc., **65**, 824, 1969

55 Conder, J.R., Young, C.L., *Physicochemical Measurements by Gas Chromatography*, John Wiley & Sons, New York, 1979

56 Laub, R.J., Pecsoc, R.L., *Physicochemical Applications of Gas Chromatography*, John Wiley & Sons, New York, 1978

57 Cremer, E., Monatsh. Chem., **92**, 112 (1961)

58 Cremer, E., Huber, H.F., Gas Chromatography, Third Intern. Symp., p. 169, Eds. N. Bremer, J.E. Cullen, M.D. Weiss, Academic Press, New York, 1962

59 Huber, J.F.K., Keulemans, A.I.M., *Gas Chromatography*, 1962, Ed. M.van Sway, Butterworths, London, 1962

60 Cremer, E., Huber, J.F.K., Angew. Chem. **73**, 461 (1961)

61 Reilley, C.N., Hildebrand, G.P., Ashley, J.W., Anal. Chem., **34**, 1198 (1962)

62 Littlewood, A.B., *Gas Chromatography, Principles, Techniques and Applications*, Academic Press, New York, 1962

63 Bird, R.B., Stewart, W.E., Lightfoot, E.N., *Transport Phenomena*, John Wiley & Sons, New York, 1960

64 Suzuki, M., *Adsorption Engineering*, Elsevier, Amsterdam, 1990

65 Kaleidagraph, Data analysis/graphics application program, Synergy Software, Reading, Pa

66 Ruthven, D.M., *Principles of Adsorption and Adsorption Processes* Wiley, New York, 1984

67 Holman, J.P., Experimental Methods for Engineers, McGraw-Hill, New York, 1978

68 Hausen, H., Z.A.V.D.I., Beihefte Verfahrenstechnik, **4**, 91 (1943)